

# **The Institute of Paper Chemistry**

**Appleton, Wisconsin**

## **Doctor's Dissertation**

**The Influence of Cobalt Ion Concentration on the  
Degradation of Methyl  $\beta$ -D-Glucopyranoside  
in Oxygen-Alkali**

**David P. Graves, Jr.**

**January, 1981**

THE INFLUENCE OF COBALT ION CONCENTRATION ON THE DEGRADATION  
OF METHYL  $\beta$ -D-GLUCOPYRANOSIDE IN OXYGEN-ALKALI

A thesis submitted by

David P. Graves, Jr.

B.S. 1975, Duke University

M.S. 1977, Lawrence University

in partial fulfillment of the requirements  
of The Institute of Paper Chemistry  
for the degree of Doctor of Philosophy  
from Lawrence University,  
Appleton, Wisconsin

Publication Rights Reserved by  
The Institute of Paper Chemistry

January, 1981

# TABLE OF CONTENTS

	Page
SUMMARY	1
INTRODUCTION	3
Perspective	3
Literature Review	3
Chain Cleavage	4
Oxidation Within the Carbohydrate Ring	5
Intermediate Peroxides	7
Mechanism of Oxidation	7
Transition Metal Ion Catalysis	9
Free Radical Generation	9
Aging of Alkali Cellulose	10
Decreased Catalysis at High Metal Ion Concentration	11
Metal-Induced Mechanism Shift	13
THESIS OBJECTIVE	16
RESULTS AND DISCUSSION	17
Experimental Approach	17
MBG Degradation	18
No added Cobalt	19
Cobalt Added at the 0.01 and 0.05 mM Levels	20
Cobalt Added at the 0.25 mM Level	21
The Chemistry of Cobalt in Alkaline Solution	25
Transition Metal Ion Precipitation and Adsorption	29
Precipitate Formation and MBG Degradation	29
Precipitate Composition	30
Color Formation	31

Adsorption by Precipitated Cobalt	32
Adsorption in the Absence of Oxygen	33
Adsorption during MBG Degradation	34
Adsorption by Precipitated Transition Metal Oxides and Hydroxides	35
Metal Hydroxide Solubility and Oxygen-Alkali Degradation	39
Inhibition of Alkaline Cobalt Precipitation	40
General Comments	40
Visible Spectrum of Cobalt(II) in Alkali	41
Influence of Silicate Anions	43
Visible Spectra	43
Coordination of Silicate Anions with Transition Metal Ions	45
Silicates as Catalysts and Inhibitors	46
Influence of Borates	48
Influence of Polyols	49
Visible Spectra	49
Metal Ion-Carbohydrate Complexation in Alkali	51
Cobalt-Carbohydrate Complexation and MBG Degradation	52
Glycosidic Bond Cleavage	54
Methanol Stability	54
Analyses for Methoxyl Content	55
Methanol Formation	55
Acidic Products	57
General Comments	57
Influence of Cobalt	60

Mechanism of Cobalt-Catalyzed MBG Degradation	66
General Comments	66
Oxidation-Reduction of Cobalt	69
Influence of Cobalt-MBG Coordination on MBG Degradation	71
Cobalt-Catalyzed MBG Degradation in H <sub>2</sub> O <sub>2</sub> -Alkali and O <sub>2</sub> -Alkali	75
CONCLUSIONS	77
EXPERIMENTAL	79
General Analytical Procedures	79
Solutions and Reagents	80
Water	80
Oxygen and Nitrogen	80
Sodium Hydroxide	80
Extracted Sodium Hydroxide	80
Ultrapure Sodium Hydroxide	81
Methyl $\beta$ - <u>D</u> -Glucopyranoside (MBG)	81
Internal Standards	82
<u>n</u> -Butyl $\beta$ - <u>D</u> -Glucopyranoside (BBG)	82
Ethanol	82
Reaction Conduct and Solution Analysis	82
Reactor System	82
Conditioning of Reactor and Labware	83
Preparation of Reaction Solutions	83
Reaction Sampling	86
Analysis of Reaction Solutions	87
Glycoside Analysis	87
Methanol Analysis	87
Methoxyl Analysis	87

Acid Hydrolysis	90
Acidic Product Analysis	91
Trace Metal Analysis	91
Plasma Emission Spectrometry	91
Atomic Absorption Spectroscopy	92
Visible Spectra of Alkaline Cobalt Solutions	93
ACKNOWLEDGMENTS	94
LITERATURE CITED	95
APPENDIX I. TRACE METALS IN ALKALINE REACTION SOLUTIONS	101
APPENDIX II. EXPERIMENTAL DATA	102
APPENDIX III. DETERMINATION OF SIGNIFICANT DIFFERENCES BETWEEN SETS OF MBG RESULTS	112
APPENDIX IV. GAS-LIQUID CHROMATOGRAPHY	114
APPENDIX V. GAS CHROMATOGRAPHIC-MASS SPECTRAL ANALYSIS	117

## SUMMARY

The influence of cobalt concentration (0.01, 0.05, and 0.25 mM  $\text{CoSO}_4 \cdot 7\text{H}_2\text{O}$ ) on the degradation of 95.5 mM methyl  $\beta$ -D-glucopyranoside (MBG) in an  $\text{O}_2$ -alkali system was studied in a Teflon-lined reactor at  $120^\circ\text{C}$  using 1.25M NaOH and 0.68 MPa oxygen pressure. The degradations were followed by quantitative gas-liquid chromatography and were analyzed for both degradation rate and product appearance.

The rate of MBG degradation was dependent on cobalt ion solubility. Increasing the concentration of cobalt(II) initially present in reaction solutions from 0.00 to 0.01 to 0.05 mM decreased the time required for 50% MBG degradation from 12 to 6 to just under 2 hours. Attempts to prepare a 0.25 mM cobalt(II) reaction solution by addition of aqueous cobalt(II) to an alkaline stock solution prior to addition of solid MBG (the procedure used in the 0.01 and 0.05 mM reactions) resulted in the formation of a highly adsorptive cobaltous precipitate which was capable of removing otherwise soluble cobalt(II) from solution. Reactions conducted with solutions prepared in this manner resulted in MBG degradation rates which were essentially the same as in uncatalyzed reactions.

The initial rate of MBG degradation at the 0.25 mM added cobalt(II) level was substantially increased if silicate anions were initially present in stock alkaline solutions, or if the reaction solution preparation procedure was reversed so that aqueous cobalt was added to an alkaline MBG solution. In these instances cobalt(II) at the 0.25 mM addition level was stabilized in alkaline solution and no precipitation occurred until after reaction initiation by oxygen pressurization. Visible spectral studies showed that silicates and selected polyols (MBG, sorbitol, glycerol, and ethylene glycol) stabilized cobalt(II) in strongly alkaline (pH 14) solutions.

Cobalt(III) gradually precipitated from solution during degradations which were initially 0.25 mM in soluble cobalt(II). The precipitate formed under degradation conditions was highly adsorptive and removed otherwise soluble cobalt ions from solution. The precipitation of cobalt(III) from reaction solutions coincided with a rapid decline in the rate of MBG degradation.

The presence of either soluble or precipitated cobalt species in reaction solutions had only a minor influence on the pattern of acidic products formed during MBG degradation. The extent of MBG degradation occurring through glycosidic bond cleavage (as detected through methanol formation) was the same (ca. 70%) both in the presence and absence of added cobalt. At later reaction times (40-60% reaction) the presence of soluble cobalt in reaction solutions increased the concentrations of dicarboxylic acids relative to uncatalyzed degradations. A mechanism involving direct oxidation of MBG by cobalt(III) is proposed to account for the enhanced formation of dicarboxylic acids. Catalysis by soluble cobalt ions is attributed to a catalytic oxidation-reduction cycle between cobalt(II) and cobalt(III). It is proposed that the initial oxidation of cobalt(II) to cobalt(III) by oxygen produces superoxide radical ( $O_2^{\cdot-}$ ), and that cobalt(III) and superoxide radical promote oxidative MBG degradation reactions.



## INTRODUCTION

### PERSPECTIVE

Delignification of pulps in alkali under oxygen pressure\* is an attractive process since molecular oxygen is both nonpolluting and, if air is the source, free. The most significant drawback of this process is a slight reduction in the strength properties of oxygen-alkali pulps compared to conventional pulps. During oxygen-alkali delignification cellulose fibers are weakened by random chain cleavage reactions, and these reactions can result in a loss in pulp strength.

The finding that magnesium compounds largely inhibit carbohydrate degradation during oxidative alkaline delignification has made oxygen-alkali a more practical process (1-4). It is likely that magnesium compounds maintain pulp strength primarily by inhibiting degradative reactions induced by catalytic quantities of transition metals (3,5-7). The manner in which transition metals promote degradative reactions, however, is poorly understood. This investigation was directed at clarifying the role of catalytic transition metal ions (in particular cobalt ions) in oxygen-alkali carbohydrate degradation.

### LITERATURE REVIEW

Degradation of carbohydrates in oxygen-alkali-transition metal ion systems can involve ionic as well as free radical reactions, the formation and decomposition of peroxides, catalysis by transition metal ions, and, if the metal ions are precipitated under the reaction conditions, heterogeneous surface

---

\*Representative oxygen bleaching conditions are 10-30% pulp consistency, 0.5-5% sodium hydroxide (based on O.D. pulp), 90-130°C, and 0.5-1.5 MPa oxygen pressure. Total bleaching time is usually less than 2 hours.

phenomena. Such systems are clearly complex, and touch on an extensive body of information. The following literature review can only briefly consider some of the more salient findings on reactions of carbohydrates under oxidative alkaline conditions in the presence and absence of transition metal ions.

#### CHAIN CLEAVAGE

The delignification of pulp with oxygen and alkali can lead to severe carbohydrate degradation. This degradation is primarily manifested as reduced pulp viscosity, attributable to chain cleavage of polysaccharides. Peeling, the alkaline stepwise elimination of monomers from the reducing end of a polysaccharide chain, is of less importance than chain cleavage in an oxidative system. Under oxidative conditions, reducing end groups are oxidized to aldonic acids which are more resistant to peeling than aldehydic end groups (8-11). Of much more consequence in oxygen-alkali is the severe reduction in the length of carbohydrate polymers associated with chain cleavage reactions (8,12).

Investigations conducted with cellulose model compounds (3,13-20) indicate that the depolymerization involved in chain cleavage is initiated by the oxidation of carbohydrate hydroxyl groups to alkali labile carbonyl groups. In alkaline media, carbohydrate units with carbonyl groups are subject to  $\beta$ -alkoxy elimination reactions. Similar reactions presumably result in cellulose chain cleavage, and an example of a reaction leading to chain cleavage is shown in Fig. 1 (21,22).

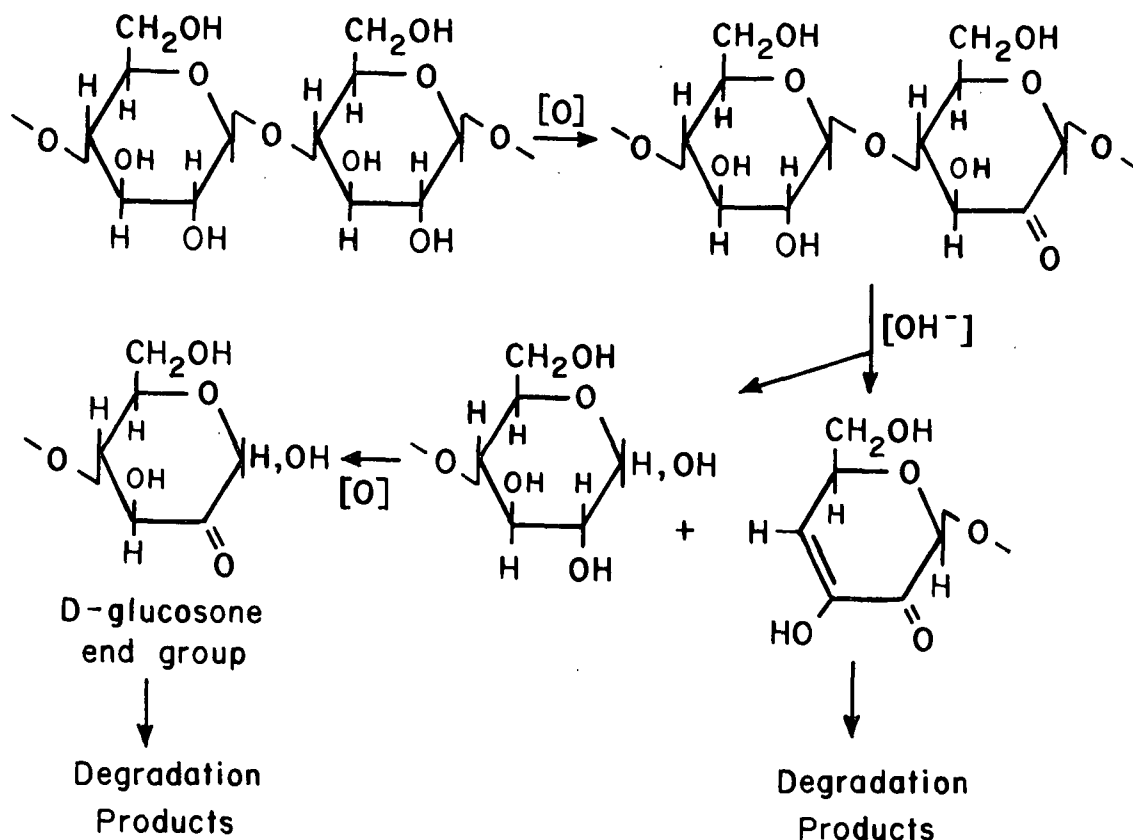


Figure 1. Mechanism for Cleavage of Cellulose by Oxygen in Alkali Proposed by Haskins and Hogsed (21)

#### OXIDATION WITHIN THE CARBOHYDRATE RING

Carbohydrate oxidation may also occur without the cleavage of polysaccharide glycosidic bonds. Studies with carbohydrate model compounds indicate that dicarboxylic acids and C-carboxy furanoid species are formed with the aglycone still intact (15-17,19,23,27,29). Oxidation of this type has been postulated to occur via a dicarbonyl intermediate which is either oxidized to a dicarboxylic acid, or rearranged in alkali to a C-carboxy furanoid acid via a benzylic acid rearrangement (15,19). This is shown in Fig. 2 for the cellulose model methyl  $\beta$ -D-glucopyranoside (MBG). Recent work, however, suggests stereoselective C-carboxy furanoid acid formation can also occur involving a single carbonyl and intramolecular hydrogen bonding via an alpha-hydroxyhydroperoxide (20,24,25).

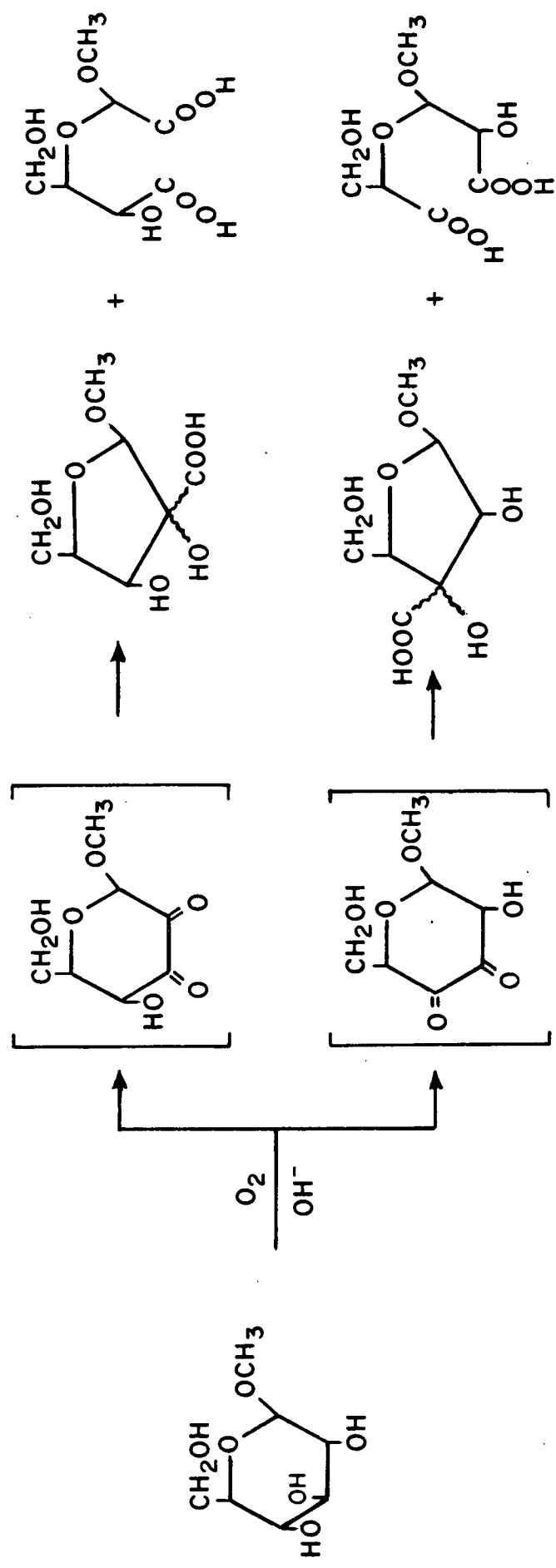


Figure 2. Oxidation Scheme for MBG According to Ericsson et al. (15)

## INTERMEDIATE PEROXIDES

Peroxides have been detected in oxygen-alkali reactions of cellulose (14) and cellulose model compounds (3,8,14,20,24,25,28,29), and are thought to be key reactive intermediates. Hydrogen peroxide and hydroperoxides are subject to highly degradative free radical decomposition reactions (30,31), and these reactions are influenced by the presence of trace contaminants or additives. Sinkey and Thompson (3) investigated the actions of the additives iron, iodide, and magnesium on the oxygen-alkali degradation of the cellulose model MBG. In each case they found that the action of the additive was related to the expected behavior of hydrogen peroxide in the presence of the additive.

Further, both oxygen-alkali and hydrogen peroxide-alkali degradations of MBG yield the same reaction products, though in slightly differing proportions (14,17), suggesting that the mechanisms of oxygen and hydrogen peroxide degradations are very similar.

Alpha-hydroxyhydroperoxides may also be very important in the mechanism of oxidative alkaline carbohydrate degradation and have been postulated as precursors in carbonyl formation (20,24-27). Relatively stable organic peroxides, possibly dialkyl peroxides arising from radical chain termination reactions (18,25,29), have also been reported in oxygen-alkali systems. The presence of transition metals in an oxygen-alkali-MBG system is reported to greatly enhance the formation of stable organic peroxides (29).

## MECHANISM OF OXIDATION

The mechanism of oxidative alkaline carbohydrate degradation leading to the formation of an alkali labile carbonyl group appears to involve free radicals and peroxidic intermediates (20). Initiation of degradation requires

ionization of a hydroxyl group to form a carbinolate anion (3,14,18,20,26). The increased electron density on carbon induced by the alkoxide ion, facilitates geminal hydrogen abstraction by oxygen (or other strong oxidizing agents) to form a hydroperoxy radical and ketyl radical as shown in Fig. 3. The ketyl radical thus formed may then add oxygen and participate in a series of steps leading to the formation of an alpha-hydroxyhydroperoxide (20,24). It is likely that the hydroperoxide intermediate then forms an alkali labile carbonyl in an irreversible step (32), ultimately leading to chain cleavage or a similar oxidative reaction within the ring.

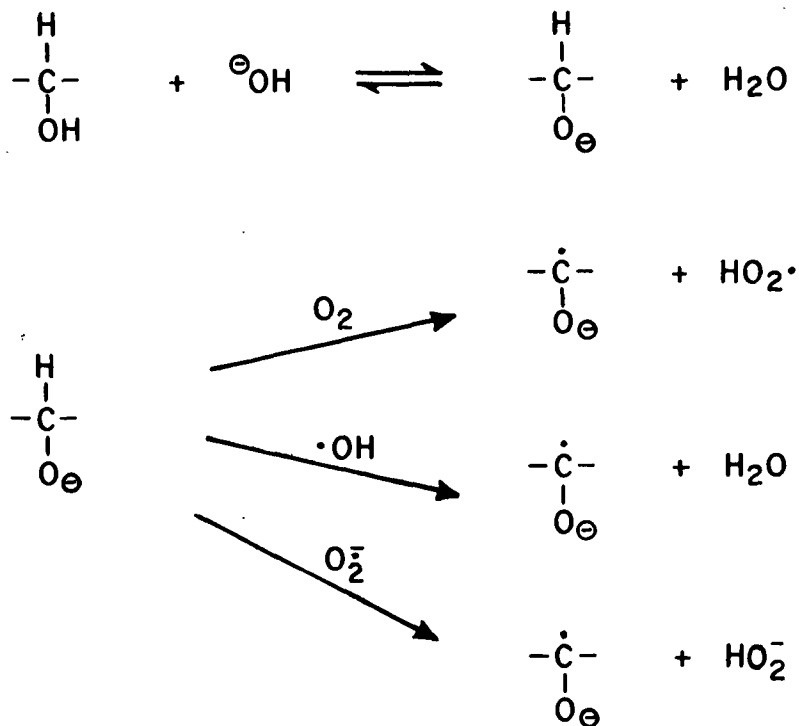


Figure 3. Initiation of Oxygen-Alkali Carbohydrate Degradation (3,20,24)

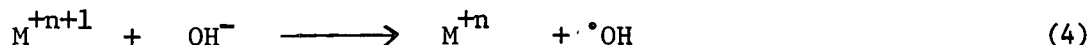
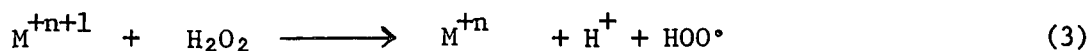
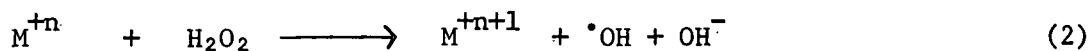
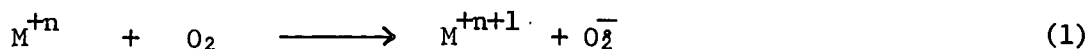
## TRANSITION METAL ION CATALYSIS

### FREE RADICAL GENERATION

The ability of transition metal ions to catalyze degradative reactions of carbohydrates in oxygen and alkali is well documented (3,5,6,9,18,29,33-42). In particular, the ionic forms of cobalt (5,9,34,35,39,40,42), iron (5,6,9,29,34,35,39,41), manganese (5,38), and copper (5,6,9,33,34,39-41) can be highly detrimental to carbohydrates under oxidative alkaline conditions. Comparable metal ion-induced catalysis has been noted in hydrogen peroxide-alkali systems (26,27,42) and during the aging of alkali cellulose (43,44).

In the absence of added transition metal ions the mechanism of oxygen-alkali carbohydrate degradation involves the participation of free radicals in the formation of alkali labile carbonyl groups (20,39). It is likely that transition metal ions catalyze degradative reactions at least partially by promoting the formation of highly degradative free radical species from intermediate peroxides (3,29,39). Hydrogen peroxide and hydroperoxides are notably sensitive to metal ion-induced free radical decomposition (30,31).

The most detrimental metal salts in oxidative alkaline systems (those of cobalt, copper, and iron) each have two principal oxidation states differing by one unit, and it is likely that these metals produce radical species via one electron oxidation-reduction reactions (30,31,45). In an oxidative alkaline solution, possible oxidation-reduction reactions leading to free radical production are shown below (34).



Reactions 2 and 3 involve participation of peroxides, while reactions 1 and 4 are dependent upon oxygen and hydroxyl ion. Hydroperoxides may participate in reactions comparable to reactions 2 and 3. Whether it is possible for ionized carbohydrate hydroxyl groups to undergo a reaction comparable to reaction 4 in alkaline solution is unknown. The radical species formed due to transition metal ion reactions such as those shown above may enhance the rate of carbohydrate degradation by increasing the likelihood of free radical degradation pathways.

#### AGING OF ALKALI CELLULOSE

In the production of rayon, the degradative alkaline-oxygen reactions promoted by transition metal ions are, for the most part, desired reactions. One of the steps in the manufacture of viscose rayon involves the aging, or autoxidation, of cellulose in contact with air at 30% consistency in ca. 17% NaOH at 20-40°C. During the aging process the degree of cellulose polymerization is decreased via ionic and radical oxidative reactions which are catalyzed by added trace metals, or by metals which are present as impurities in the pulp or the sodium hydroxide (43,44,46).

Entwistle, et al. (43) reported the relative catalytic ability of selected transition metal ions in viscose aging to be Co>Mn>Fe>Ni. As described in the next section, a similar trend has been noted in oxygen bleaching. MacDonald (44)



also investigated the action of the metals copper, manganese, iron, and cobalt on the alkaline aging of cellulose and found cobalt to be the most degradative metal. Further, MacDonald (44) found hydrogen peroxide to be produced during aging [as it is during oxygen alkali reactions (3,14)], and he proposed that metal ions interacted with hydrogen peroxide and cellulose to produce chain-initiating free radical species. Thus, although the conditions for aging differ from those for oxygen bleaching, it seems likely that similar metal-catalyzed reactions take place in both systems (5,47,48).

#### DECREASED CATALYSIS AT HIGH METAL ION CONCENTRATION

An interesting but poorly understood phenomenon in the transition metal ion-catalyzed degradation of carbohydrates is the loss in catalytic ability exhibited by particular transition metal ions as their concentration in an oxidative alkaline system is raised above a critical level. This effect has been observed for salts of iron (5), cobalt (35,39,42), and manganese (5,38,43), but has not been reported for copper (9,35,40,49).

In their work with alkali cellulose, Entwistle *et al.* (43) found manganese ions to accelerate the aging process in concentrations of 30 ppm on pulp, while inhibiting degradation when added in amounts over 100 ppm.

Manouchehri and Samuelson (38) found that a small addition of  $\text{MnCl}_2$  (0.1 mM) during oxygen-sodium bicarbonate treatment of cellobiose promoted oxidative reactions, while a larger addition (15 mM) led to a retardation of oxidative reactions. They ascribed the protective effect of a high manganese concentration to the precipitation of hydrous manganese oxide, though they did not suggest how the precipitate might inhibit degradation. Manouchehri and Samuelson (38) also noted that the inhibitory ability of the precipitate decreased on aging of the precipitate.

In an oxygen-alkali system Gilbert et al. (5) found the transition metal ions cobalt(II), iron(III), and copper(II), in order of decreasing effect, to catalyze cellulose depolymerization in a manner analogous to that occurring in alkali cellulose. They also found nickel(II) to be inert and determined that manganese(II) acts as a degradative catalyst below 10 ppm on pulp and as a protective agent above 60 ppm on pulp. In addition, they found that with an increasing iron(III) concentration in the range of 1000-6000 ppm on pulp, the pulp viscosity increased dramatically. At the higher levels of manganese(II) and iron(III) addition Gilbert et al. (5) noticed the formation of precipitates and concluded that precipitated hydrous ferric and manganese oxides acted as inhibitors.

Samuelson and Stolpe (35), in experiments on the rate of cellobiitol attack by oxygen in an alkaline medium, found that in the presence of cobalt(II) the highest rate of reaction, as evidenced by oxygen consumption, was obtained with an intermediate level of cobalt(II) addition. Of the three concentrations of cobalt(II) employed (0.01, 0.05, and 0.25 mM), the reaction at the 0.05 mM level resulted in the greatest catalytic effect. Samuelson and Stolpe (35) postulated that cobalt(III) hydroxide precipitated under oxidative conditions and acted as an inhibitor of carbohydrate degradation.

Sjostrom and Valttila (39) have reported that cobalt(II) is much stronger than copper(II) or manganese(II) in causing cellulose degradation in oxygen bleaching of kraft pulp. They also found that 100 mg of cobalt(II) per kg of pulp caused less degradation than addition of 10 mg/kg.

Studies by Ericsson (42) of metal ion-catalyzed cellulose degradation in oxygen-alkali and in hydrogen peroxide-alkali indicated an order of metal ion catalytic strength comparable to the relative orders reported by Entwistle et al.

(43), Gilbert et al. (5), and Sjostrom et al. (39). For both oxygen and hydrogen peroxide oxidations, the extent of metal-effected viscosity loss followed the order  $\text{Co(II)} > \text{Cu(II)} \approx \text{Fe(III)} > \text{Mn(II)} > \text{Ni(II)}$ . Ericsson (42) also found that in the oxygen bleaching of a pine kraft pulp the greatest catalytic effect was found at an intermediate cobalt ion concentration.

Copper salts have not been reported to display a reduction in catalytic effect with increasing copper concentration. Oxygen-alkali experiments with cellobiose (40), cellulose (9), cellobiitol (35), and wood meal (49) over a range of copper ion concentrations all show copper salts to be highly degradative. Nickel salts, on the other hand, are generally considered to be inert or only mildly degradative in oxygen-alkali systems (5,34,43,44).

#### METAL-INDUCED MECHANISM SHIFT

There is some evidence from model compound studies that the mechanism of carbohydrate degradation may be significantly altered in the presence of transition metal ions. In working with an alkaline hydrogen peroxide system and the cellulose model methyl  $\beta$ -D-glucopyranoside (MBG) Weaver (27) found that a trace concentration of added cobalt ( $10^{-4}$  mM) resulted in greatly enhanced formation of methanol relative to uncatalyzed systems. Formation of methanol, indicative of glycosidic bond cleavage, accounted for ca. 90-95% of MBG degradation in the presence of cobalt, and ca. 60% in the absence of cobalt. Unfortunately, Weaver (27) did not investigate the types or relative quantities of acids formed under the cobalt-catalyzed conditions. If such analyses had been conducted, methoxy-stable products (resulting from oxidation of the pyranoside structure without glycosidic bond cleavage) would presumably have been present in comparatively low concentration.

Another important finding by Weaver et al. (50) was that increasing the cobalt concentration in an alkaline hydrogen peroxide-MBG system from  $10^{-4}$  to  $10^{-3}$  mM reduced the proportion of methanol liberated due to oxidation almost to the level of uncatalyzed degradations. These results suggest that the mechanism of cobalt-induced MBG degradation under oxygen alkali conditions is dependent upon metal ion concentration.

Experiments on MBG degradation in an alkaline hydrogen peroxide system in the presence of chromium ion also suggest that metal ions alter degradation mechanisms. Weaver et al. (26) found that chromium ion enhanced glycosidic bond cleavage (75% vs. 60% in the absence of metal ion) and also increased pentonic acid formation, suggesting a metal ion-induced shift in degradation pathways. The mechanism for enhanced pentonic acid and methanol formation proposed by Weaver et al. (26) is shown in Fig. 4.

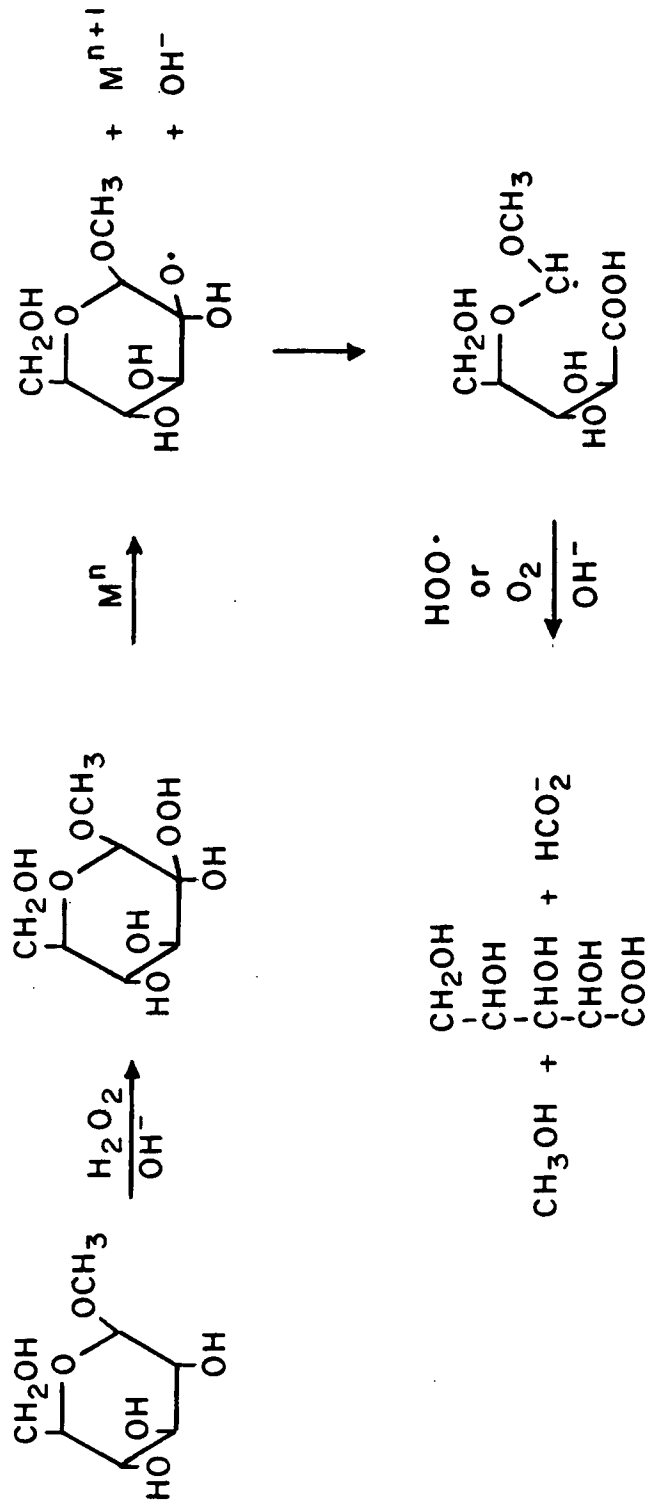


Figure 4. Methanol and Pentonic Acid Formation from MBG Degradation in Hydrogen Peroxide-Alkali According to Weaver et al. (26,27)

## THESIS OBJECTIVE

The objective of this study was to clarify the influence of catalytic transition metal ions on the rate and mechanism of carbohydrate degradation under conditions approximating those of oxygen bleaching. In particular, the relationship between metal ion concentration and carbohydrate degradation was of interest. The findings of Weaver and coworkers (26,27,50) in a hydrogen peroxide-alkali system suggested that trace concentrations of certain transition metal ions shifted the mechanism of carbohydrate degradation in favor of enhanced glycosidic bond cleavage. Other studies, primarily conducted in pulp systems, indicated that particular metal ions (cobalt, iron, manganese) could be less degradative when present in high concentration than in low concentration under oxidative alkaline conditions (5,35,38,39,42,43). Although numerous oxygen-alkali studies involving metal ion-catalyzed carbohydrate degradation has been conducted, no work relating the influence of metal ion concentration to both the rate and mechanism of carbohydrate degradation (as reflected in carbohydrate degradation products) had been reported. This study was conducted to clarify the influence of metal ion concentration (specifically cobalt ion) on the rate and mechanism of cellulose degradation, using methyl  $\beta$ -D-glucopyranoside (MBG) as a cellulose model compound.

## RESULTS AND DISCUSSION

### EXPERIMENTAL APPROACH

The cellulose model methyl  $\beta$ -D-glucopyranoside (MBG) was chosen to investigate the influence of transition metal concentration on the rate and mechanism of carbohydrate degradation under oxygen bleaching conditions. In addition to being readily available, MBG contains the glucose monomer of which cellulose is composed, and also possesses a glycosidic linkage which is of key importance in depolymerization reactions. Furthermore, MBG has frequently been used as a cellulose model in oxygen-alkali (3,15,18,19,26,29), allowing the results of this work to be compared with the findings of previous workers.

Cobalt, as  $\text{CoSO}_4 \cdot 7\text{H}_2\text{O}$ , was chosen as the transition metal ion since it exhibits a very pronounced catalytic ability in oxygen-alkali (5,9,34,35,39,40,42), yet displays a decrease in degradative activity as its concentration is increased in oxygen-alkali systems (35,39,42). Cobalt sulfate ( $\text{CoSO}_4 \cdot 7\text{H}_2\text{O}$ ) was the only cobalt salt used in this study.

Two sodium hydroxide solutions of different origin were used for MBG degradations. One solution was purified to minimize trace metal contaminants via an extractive procedure (51) and contained impurities introduced from contact with glassware during the purification procedure (extracted NaOH). Reactions conducted with extracted NaOH contained, on average, 500 ppm Si, 250 ppm B and 13 ppm Al as determined by atomic absorption and plasma emission techniques (Appendix I).

The second sodium hydroxide solution, produced via hydrolysis of ultrapure sodium, was purchased from Alpha Products, Ventron Corporation and was used as received (ultrapure NaOH). Both sodium hydroxide solutions contained very low

levels of transition metal ions (Appendix I). Under certain circumstances the dissolved silica in extracted NaOH was found to significantly alter cobalt-catalyzed MBG degradation. Since dissolved silica is a major constituent in natural waters (52), and since silicate ions are a common contaminant of sodium hydroxide solutions; the influence of soluble silicate ions on cobalt-catalyzed reactions was also pursued.

Reaction conditions for all MBG degradations, chosen to be comparable to previous work with cellulose model compounds under oxygen bleaching conditions (3,10,18,24,25,29), were: 1.25M NaOH, 120°C; and 0.68 MPa partial O<sub>2</sub> pressure\*. Reactions were conducted in a magnetically-stirred Teflon-lined reactor which could be sampled while hot and under pressure. Reaction solutions were prepared at room temperature and were heated to reaction temperature (120°C) prior to reaction initiation by oxygen pressurization. Reaction samples were periodically obtained and were analyzed for remaining starting material (MBG) and for selected MBG degradation products. Experimental procedures are described in the Experimental section and tabulated reaction results appear in Appendix II.

#### MBG DEGRADATION

The decrease in MBG concentration with reaction time was followed by quantitative gas-liquid chromatography (GLC). MBG was analyzed as its per-O-acetylated derivative and n-butyl- $\beta$ -D-glucopyranoside (BBG) was used as an internal standard. Appendix III describes the statistical approach used to determine significant differences between sets of MBG results.

---

\*Total reactor pressure at 120°C was 1.01 MPa (147 psia). This pressure accounted for 0.20 MPa (28.8 psia) water vapor and 0.13 MPa (19.4 psia) nitrogen.



NO ADDED COBALT

In the absence of added cobalt sulfate the rate of MBG degradation was the same in either extracted or ultrapure NaOH (Fig. 5, reactions IV and X), showing that the contaminants in extracted NaOH did not significantly alter the rate of MBG degradation.

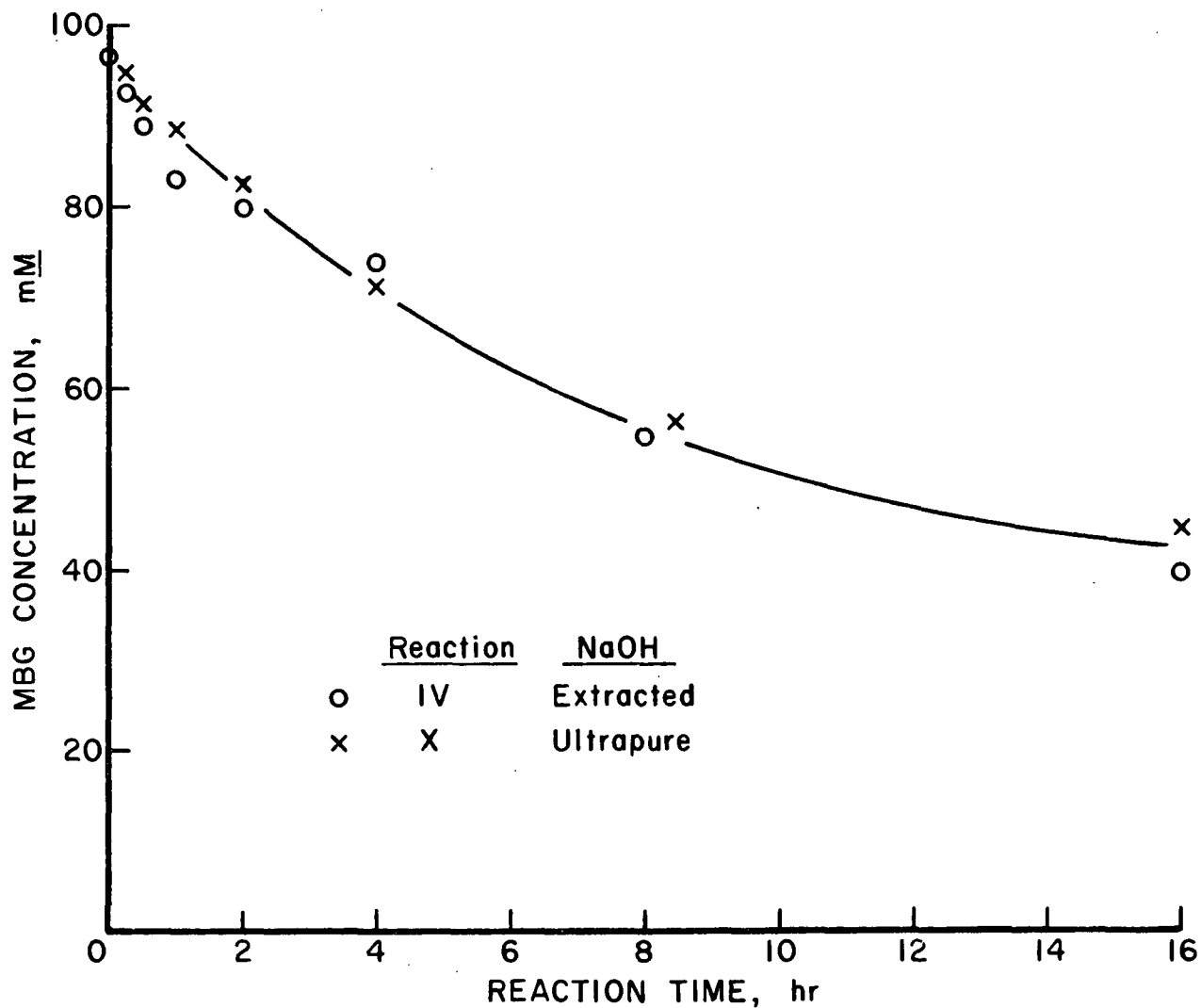


Figure 5. MBG Degradation in 1.25M NaOH at 120°C and 0.68 MPa Partial Oxygen Pressure

# COBALT ADDED AT THE 0.01 AND 0.05 mM LEVELS

The influence of  $\text{CoSO}_4 \cdot 7\text{H}_2\text{O}$  at the 0.01 and 0.05 mM levels on the rate of MBG degradation is shown in Fig. 6. In a reaction in extracted NaOH the rate of MBG degradation was accelerated by 0.01 mM added cobalt(II) (reaction V). The rate of MBG degradation was even greater at the 0.05 mM cobalt(II) level (Fig. 6, reactions XII, XIII, and XVII). The MBG degradation rate was essentially the same in either extracted or ultrapure NaOH at the 0.05 mM cobalt(II) addition level. MBG degradation rates reflected a 0.5 order pseudo rate dependence on dissolved cobalt ions.

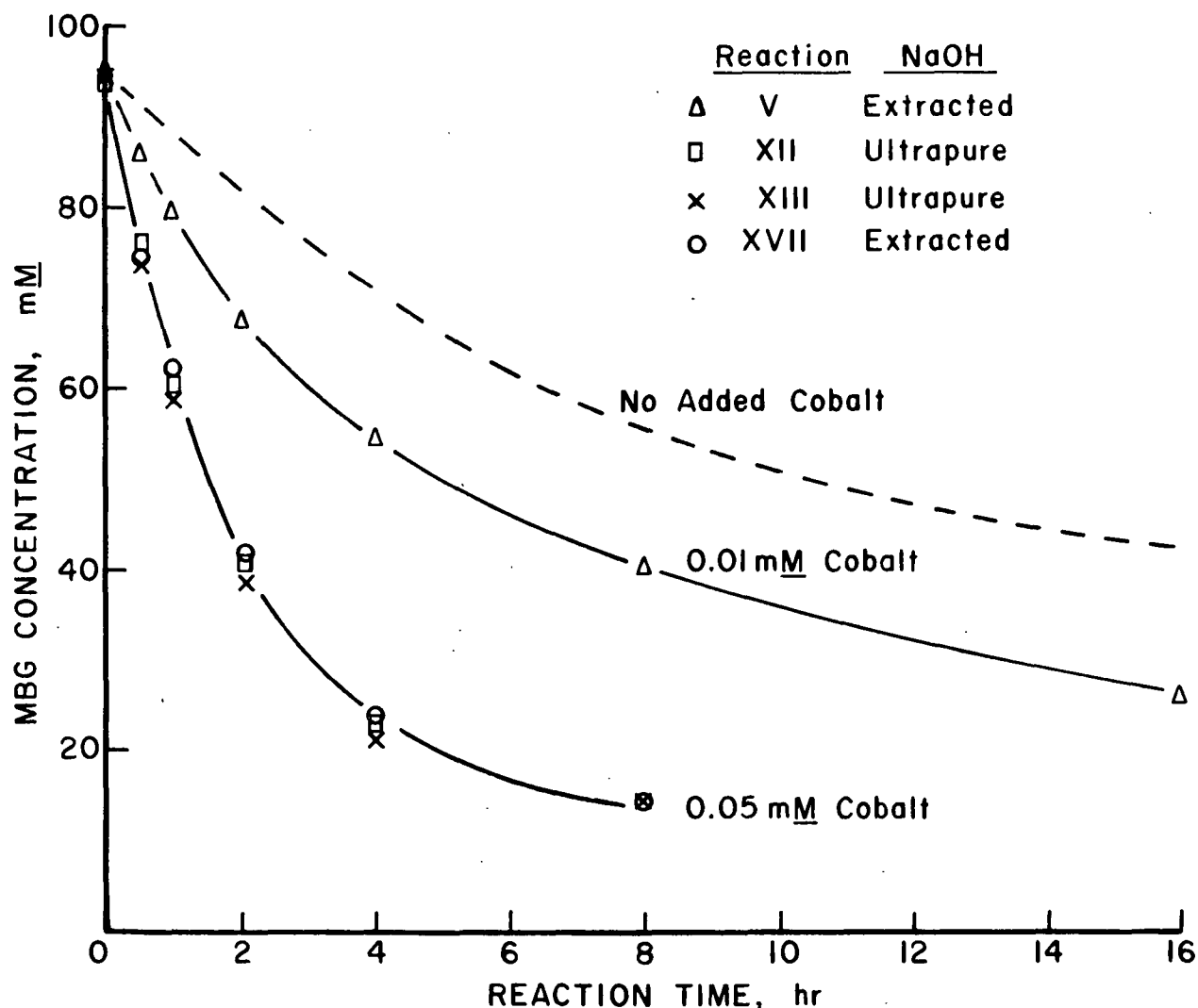


Figure 6. MBG Degradation in 1.25 mM NaOH Containing 0.01 and 0.05 mM Added  $\text{CoSO}_4 \cdot 7\text{H}_2\text{O}$ . Reactions Conducted at 120°C and 0.68 MPa Partial Oxygen Pressure

#### COBALT ADDED AT THE 0.25 mM LEVEL

At the 0.25 mM added cobalt(II) level both the NaOH employed (ultrapure vs. extracted) and the reaction solution preparation procedure had a major influence on both the initial solubility of cobalt(II) in reaction solutions and on the subsequent rate of MBG degradation. Except for a reaction in which the order of addition of reagents was reversed, MBG reaction solutions were prepared by addition of an aqueous cobalt(II) solution to a solution of NaOH. Solid MBG was then added to the alkaline cobalt salt mixture. In reactions at the 0.25 mM added cobalt(II) level prepared with ultrapure NaOH, precipitation of cobalt(II) from solution began before MBG could be added and mixed into alkaline solution. In the two other reactions containing 0.25 mM added cobalt(II) (reaction in ultrapure NaOH with a reversed reaction solution preparation sequence and reaction in extracted NaOH) no cobalt ions precipitated from solution prior to reaction initiation by oxygen pressurization. During these MBG degradations, which were initially homogeneous at the 0.25 mM addition level, precipitation of cobalt(III) from solution occurred over the course of reaction.

Results from reactions in which cobalt(II) precipitated from solution prior to reaction initiation (Fig. 7, reactions IX and XI) show that the degradation rate of MBG in these reactions was initially only slightly greater than in the absence of added cobalt(II). By reversing the reaction solution preparation procedure such that MBG was dissolved in ultrapure NaOH prior to addition of aqueous cobalt(II), no precipitation of cobalt(II) occurred during reaction solution preparation. As discussed in the section Influence of Polyols, MBG stabilized cobalt(II) in alkaline solution. MBG degradation results for a reaction solution prepared in this manner (Fig. 7, reaction XVIII) show an initial rate of MBG degradation which is even faster

than that found at the 0.05 mM added cobalt(II) level. However, the rate of MBG degradation declined rapidly after ca. 1 hour. After 4 hours of reaction, the remaining MBG concentration was actually greater than in reactions at the 0.05 mM added cobalt(II) level (Fig. 7, reaction XVIII). Coincident with the rapid decline in the rate of MBG degradation at the 0.25 mM added cobalt(II) level (reaction XVIII) was the precipitation of cobalt(III) from solution. Precipitation of cobalt(III) from reaction solution also coincided with a decrease in the intensity of the yellow color of subsequent reaction solution samples\*.

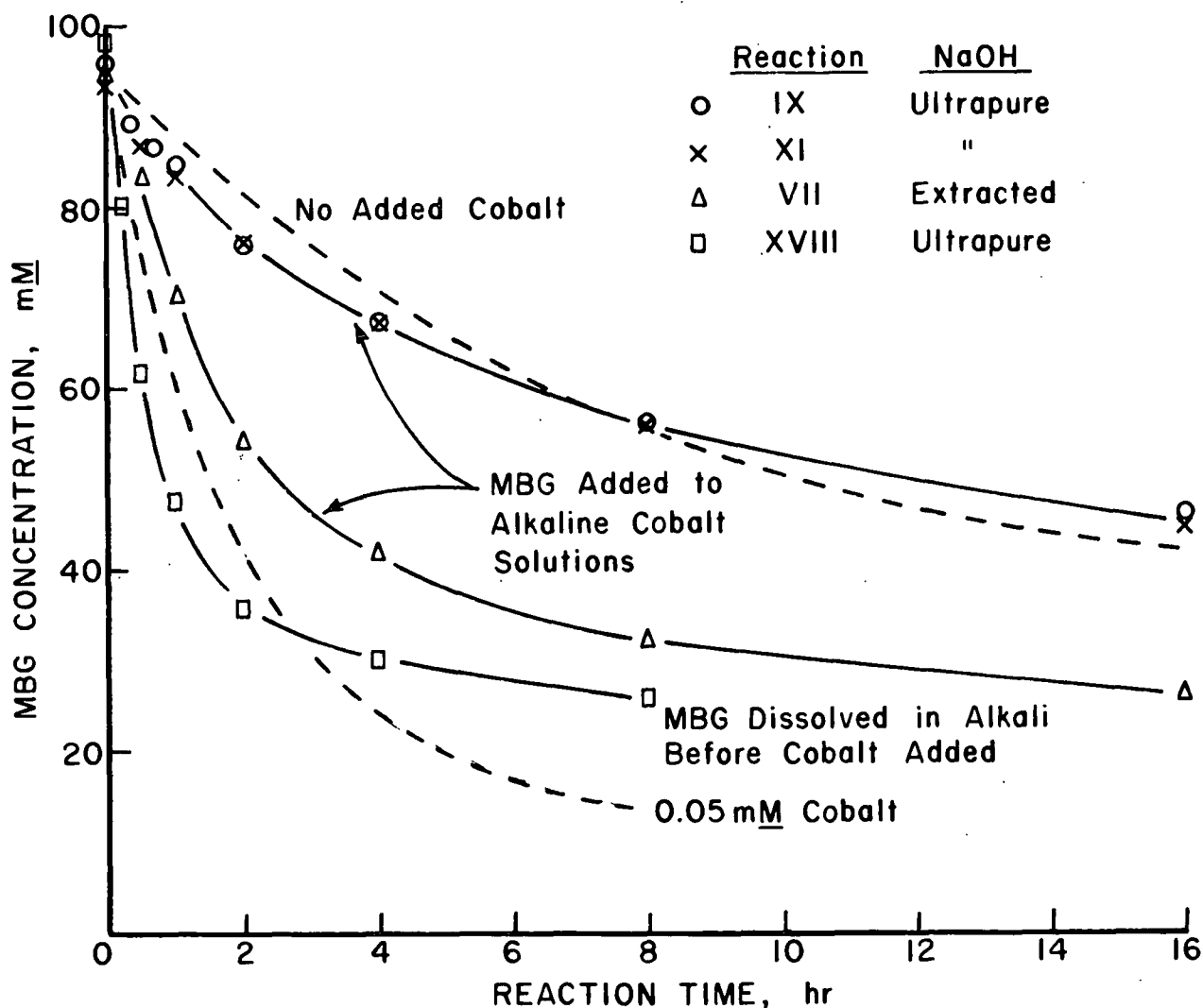


Figure 7. MBG Degradation in 1.25M NaOH Containing 0.25 mM Added  $\text{CoSO}_4 \cdot 7\text{H}_2\text{O}$ . Reactions Conducted at 120°C and 0.68 MPa Partial Oxygen Pressure

\*Yellow color developed in all cobalt(II)-containing degradations following reaction initiation. Precipitation and color formation are described in the section on Transition Metal Ion Precipitation and Adsorption.

The use of extracted NaOH in preparation for a degradation of MBG at the 0.25 mM cobalt(II) level also resulted in the stabilization of cobalt(II) in alkaline solution. As discussed in the section Inhibition of Alkaline Cobalt Precipitation, silicate anions in extracted NaOH stabilized cobalt(II) in alkaline solution through coordination. Both reaction XVIII (with the reversed order of reagent addition) and reaction VII (conducted in extracted NaOH) were initially homogeneous. Only after reaction initiation by oxygen pressurization did precipitation of cobalt(III) from these reactions occur. In extracted NaOH (reaction VII), however, the quantity of precipitate formed after 1 hour of reaction appeared to be slightly greater than in ultrapure NaOH (reaction XVIII) after the same period of reaction.

Thus, in extracted NaOH (reaction VII) and in ultrapure NaOH in which aqueous cobalt(II) was added to an alkaline MBG solution (reaction XVIII), MBG degradation was greatly enhanced relative to degradations in ultrapure NaOH in which MBG was added to alkaline cobalt(II) solutions (reactions IX and XI). Both the impurities in extracted NaOH, and the presence of MBG in alkaline solution prior to mixing with aqueous cobalt(II), stabilized cobalt(II) in alkaline solution and inhibited the initial precipitation of cobalt (II). The stabilization of cobalt(II) in alkali enhanced the initial rate of MBG degradation.

Cobalt(II) which precipitated from solution during reaction solution preparation did not redissolve to any detectable degree upon heating of reaction solutions prior to reaction initiation. After cobalt(II) precipitated from solution, the rate of MBG degradation following oxygen pressurization was initially only slightly faster than in the absence of added cobalt(II) (Fig. 7, reactions IX and XI). As will be discussed in the section on Transition Metal Ion Precipitation and Adsorption, precipitation of cobalt(II) from alkaline

solution resulted in the formation of a highly adsorbent cobalt(II) solid which removed otherwise soluble cobalt ions from solution. Other than being adsorbent, the precipitated cobalt(II) was relatively inert, and the low concentration of soluble cobalt ions in the presence of precipitated cobalt(II) resulted in a relatively slow rate of MBG degradation (Fig. 7, reactions IX and XI).

Cobalt(III) which precipitated from solution during MBG degradation was also highly adsorptive of soluble cobalt ions, as discussed in the section on Transition Metal Ion Precipitation and Adsorption. Adsorption of soluble cobalt ions by precipitated cobalt(III) resulted in a decreased rate of MBG degradation. The effects of adsorptive precipitate formation are most clearly shown in reaction XVIII of Fig. 7. Precipitate formation in this reaction became evident after 1 hour of reaction and it was at that point that the rate of MBG degradation began to decline rapidly.

To test the adsorptive ability of precipitated cobalt(III), the precipitate from a 0.25 mM reaction was isolated and added to a reaction prepared to be 0.05 mM in soluble cobalt(II). Results for this reaction (Fig. 8, reaction VIII) show that precipitated cobalt slightly inhibited the rate of MBG degradation at the 0.05 mM cobalt addition level. It is likely that the adsorptive ability of the precipitate was weakened by aging during precipitate isolation and reaction solution preparation. Aging of transition metal ion precipitates is discussed further in the section on Adsorption by Precipitated Metal Oxides and Hydroxides.

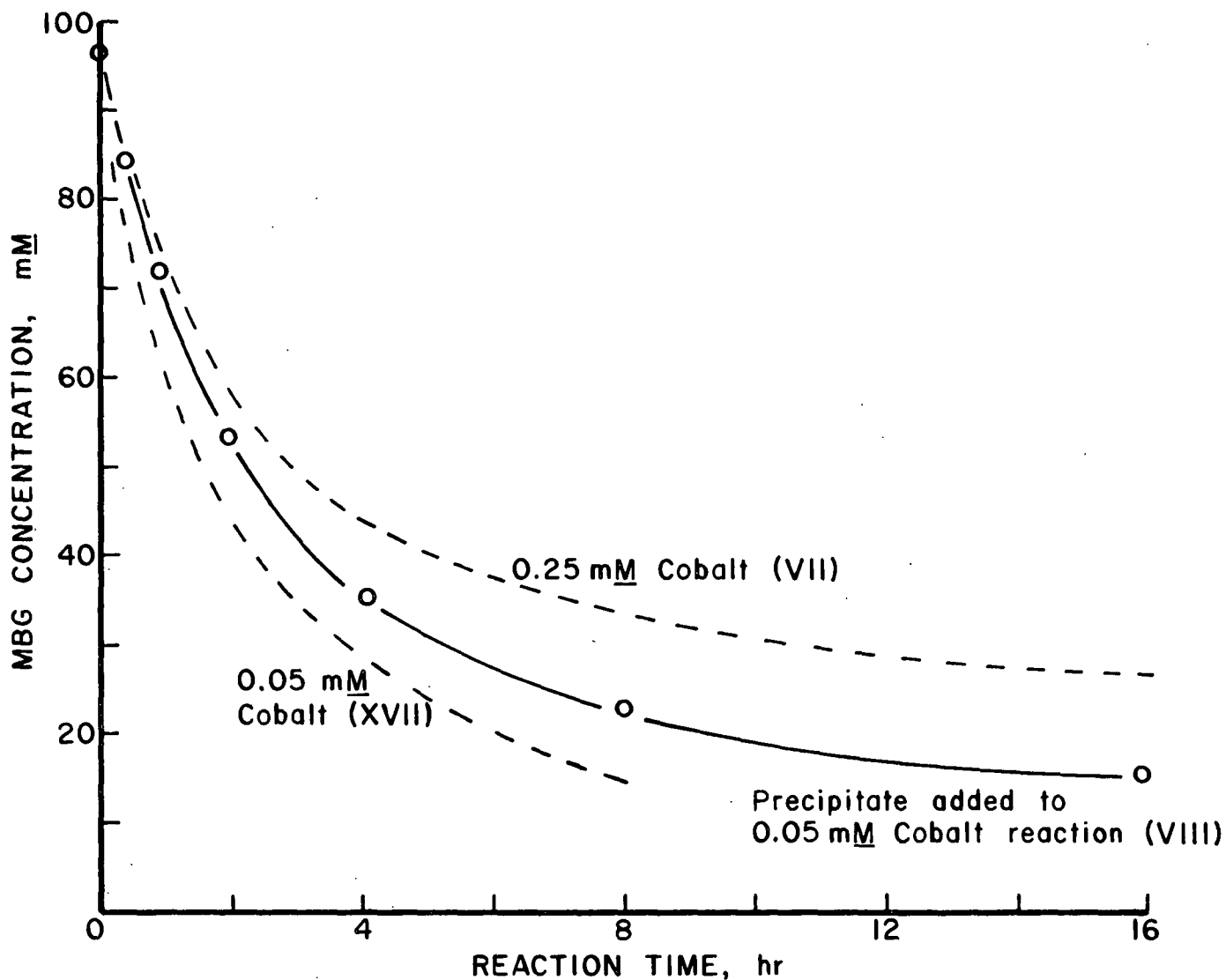


Figure 8. Influence of Precipitated Cobalt from a 0.25 mM Reaction on MBG Degradation in Extracted NaOH Containing 0.05 mM  $\text{CoSO}_4 \cdot 7\text{H}_2\text{O}$  (Reaction VIII)

#### THE CHEMISTRY OF COBALT IN ALKALINE SOLUTIONS

The influence of cobalt ions on the degradation rate of MBG in oxygen-alkali can be explained in terms of the solubility and precipitation characteristics of cobalt(II), and in terms of alkaline oxidation-reduction properties of cobalt. To provide the proper background for interpretation of glucoside results, the appropriate physical and chemical properties of alkaline cobalt solutions are here briefly reviewed.

When alkali is added to an aqueous solution of a cobalt(II) salt (or vice versa) in the absence of oxygen, hydrolysis reactions occur which lead to the precipitation of cobalt(II) hydroxide  $[\text{Co}(\text{OH})_2]$  (Table I) (53-57). Although cobalt(II) hydroxide is relatively insoluble in water  $K_{\text{sp}} = 10^{-15}$  (58), it is slightly amphoteric and dissolves in more concentrated alkali to give deep blue solutions containing  $\text{Co}(\text{OH})_3(\text{H}_2\text{O})^-$  and  $\text{Co}(\text{OH})_4^{2-}$  ions (58,59). The reactions defining alkaline cobalt(II) hydrolysis equilibria are given in Table I. The distribution of hydrolysis products with pH for a  $10^{-5}\text{M}$  cobalt(II) solution, as calculated from the hydrolysis data of Table I, is shown in Fig. 9 (58). The amphoteric nature of cobalt(II) in alkaline solution is illustrated in Fig. 10, which shows the increase in cobalt(II) hydroxide solubility with increasing alkalinity. From tabulated results reported by Gayer and Garrett (60), the solubility of cobalt(II) hydroxide in  $1.25\text{M}$  NaOH at  $25^\circ\text{C}$  may be estimated as ca.  $3 \times 10^{-5}\text{M}$ . Their work also indicates that the solubility of cobalt(II) hydroxide in alkali increases with temperature.

TABLE I

SUMMARY OF Co(II) HYDROLYSIS AT  $25^\circ\text{C}$  (56,57)

Equilibria	Log K (Formation Constant)	
$\text{Co}^{2+} + \text{H}_2\text{O} \rightleftharpoons \text{Co}(\text{OH})^+ + \text{H}^+$	-9.6	(5)
$\text{Co}(\text{OH})^+ + \text{H}_2\text{O} \rightleftharpoons \text{Co}(\text{OH})_2(\text{aq}) + \text{H}^+$	-9.2	(6)
$\text{Co}(\text{OH})_2(\text{s}) + \text{H}_2\text{O} \rightleftharpoons \text{Co}(\text{OH})_3^- + \text{H}^+$	-12.7	(7)
$\text{Co}(\text{OH})_3^- + \text{H}_2\text{O} \rightleftharpoons \text{Co}(\text{OH})_4^{2-} + \text{H}^+$	-14.8	(8)
$\text{Co}(\text{OH})_2(\text{s}) \rightleftharpoons \text{Co}(\text{OH})_2(\text{aq})$	-5.7	(9)
$\text{Co}(\text{OH})_2(\text{s}) \rightleftharpoons \text{Co}^{2+} + 2\text{OH}^-$	-14.9	(10)



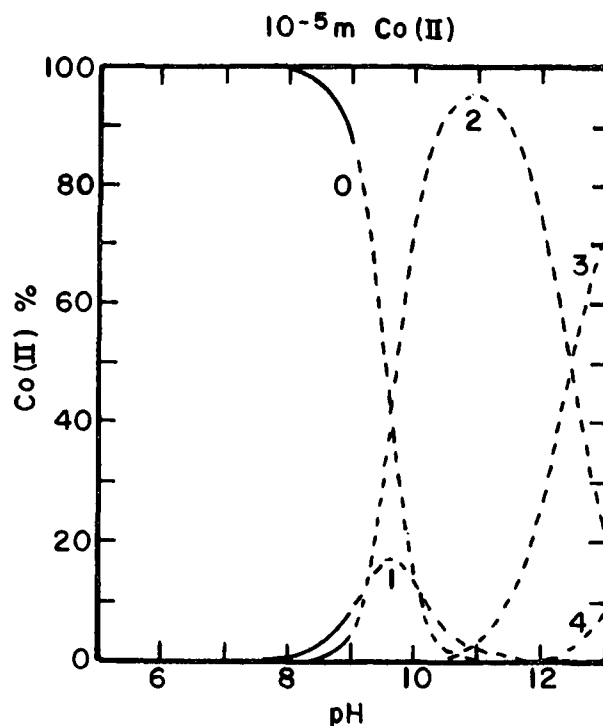


Figure 9. Distribution of Hydrolysis Products for  $10^{-5}\text{M}$  Co(II) at Ionic Strength =  $1\text{M}$  and  $25^\circ\text{C}$ . Dashed Curves Denote Regions of Supersaturation with Respect to  $\text{Co}(\text{OH})_2$  (58). Numbers Indicate the Number of Hydroxyl Groups Coordinated with Each Cobalt Cation

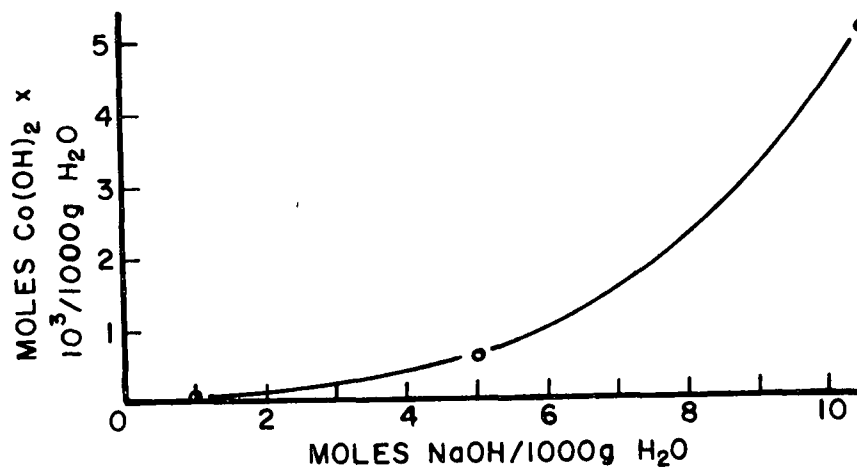
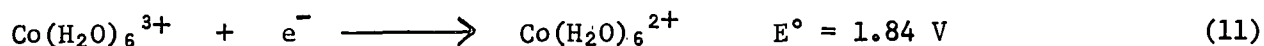


Figure 10. Solubility of  $\text{Co}(\text{OH})_2$  in Sodium Hydroxide Solutions at  $25^\circ\text{C}$  (61)

In aqueous solutions containing no complexing agents the oxidation of Co(II) to Co(III) is very unfavorable;



and water rapidly reduces uncomplexed Co(III) at room temperature to liberate oxygen (53). In strongly acid or alkaline solutions in the presence of complexing agents the stability of trivalent cobalt is greatly improved. Co(III) shows a particular affinity for nitrogen donors, and Co(II)-amine complexes are readily oxidized by oxygen to Co(III) complexes (53). Reducing sugars and polyols are also known to form stable complexes with Co(II) under mildly alkaline conditions (56,61,62). Further, oxidation of strongly alkaline cobalt(II) solutions containing glycerol has been found to produce a stable cobalt(III)-glycerol complex (57). In aqueous acidic solution cobalt(III) complexes commonly oxidize organic compounds (53).

In the presence of alkali, suspensions of  $\text{Co}(\text{OH})_2$  are oxidized by air to solid  $\text{CoO}(\text{OH})^*$ , and the oxidation may be brought about more rapidly by an oxidizing agent such as hydrogen peroxide (54). Although no precise information could be found in the literature on the solubility of  $\text{CoO}(\text{OH})$  in alkaline solution, the solubility of  $\text{CoO}(\text{OH})$  is reported to be negligible in comparison to  $\text{Co}(\text{OH})_2$  (63).

---

\* The oxidation of aqueous suspensions of cobaltous hydroxide or the destruction of a cobalt(III) complex with alkali gives a brown or black precipitate,  $\text{Co}_2\text{O}_3 \cdot \text{aq}$ . Upon heating,  $\text{Co}_2\text{O}_3 \cdot \text{aq}$  yields the monohydrate  $\text{Co}_2\text{O}_3 \cdot \text{H}_2\text{O}$  which is usually formulated as  $\text{CoO}(\text{OH})$  (54).

## TRANSITION METAL ION PRECIPITATION AND ADSORPTION

### PRECIPITATE FORMATION AND MBG DEGRADATION

Before and during reactions containing 0.01 and 0.05 mM added cobalt(II), no visible evidence of precipitate formation was observed. However, reaction samples obtained at the end of 0.05 mM cobalt-containing reactions and stored at room temperature for extended periods of time (over 4 months) gradually formed a fine black precipitate. Samples obtained during MBG degradation in extracted NaOH containing 0.01 mM cobalt(II) did not form a precipitate even after more than one year of storage.

Precipitate formation was most evident for reactions at the highest level of cobalt(II) addition (0.25 mM) when reaction solutions were prepared by addition of solid MBG to an alkaline (ultrapure NaOH) cobalt(II)-containing solution (reactions IX and XI). During preparation of 0.25 mM cobalt(II)-ultrapure NaOH solutions, cobalt(II) began flocculating immediately upon addition of aqueous cobalt salt to ultrapure NaOH, and before MBG was added. At the same cobalt(II) level (0.25 mM), cobalt(II) was stabilized in ultrapure NaOH by MBG (giving a deep blue solution) if MBG was already present in the stock NaOH when aqueous cobalt(II) was added (reaction XVIII). Formation of a fine black precipitate in reaction solution samples became evident only after ca. 1 hour of reaction.

Soluble silicate anions present in extracted NaOH also stabilized alkaline cobalt(II) in solution. During preparation for reaction of MBG in extracted NaOH containing 0.25 mM added cobalt(II) (reaction VII) the reaction solution was initially a deep blue (no precipitate was evident). Upon oxygen pressurization, reaction samples became increasingly yellow in color until a black

precipitate began to form. Following the onset of precipitate formation, the yellow color of reaction solution samples decreased. Color development and precipitate formation was very similar to that observed in ultrapure NaOH in which 0.25 mM cobalt(II) was initially soluble (reaction XVIII). However, the quantity of precipitate formed after 1 hour of reaction in extracted NaOH appeared to be greater than in ultrapure NaOH.

The precipitate formed during initially homogeneous degradations at the 0.25 mM cobalt(II) level (reactions VII and XVIII) was not immediately obvious as early reaction samples were taken. The black precipitate was very fine and had to settle from solution before being easily visible. No precipitate was evident in samples obtained at 15 and 30 minutes reaction times even after settling of samples. The amount of precipitate formed increased with increasing reaction time, and precipitate formation coincided with a decrease in the intensity of the yellow color of cobalt-containing reaction solutions (see Color Formation). It was not possible to determine the precise amount of precipitate formed at particular reaction times. The limited sample volumes withdrawn from the reactor for each sample (< 10 mL) and the low level of cobalt addition (maximum of 0.25 mM  $\text{CoSO}_4 \cdot 7\text{H}_2\text{O}$ ) precluded gravimetric analysis. However, various reaction solution samples obtained after reactions were terminated were analyzed for soluble cobalt, and the results are discussed in the section Adsorption by Precipitated Cobalt.

#### PRECIPITATE COMPOSITION

A sample of precipitate from a reaction in extracted NaOH containing 0.25 mM added cobalt(II) (obtained after 32 hours reaction from reaction VII) was analyzed for elemental composition by energy dispersive x-ray analysis (EDAX). This technique is qualitatively sensitive to all elements of atomic

weight greater than sodium. No trace of any element other than cobalt was detected. The precipitate was inspected with a scanning electron microscope, and no evidence of crystallinity could be discerned up to 3000X magnification. An x-ray diffraction analysis of the precipitate gave no discernible pattern, further suggesting that the precipitate was amorphous rather than crystalline. The amorphous nature of the precipitate precluded structural identification of precipitate composition by x-ray techniques.

#### COLOR FORMATION

In the absence of added cobalt(II), reaction solutions remained clear and entirely colorless over the course of reaction. During all reactions conducted with cobalt, however, a yellow discoloration of reaction solutions was noticed after reaction initiation. The discoloration was relatively faint in reactions where cobalt(II) precipitated from solution prior to reaction initiation (reactions IX and XI). All cobalt-containing reactions, except for those in which cobalt(II) precipitated immediately upon reaction solution preparation (reactions IX and XI), were initially blue and did not show evidence of precipitate of yellow color formation until solutions were pressurized with oxygen. Reaction solutions in which cobalt(II) precipitated during reaction solution preparation (reactions IX and XI) were colorless (except for a brown-black precipitate) just prior to reaction initiation.

In cobalt-containing reactions in which precipitation from solution during reaction did not occur (reactions V, VI, XII, XIII, and XVII), the yellow color of cobalt-containing reaction solutions intensified with increasing reaction time. In reactions in which precipitation from solution occurred after reaction initiation (reactions VII and XVIII) the yellow color of reaction solutions was most intense just prior to the apparent onset of

cobalt precipitation. Once precipitation had begun, the yellow color of reaction solutions became more faint.

The yellow color of cobalt-containing reaction solutions also faded upon storage of samples, and precipitate formation during sample storage coincided with fading. Precipitation of cobalt from reaction solution samples during sample storage was noted in the section on Precipitate Formation and MBG Degradation.

Visible spectra of the yellow solutions produced during cobalt-containing MBG degradations showed only a broad band of poor diagnostic value. The band began at 450 nm and extended, with gradually increasing intensity, into the ultraviolet region.

McCloskey (28) has reported discoloration of reaction solutions in oxygen-alkali MBG degradation in unlined stainless steel reactors.

#### ADSORPTION BY PRECIPITATED COBALT

MBG degradation results (Fig. 5-8) indicate that the greatest extent of MBG degradation occurred in reactions in which the greatest concentration of soluble cobalt was present in solution. The rate of MBG degradation increased with increasing cobalt concentration, 0.05 mM cobalt(II) being much more degradative than 0.01 mM cobalt(II) (Fig. 6). At the 0.25 mM cobalt(II) level, however, the solubility (and consequently the rate of MBG degradation) was dependent upon both the reaction solution preparation sequence and the sodium hydroxide used (Fig. 7). The precipitation of cobalt ions from solution either before or during MBG degradation at the 0.25 mM added cobalt(II) level was found to result in the removal of otherwise

soluble cobalt ions from solution. Adsorption of soluble cobalt ions resulted in markedly decreased rates of MBG degradation.

#### Adsorption in the Absence of Oxygen

At the 0.25 mM cobalt(II) level in ultrapure NaOH the rate of MBG degradation depended upon the sequence of reaction solution preparation (Fig. 7). Attempts to prepare an ultrapure NaOH-0.25 mM cobalt(II) solution which did not initially contain MBG solubilized in the alkali (reactions IX and XI) resulted in the precipitation of cobalt(II) from solution during reaction solution preparation. The rate of MBG degradation in solutions prepared in this manner was initially only slightly greater than in the absence of added transition metal (Fig. 7, reactions IX and XI).

The ability of precipitated cobalt(II) to remove soluble cobalt ions from solution was investigated by atomic absorption techniques. Cobalt(II) which precipitated (in the absence of oxygen) from an alkaline solution initially supersaturated with cobalt ions adsorbed otherwise soluble cobalt ions from solution (Table II). The presence of precipitated cobalt dropped the concentration of soluble cobalt(II) in alkaline solution well below the cobalt(II) solubility in the absence of precipitate.

TABLE II

COBALT(II) SOLUBILITY IN 1.25M ULTRAPURE NaOH AT  
18°C, 24 HOURS AFTER SOLUTION PREPARATION<sup>a</sup>

Alkaline Cobalt(II) Concentration When Solution Prepared, x 10 <sup>5</sup> moles/L	Cobalt(II) Concentration of Filtrate After 24 Hours, x 10 <sup>5</sup> moles/L
5.0	5.0
25.0	2.2
83.0	1.4

<sup>a</sup>Samples were prepared and stored under nitrogen.

### Adsorption During MBG Degradation

If, during reaction solution preparation, MBG was already present in ultra-pure NaOH when aqueous cobalt(II) was added to the alkali, or if extracted NaOH was employed, then cobalt remained in solution until well after reaction initiation. However, cobalt ions did begin to precipitate after ca. 1 hour from reaction solutions which were initially 0.25 mM in soluble cobalt(II) (reactions VII and XVIII). Precipitate formation coincided with a marked decrease in the rate of MBG degradation.

The cobalt concentrations of reaction solution samples obtained at the end of MBG degradations indicate that cobalt(III) which precipitated under oxidative conditions could be highly adsorptive of soluble cobalt ions (Table III). The lowest level of soluble cobalt remaining in solution was found in reaction solution samples which initially had been prepared to have the highest level of cobalt(II) concentration (0.25 mM) (Table III, reactions VII and XI). Also very low in soluble cobalt concentration were reaction solution samples obtained from reactions initially intermediate in cobalt(II) concentration (0.05 mM), but from which cobalt ions precipitated on sample storage (Table III, reactions VI and XIII). Cobalt did not precipitate from samples obtained at the end of a reaction conducted at the 0.01 mM added cobalt(II) level (reaction V). The final soluble cobalt concentration was actually higher for the reaction at the 0.01 mM added cobalt(II) level (reaction V) than for reactions at the 0.25 mM added cobalt(II) level (reactions VII and XI). Reaction solution samples obtained from one reaction at the 0.05 mM added cobalt(II) level (reaction XVII) were analyzed for cobalt content before precipitation was evident. The soluble cobalt concentration for this reaction thus corresponded more closely to the concentration of cobalt initially present in reaction solution.



TABLE III  
COBALT REMAINING IN SOLUTION AT THE END OF  
COBALT-CONTAINING MBG DEGRADATIONS

Reaction	Initial Co Concentration, $\times 10^5$ moles/L	NaOH	Soluble Co, $\times 10^5$ moles/L	
			Atomic Absorption	Plasma Emission
V <sup>a</sup>	1.0	Extracted	1.0	0.70
VI <sup>b</sup>	5.0	Extracted	0.7	0.39
XVII <sup>c</sup>	5.0	Extracted	3.9	3.9
XIII <sup>b</sup>	5.0	Ultrapure	0.3	0.19
VII <sup>d</sup>	25.0	Extracted	---	<0.08
XI <sup>e</sup>	25.0	Ultrapure	0.1	<0.08

<sup>a</sup>No precipitate evident even after prolonged storage.

<sup>b</sup>Precipitate formed only after reaction termination and sample storage.

<sup>c</sup>Analyzed within 2 weeks of reaction termination and before fading of yellow reaction solution color or evidence of precipitate formation.

<sup>d</sup>All other samples were analyzed after a minimum of two months storage.

<sup>e</sup>Precipitate formed during MBG degradation.

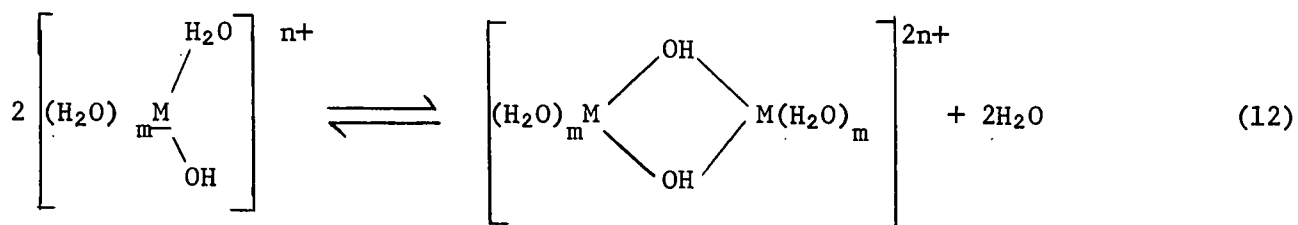
<sup>e</sup>Precipitate formed before reaction initiation.

#### ADSORPTION BY PRECIPITATED TRANSITION METAL OXIDES AND HYDROXIDES

Under the proper conditions both transition metal oxides and hydroxides can adsorb (through chemisorption) metal ions at particle-water interfaces (64,65). Precipitated oxides and hydroxides exhibit similar adsorption properties since oxides are known to hydrate at the surface and convert to surface hydroxides (64).

Adsorptive hydroxides of transition metals may be formed through hydrolysis reactions which involve the sequential loss of  $H^+$  ions from hydrated metal ions. Hydrolysis reactions can convert cationic species to uncharged and ultimately anionic hydroxo metal complexes, as shown for cobalt(II) in Table

I. However, dimeric and higher polymeric hydrolyzed species have also been reported for most metal ions (64). The polymerization process is thought to involve condensation reactions which produce hydroxo bridging groups, as shown in reaction 12 (64,66).

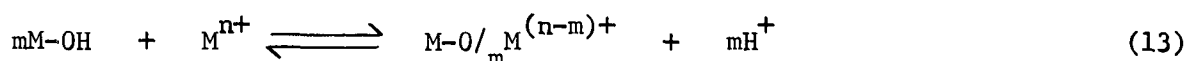


Species such as the dimer in reaction 12 can undergo additional condensation reactions resulting in the formation of multinuclear condensation products (64,66). Under conditions of oversaturation with respect to metal hydroxide, colloidal hydroxo polymers can form, ultimately resulting in the formation of adsorptive precipitates (64). The sequence of hydrolytic and condensation reactions leading to hydroxo-bridged species is called olation, and increasing temperature, alkalinity, and metal ion concentration all promote the process of olation (66). Cobalt is not thought to form polymeric species except under conditions of precipitation, which favor adsorptive precipitate formation (58,64,67).

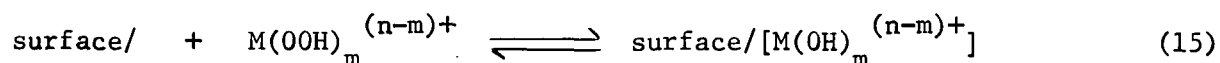
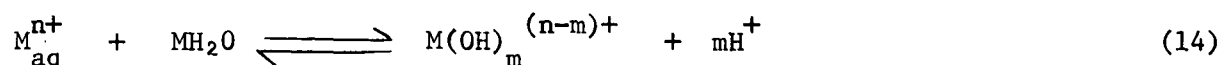
Transition metal oxides and oxy hydroxides have been noted to adsorb soluble metal species from solution in a number of systems. Morgan and Stumm (68) investigated the kinetics of removal of manganese(II) ion from aqueous solution due to oxygen oxidation and observed that the extent of removal could not be accounted for by the stoichiometry of the oxidation reaction alone. Their results indicated that Mn(II) was adsorbed by incipiently formed solid oxidation products. They also noted that their solutions became more acid due to the adsorption process. Murray *et al.* (69) found that Ni(II), Cu(II), and Co(II) were strongly adsorbed by colloidal hydrous

manganese oxide, and that the extent of adsorption increased with pH in an acidic to neutral pH range. Kurbatov and coworkers (70) have reported that cobalt(II) was adsorbed on hydrous ferric oxide, and that adsorption increased with increasing adsorbent, adsorbate, and pH. Thus, the abilities of metal oxides and oxy hydroxides to adsorb soluble metal species from aqueous solutions is well recognized, and alkaline conditions favor adsorption.

The mechanism of metal ion adsorption by precipitated metal hydroxides and oxides has been interpreted by a number of mechanisms. Surface complex formation (which can also be viewed as an ion exchange reaction) could occur as follows (64):



Another model proposed to account for the removal of aqueous metal ions from solutions involves hydrolysis followed by an adsorption reaction (65) (reactions 14 and 15).



Both mechanisms for removal of metal ions from solution are compatible with the decrease in pH noted during adsorption in the manganese system investigated by Morgan and Stumm (68). However, the latter mechanism of hydrolysis followed by adsorption is much more likely under the alkaline conditions used in this work (1.25M NaOH), since increased adsorption with increasing pH (64,65) suggests participation of metal ion hydrolysis products in the adsorption process. Indeed, the alkaline hydrolysis products of multivalent ions are more readily adsorbed at solid solution interfaces than are nonhydrolyzed

metal ions (64,65). It is also notable that the tendency for metal ion species to be adsorbed, even against electrostatic repulsion, is especially pronounced for polynuclear species, although the reasons for this are not clear (64,65). The relationship between adsorption and hydrolysis appears to be very complex, and the reader is referred to the work of James and coworkers (65,67,73) for a more in-depth discussion of the mechanisms of adsorption of hydrolyzable metal ions (and in particular cobalt) at the solid oxide/solution interface.

Freshly precipitated metal oxides and hydroxides often continue to change with time (age) after precipitation. On standing, hydrous oxides and hydroxides can become less hydrous and exhibit a decrease in solubility, adsorptive capacity, and catalytic activity (64,66,71). During aging of hydroxo species, for instance, bridging hydroxo groups ( $\text{-OH-}$ ) can be converted to bridging oxo groups ( $\text{-O-}$ ), a process known as oxolation (64,66). Oxo compounds are in general less readily depolymerized than hydroxo-bridged compounds, and completely oxolated oxides are relatively inert (66). Some initially amorphous precipitates which continue to age after precipitation become crystalline during the aging process (72).

It is likely that the precipitate isolated from a 0.25 mM cobalt(II)-containing reaction for use in a 0.05 mM cobalt(II)-containing reaction (Fig. 8, reaction VIII) aged during the isolation procedure. The aging process would decrease the adsorptive ability of the cobalt(III) precipitate, accounting for the relatively weak inhibitory ability of the added precipitate (reaction VIII). Nonetheless, the adsorptive ability of cobalt ions precipitated either prior to, or during, MBG degradation is clearly evident from MBG degradation results (Fig. 7 and 8) and from trace metal analyses (Tables II and III). It also seems likely that the mechanism of adsorption is

similar for both precipitated cobalt(II) and cobalt(III), even though the conditions of precipitation (reaction solution preparation versus oxidative MBG degradation) were quite disparate. Since oxides are known to hydrate at the surface and convert to surface hydroxides (64), it is not unreasonable that both precipitated cobalt(II) hydroxide and hydrous cobalt(III) oxide can adsorb soluble cobalt ions from solution.

#### METAL HYDROXIDE SOLUBILITY AND OXYGEN-ALKALI DEGRADATION

The importance of transition ion metal solubility as a prime determinant of transition metal catalytic activity in oxygen-alkali systems may have been largely overlooked. Under oxidative alkaline conditions the order of catalytic ability of trace quantities of transition metal ions is roughly  $\text{Co(II)} > \text{Cu(II)} \approx \text{Fe(III)} > \text{Mn(II)} > \text{Ni(II)} (\text{inert})$  (5,39,42,43). The solubilities of these metals as hydroxides in aqueous solutions provide no insight into this particular ordering of metals (see Table IV). The solubilities of the hydroxides of nickel, iron, cobalt, manganese and copper in alkaline solution (Table IV), however, do suggest how transition metal ions fit into the above order. Nickel(II) is the least amphoteric of the metal ions in Table IV and is thus the least soluble in alkaline solution. If the catalytic activities of the metal ions in solution are assumed to be the same for the point of illustration, then it is not surprising that nickel(II) compounds are relatively inert since nickel(II) hydroxide is highly insoluble in alkali. Copper(II), at the other extreme, is the most soluble of the metal ions in alkaline solution. It is perhaps for this reason that no maximum in catalytic effect has been reported for an intermediate copper ion concentration in oxygen-alkali systems. It is likely that degradative reactions with copper ions have not been conducted at sufficiently high concentrations for copper precipitation and inhibition by such precipitates to become significant.

Iron(III), cobalt(II), and manganese(II) are intermediate between nickel(II) and copper(II) in their solubilities, and all three have been noted for inducing maximum carbohydrate degradation at an intermediate metal ion concentration (5,38,39,42,43). Conduct of oxygen-alkali reactions in the range of 1M alkali with  $10^{-5}$ M added Fe, Co, or Mn salts could result in transition metal ion precipitate formation, and in the inhibitory action associated with such precipitates. Thus, the solubility data for alkaline transition metal ion solutions suggests that a key determinant of metal degradative activity, in accord with the results found in this work, is metal ion solubility.

TABLE IV  
SOLUBILITIES OF TRANSITION METAL CATALYSTS  
IN AQUEOUS AND ALKALINE SOLUTIONS

	Solubility in Cold H <sub>2</sub> O (g/100 cc) ( <u>74</u> )	Interpolated Solubility in 1.25M Alkali, 25°C (moles/L)	Reference
Ni(OH) <sub>2</sub>	0.013	$6 \times 10^{-6}$	( <u>75</u> )
Fe(OH) <sub>2</sub> <sup>a</sup>	0.00015	$1 \times 10^{-5}$	( <u>76</u> )
Co(OH) <sub>2</sub>	0.00032	$3 \times 10^{-5}$	( <u>60</u> )
Mn(OH) <sub>2</sub>	0.0002	$4 \times 10^{-5}$	( <u>77</u> )
CuO <sup>b</sup>	Insoluble	$3 \times 10^{-4}$	( <u>78</u> )

<sup>a</sup>Fe(OH)<sub>3</sub> is insoluble in cold water (74) and is ca. 1/100 as soluble in 1.25M alkali as Fe(OH)<sub>2</sub> (76).

<sup>b</sup>The solubility of Cu(OH)<sub>2</sub> in alkaline solutions is not accurately known, but it is reported to be more soluble than the oxide by several fold (78).

#### INHIBITION OF ALKALINE COBALT PRECIPITATION

#### GENERAL COMMENTS.

MBG degradation results (Fig. 7; reaction VII) indicated that impurities in extracted NaOH (consisting primarily of ca. 500 ppm Si and ca. 250 ppm B)

initially stabilized 0.25 mM cobalt(II) in 1.25M NaOH. The ability of silicate and borate anions to stabilize cobalt(II) in alkaline solution was investigated with visible spectra. Silicate anions were found to stabilize cobalt(II) in alkaline solution, while borate anions were found to exert no influence on alkaline cobalt(II) solubility.

Since MBG, under certain conditions, was also found to stabilize cobalt(II) in alkaline solution [and hence enhance MBG degradation (Fig. 7; reaction XVIII)], the ability of MBG and certain polyols (ethylene glycol, glycerol, and glucitol) to stabilize cobalt(II) in solution was briefly investigated using visible absorption techniques.

The lack, or inhibition, of precipitate formation, and the consequent enhancement of cobalt(II) solubility (evidenced by more intense cobalt(II) absorbance) was taken as evidence for complex formation. Mixtures for analysis were prepared by addition of aqueous  $\text{CoSO}_4 \cdot 7\text{H}_2\text{O}$  to an alkaline solution containing the additive (silicate, borate, or polyol) of interest. Solutions were prepared to be 3.3M in NaOH since cobalt(II) solubility increases with increasing alkalinity (Fig. 10). This allowed more concentrated (and thus more easily analyzed) cobalt(II) solutions to be studied in 3.3M NaOH than in 1.25M NaOH. Cobalt(II) which precipitated from solution upon mixing of aqueous cobalt(II) and alkaline solutions was removed by centrifugation, and visible spectra of supernatant solutions were immediately obtained.

#### VISIBLE SPECTRUM OF COBALT(II) IN ALKALI

The intense blue color of very strongly alkaline (3-12M) cobalt(II) solutions is attributed to tetrahedral  $\text{Co}(\text{OH})_4^{2-}$  ions (53), and the absorption spectrum responsible for the blue color is shown in Fig. 11. At lower

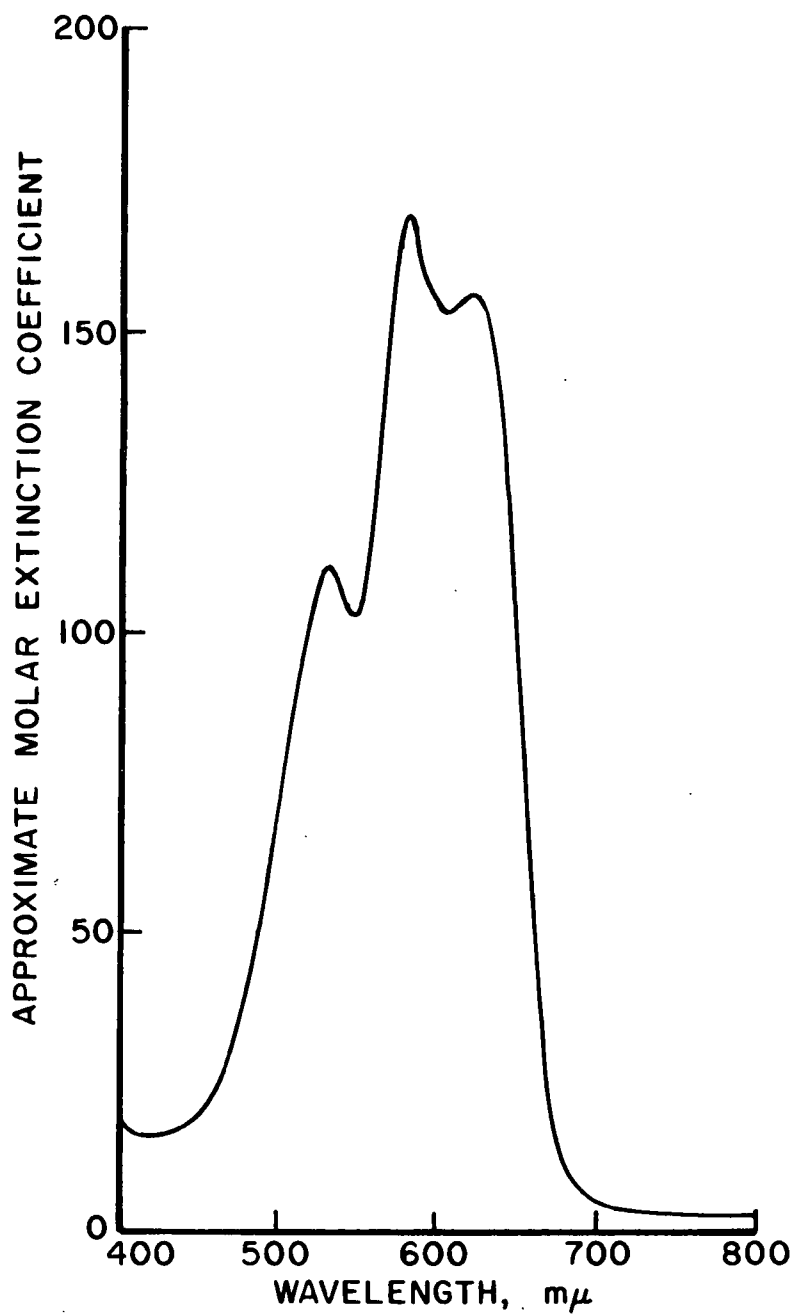


Figure 11. The Visible Spectrum of Co(II) in 50% Aqueous NaOH. The Molar Extinction Coefficients are Only Approximate ( $\pm 20\%$ ) Since the Co(II) Concentration is Only Approximately 0.005M (59)



alkalinities  $\text{Co}(\text{OH})_3(\text{H}_2\text{O})^-$  is also present in alkaline cobalt(II) solutions (Table I) (58,59). The spectrum of alkaline cobalt(II) shown in Fig. 11 is typical of tetrahedrally coordinated cobalt (53,59). The well defined absorption spectrum of alkaline cobalt(II) allowed inhibition of cobalt(II) precipitation to be monitored through visible absorption spectra. Alkaline cobalt(II) solutions have been found to obey Beer's Law in the range of 53-511 mg cobalt/liter in 12M NaOH (53,79), and the absorbing species is known to be in true solution, as opposed to being in colloidal suspension (57,60,71,79,80).

#### INFLUENCE OF SILICATE ANIONS

##### Visible Spectra

The ability of relatively low sodium silicate concentrations (7.1-36.0 mM) to increase cobalt(II) solubility in 3.3M NaOH is clearly demonstrated in Fig. 12. Curves C, D, and E all contain equivalent NaOH and cobalt(II) concentrations, but increasing the sodium silicate concentration from 7.1 to 36 mM resulted in a very substantial increase in alkaline cobalt solubility. In curve E sodium silicate was present in excess as all cobalt(II) was solubilized and no precipitate settled during sample centrifugation immediately prior to visible absorption analysis. Curve A was obtained in the absence of NaOH and in the presence of 71.0 mM sodium silicate. Curve B shows the absorption attributable to 2.08 mM cobalt(II) in 3.3M NaOH in the absence of added sodium silicate.

The trimodal cobalt(II) absorption intensities of spectra in Fig. 12 indicate that the absorption due to cobalt(II) in 3.3M NaOH containing 12 mM sodium silicate is roughly twice as intense as the combined absorbance in 3.3M NaOH and 71 mM sodium silicate solutions individually. Since the silicate concentration at the 12 mM level is only 0.4% as strong as 3.3M NaOH on a molar

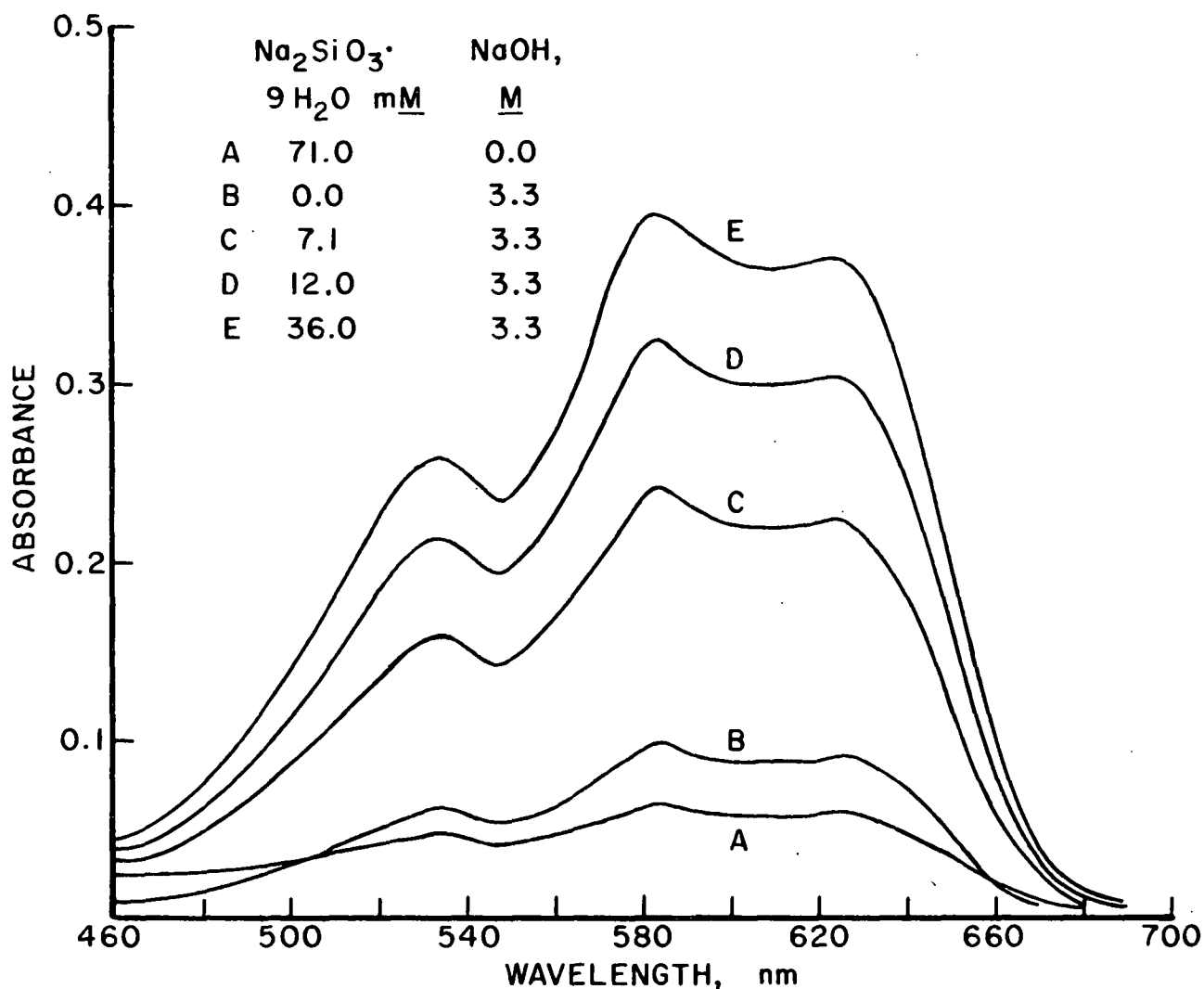


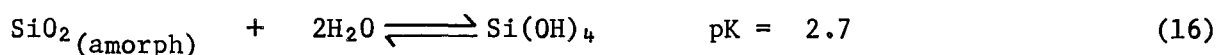
Figure 12. Visible Spectra of Ultrapure Sodium Hydroxide and/or Sodium Silicate Solutions Containing 2.08 mM Added  $\text{CoSO}_4 \cdot 7\text{H}_2\text{O}$ . Samples were Centrifuged to Remove Precipitated Cobalt(II) Prior to Analysis

basis, the ability of alkaline silicate anions to inhibit cobalt precipitation is clearly substantial. The molar absorptivity of cobalt(II) at a given visible wavelength in alkaline solution is not altered by complexation of cobalt(II) with either silicates or polyols (discussed in the section on Influence of Polyols). The absorption intensity of 2.08 mM cobalt(II) in 3.3M NaOH is not affected by variation in silicate ion concentration so long as all cobalt(II) is in solution. The visible absorption intensity of 2.08 mM cobalt(II) at 585 nm in alkaline silicate solution (Fig. 12) also corresponds to a molar absorptivity

(extinction coefficient) of 188 L/mole-cm which is in general agreement with the  $170 \pm 34$  L/mole-cm at 585 nm evident from the work of Cotton et al. (59) with cobalt(II) in 50% NaOH (Fig. 11). The similarity in trimodal absorption spectra in either NaOH (curve B) or sodium silicate solution (curve A) in Fig. 12 also indicates that silicate anions coordinate with cobalt(II) in much the same manner as hydroxyl ion. Dugger (81) has pointed out that the environments of the oxygen atoms of  $-\text{SiO}^-$  and  $\text{HO}^-$  are similar enough so that each species interacts with metal ions in a comparable manner.

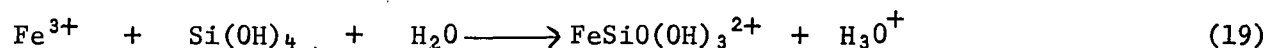
#### Coordination of Silicate Anions with Transition Metal Ions

The dissolution of amorphous solid silica in water or alkaline solution involves a simultaneous hydration and depolymerization which is catalyzed by  $\text{OH}^-$  ions (82). Under the strongly alkaline conditions employed in this work (1.25M NaOH, pH > 14) dissolved silica would remain in the monomeric state and the condensation to polysilicic acids encountered at pH's below 10.9 would not occur (82,83). The equilibrium relationships between dissolved species of silica at 25°C in strongly alkaline solution are shown below (52).



Thus, in strongly basic solutions silicate anions are retained as monomers, and polymerization reactions are highly unfavorable. Coordination of silicates with transition metals under the alkaline conditions employed in this work (1.25M NaOH) would have to occur via silicate monomers.

The occurrence of a complex formation reaction between monomeric silica and dissolved iron(III) has been established by Weber and Stumm (84) for a pH range below 3.5. The reaction is as follows:



The reaction is also thought to occur in the more neutral pH range encountered in natural waters (52). Schenk and Weber (52) found that monomeric silica inhibited the hydrolysis and precipitation of iron(III) from acidic solutions. In the pH range of 6-8 a three-fold excess of monomeric silica to iron(III), on a molar basis, prevented the hydrolytic precipitation of iron(III). Schenk and Weber (52) have also established, however, that silicate anions promote the oxidation of iron(II) to iron(III). Schenk (85) found that monomeric silica decreased the rate of hydrolytic precipitation of manganese(II) from alkaline (pH 9) solution, and that inhibition of precipitation by silica increased with increasing pH. In a comparable manner, Schenk (85) observed that a five-fold excess of silica maintained aluminum in solution.

Evidently, monomeric silica and its hydrolysis products compete very effectively with water and hydroxide ion for coordination sites on transition metal ions such as iron(III) (52,84), manganese(II) (85), and aluminum(III) (85), even in alkaline solution. Since the similarity between the surface  $\text{SiO}^-$  groups of amorphous silica and  $\text{OH}^-$  ions, as ligands, is well recognized (81,82), it is not surprising that soluble silicate anions may exhibit a considerable affinity toward metal ions.

#### Silicates as Catalysts and Inhibitors

The coordination of silicate anions with cobalt(II) inhibited the initial precipitation of cobalt(II) during preparation for a reaction at the 0.25 mM added cobalt(II) level in extracted NaOH (reaction VII). During

preparation of reaction solutions at the 0.25 mM added cobalt(II) level in ultrapure NaOH (reactions IX and XI) cobalt(II) precipitated from solution before reactions could be initiated. However, the rate of MBG degradation in extracted NaOH at the 0.25 mM cobalt(II) level (reaction VII, no initial precipitation) was slower than in a 0.25 mM cobalt(II)-containing reaction in which MBG was initially dissolved in ultrapure NaOH prior to mixing with aqueous cobalt(II) (reaction XVIII, no initial precipitation). These results indicate that silicates can act as catalysts of MBG degradation by stabilizing cobalt(II) ions in alkaline solution. These results also suggest that silicates can inhibit MBG degradation under oxidative conditions. Since more precipitate appeared to be formed after 1 hour of reaction in extracted NaOH (reaction VII) than was formed after 1 hour of reaction in an initially homogeneous degradation in ultrapure NaOH (reaction XVIII), it seems likely that silicates may have slightly promoted the oxidative precipitation of cobalt(III). Silicate monomers have been noted to promote the oxidation of iron(II) to iron(III) (52), and it is probable that silicates also promote the oxidation of cobalt(II) to cobalt(III), resulting in the precipitation of cobalt(III). This earlier precipitation from reaction solution could account for the slower rate of MBG degradation at the 0.25 mM added cobalt(II) level in extracted NaOH (reaction VII) relative to ultrapure NaOH (reaction XVIII). It seems unlikely that silicates acted to inhibit the catalytic activity of cobalt ions at the 0.25 mM cobalt addition level by inhibiting interaction of cobalt ions with other species in solution. MBG degradation catalyzed by 0.05 mM added cobalt proceeded at the same rate in both ultrapure (no silicates) and extracted (containing silicates) NaOH (Fig. 6). Thus, silicate anions can stabilize cobalt(II) in alkaline solution by inhibiting precipitation of cobalt(II) and thereby

act as degradation catalysts. However, silicates may also promote oxidative precipitation of cobalt(III) during MBG degradation, and hence act as degradation inhibitors.

Silicates have been used to inhibit peroxide decomposition during peroxide bleaching. It is possible that silicates may act as protectors in such systems by promoting the oxidative precipitation of catalytic metal ions from solution. It also seems likely, however, that pH plays a very important role in the action of silicates. In contrast to the oxygen bleaching conditions used in this work, peroxide bleaching is generally conducted under mildly alkaline conditions [ca. pH 10 (86)]. It is possible that the protective action of silicates at this pH may be partially attributable to the condensation of polysilicic acids to dimensions which are highly adsorptive (31). Soluble metal ions (e.g.,  $Zn^{2+}$ ,  $Fe^{2+}$ , and  $Co^{2+}$ ) are known to be strongly adsorbed on solid silica (82), and adsorption of polybasic ions by silica is considered to be essentially irreversible (87). Under the high pH conditions employed in the work (pH 14) the affinity of silicates for cobaltous ions was manifested as a stabilization of cobalt(II) ions in solution, evidently through coordination. At the lower pH's of peroxide bleaching the protective action attributed to silicates may be a result of purification of bleaching solutions by adsorption and deactivation of catalytic transition metal ions by polymeric silicates.

#### INFLUENCE OF BORATES

Mixtures for visible spectral analysis were prepared by addition of aqueous cobalt sulfate to alkali and/or sodium borate solutions. Borates did not detectably influence the visible spectrum of alkaline cobalt. The presence of 0.07M sodium borate did not alter the visible absorbance spectrum of 2.08 mM cobalt(II) in 3.3M NaOH from that found in the absence of added sodium borate.

## INFLUENCE OF POLYOLS

### Visible Spectra

The ability of selected polyols to stabilize cobalt(II) in alkaline solution was investigated using visible spectrometry. Mixtures for visible spectral analysis were prepared by addition of aqueous cobalt sulfate to alkaline polyol solutions, and mixtures were centrifuged prior to analysis. The ability of MBG and selected polyols to stabilize cobalt(II) in solution is shown in Fig. 13. The order of polyol-induced cobalt(II) stabilization followed the sequence MBG≈glycerol>sorbitol>ethylene glycol>no polyol (H<sub>2</sub>O only). No precipitate was noticed in either MBG or glycerol solutions, indicating that all cobalt(II) was solubilized. For this reason, the relative solubilizing ability of MBG versus glycerol was not distinguishable at the alkaline cobalt(II) concentrations analyzed. As in the case of silicates (see Influence of Silicate Anions), polyols did not alter the molar absorptivity of alkaline cobalt(II) in the visible region. So long as cobalt(II) remained in solution, variations in polyol concentrations did not alter visible absorption intensities. The enhanced absorption shown by curve C relative to curve D in Fig. 13 at wavelengths lower than 500 nm is attributable to visible light scattering due to precipitate formation during spectral analysis.

The order of solution preparation was very important in the stabilization of cobalt(II) in alkaline solution. After precipitation of cobalt(II) from alkaline solution had begun, the addition of polyols to alkaline cobalt(II) mixtures did not result in the stabilization of cobalt(II) in solution. This indicated that the precipitation process in the absence of oxygen could occur in an essentially irreversible manner (i.e., any redissolution of precipitated

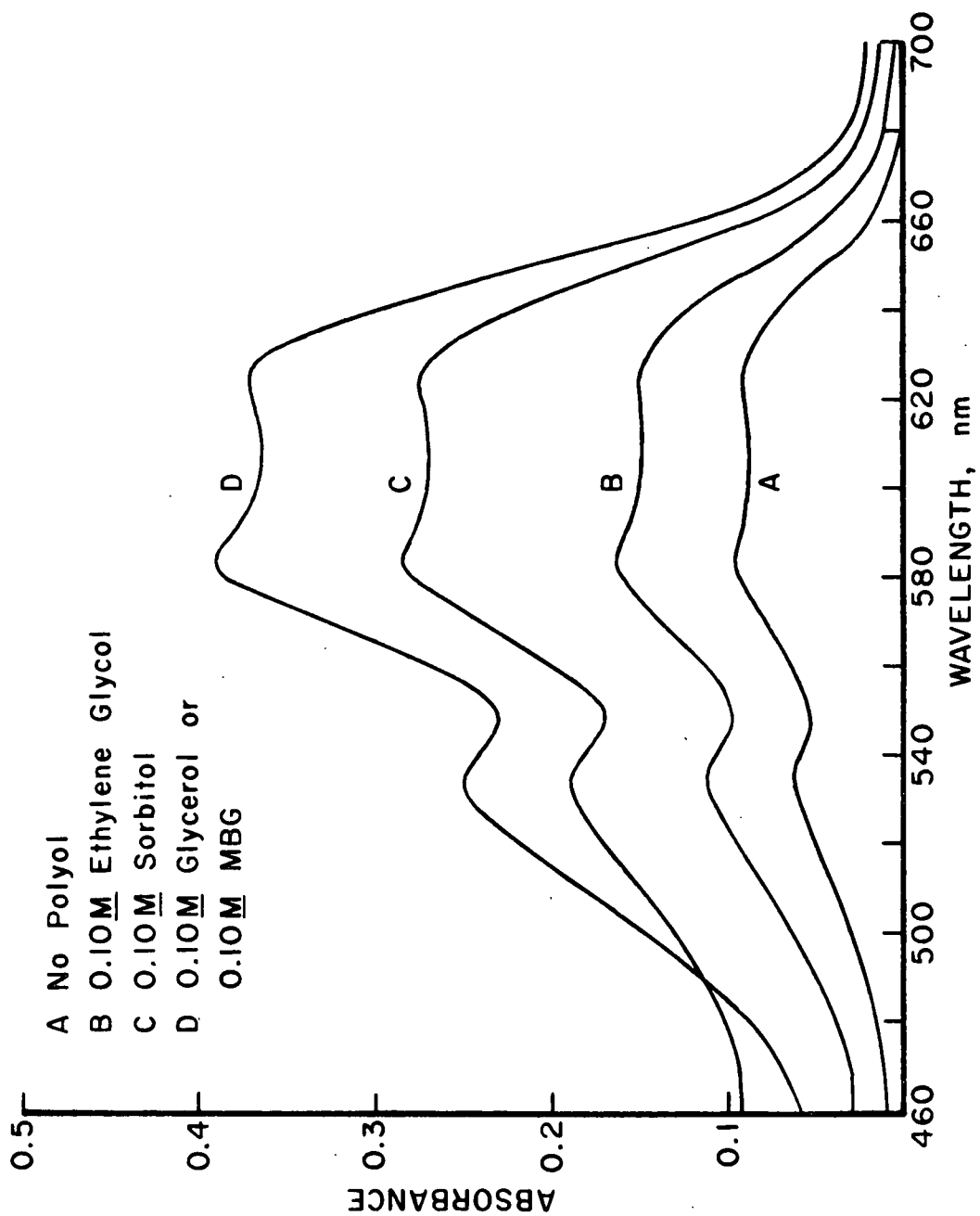


Figure 13. Visible Spectra of 3.3M Ultrapure NaOH Solutions Containing Polyols and 2.08 mM Added  $\text{CoSO}_4 \cdot 7\text{H}_2\text{O}$ . Samples were Centrifuged to Remove Precipitated Cobalt(II) Prior to Analysis



cobalt(II) was extremely slow) and that stabilization of cobalt(II) in solution by polyols had to occur prior to precipitation. Precipitation which took place during reaction solution preparation at the 0.25 mM added cobalt(II) level in ultrapure NaOH (reactions IX and XI) occurred in an essentially irreversible manner, since redissolution of precipitated cobalt(II) did not occur to any significant degree between reaction solution preparation and reaction initiation (a period of ca. 12 hours).

#### Metal Ion-Carbohydrate Complexation in Alkali

The formation, stability, and structure of transition metal-polyol chelates in alkaline solution has been only sparsely investigated, though the fact that alkali-stable complexes are formed is, in some instances, well established. Charley et al. (62) found Fe(II), Fe(III), Cu(II) and Co(II) to form soluble complexes with sugars in acid solution which remained soluble until the pH was raised to approximately 12 (well beyond the point of metal hydroxide precipitation in the absence of sugars). They also found the relative sequestering ability of sugars and polyols for iron(II) to be fructose>sorbitol>glucose = galactose ≈ maltose = lactose>sucrose>ribose>erythrose. Bourne and coworkers (61) added metal salts to a pH 12 solution of D-mannitol and found that Cu(II), Fe(II), Fe(III), and Co(II) all formed soluble chelates. With glucose, however, they were unable to detect complex formation with either iron or cobalt, though complexation was detected with copper.

Metal ion complexation with hydroxy acids under alkaline conditions is also well established. Copper(II), for instance, forms soluble complexes in alkaline solution with tartaric acid (used to prepare Fehling's solution) and citric acid (used to prepare Benedict's solution). Fehling's solution

is made by mixing an aqueous copper sulfate solution with a solution containing sodium potassium tartrate and sodium hydroxide. The soluble cupric tartrate ions thus formed serve as oxidizing agents toward aldehydes which, in the case of reducing sugars, results in decomposition of the sugar and the precipitation of cuprous oxide. The complex form of copper in Fehling's solution is not well understood (53).

#### Cobalt-Carbohydrate Complexation and MBG Degradation

The stabilization of cobalt(II) in alkaline solution by MBG and other polyols (Fig. 13) indicates two key points. First, the sequence of reaction solution preparation for oxygen-alkali MBG degradation can be very important in the formation of metal ion-carbohydrate complexes. If cobalt(II) is stabilized in alkaline solution by complexation, then the rate of MBG degradation is enhanced (Fig. 7, reaction XVIII). Once precipitated from alkaline solution, cobalt(II) resists redissolution, and precipitated cobalt(II) is relatively inert (Fig. 7, reactions IX and XI). Second, metal ion complexation or interaction with MBG degradation products may also influence the stability of cobalt ions under oxidative conditions. Particular degradation products may stabilize cobalt(III) in alkaline solution. The stabilization of cobalt(III) in solution may promote a catalytic cycle of cobalt oxidation-reduction between the  $2^+$  and  $3^+$  states to occur.

It is possible that the yellow color noted only in cobalt-containing reaction solutions was due to the formation of a soluble cobalt(III) complex with an acidic MBG degradation product. A sample of the reaction solution prepared for an initially homogeneous reaction in ultrapure NaOH at the 0.25 mM cobalt(II) addition level (reaction XVIII), and stored under ambient conditions, went from blue to clear in color when cobalt(III) precipitated.

from the solution due to air oxidation. However, the same solution turned yellow in color prior to cobalt(III) precipitation during MBG degradation. This suggests that the yellow color of cobalt-containing reaction solutions may be due to the formation of a stable complex between cobalt(III) and an acidic MBG degradation product (or products). A visible spectrum of a yellow reaction solution sample from reaction XVIII showed only a broad absorption band of gradually increasing intensity extending into the ultraviolet region beginning at 450 nm. The concentration of cobalt in reaction solution samples was too low to detect absorption by alkaline cobalt(II).

The oxidation of strongly alkaline (8M) glycerol-containing solutions of cobalt(II) by oxygen produces a cobalt(III)-glycerol complex which is stable in alkaline solution (57). This oxidation of cobalt(II) to a cobalt(III)-glycerol complex is also reported to result in a broad intensification of absorption in the visible region below 450 nm (57). These results suggest the possibility that the products of MBG degradation may stabilize cobalt(III) in solution, and may thereby inhibit the precipitation of cobalt(III) from solution. Significantly, Gordon (57) has reported that alkaline cobalt(III)-glycerol solutions react with aldehydes and methyl ketones, resulting in reduction of cobalt(III) to cobalt(II). This reaction is somewhat similar to the oxidation of aldehydes with Fehling's solution mentioned in the last section, except that Gordon (57) found the reduction of cobalt(III) to cobalt(II) to be reversible. Oxidation-reduction of cobalt ions is discussed further in the section Mechanism of Cobalt-Catalyzed MBG Degradation.

## GLYCOSIDIC BOND CLEAVAGE

To determine the extent of glycosidic bond cleavage induced by varying concentrations of cobalt, the formation of methanol with time was monitored. Methanol, however, was found to be degraded in cobalt-containing reaction solutions and this complicated the interpretation of results with methanol. For comparative purposes the total methoxyl content of selected reaction samples was determined to evaluate the extent of methoxyl loss attributable to cobalt.

### METHANOL STABILITY

Methanol is stable under the conditions of temperature, oxygen pressure, and alkalinity used in this work (25,28). Under oxidative-alkaline conditions in the presence of cobalt, however, methanol was found to be degraded (Table V).

TABLE V

THE DECOMPOSITION OF METHANOL IN 1.25M ULTRAPURE NaOH AT 120°C AND 0.68 MPa OXYGEN PRESSURE IN THE PRESENCE OF 0.25 mM CoSO<sub>4</sub>·7H<sub>2</sub>O

Reaction Time, hrs.	Methanol Concentration, mM
0	52.9
1	51.4
5	45.4
9	43.4

The extent to which methanol and methoxyl groups were degraded in cobalt-containing reaction solutions was determined by analyzing reaction samples for total methoxyl content as described in the next section.

## ANALYSES FOR METHOXYL CONTENT

Reaction solution samples were acid hydrolyzed using either hydrochloric or hydriodic acid to determine the extent of cobalt-induced methoxyl degradation, and to determine if methoxyacetic acid (MAA) constituted a major reaction product. MAA has been reported as a degradation product in both oxygen-alkali (25) and hydrogen peroxide-alkali (26) degradations of methyl glycosides, but its detection in reaction solutions via GLC and GLC-mass spectral procedures has presented difficulties (25). In this work, authentic MAA was found to be stable to a mild hydrolysis with dilute hydrochloric acid, while it hydrolyzed under the more severe conditions afforded by hydrolysis in concentrated hydriodic acid.

The total methoxyl content of reaction samples as determined by both HCl and HI hydrolyses (Table VI) was found to be very similar, showing that MAA was not a major reaction product in either the cobalt-catalyzed or uncatalyzed reactions. The results of HCl and HI hydrolyses (Table VI) also indicate that the methoxyl content of reaction solutions decreased with reaction time in a manner reminiscent of the degradation pattern exhibited by MBG. In other words, the greatest loss in methoxyl concentration was found in reaction samples which contained the greatest concentration of soluble cobalt ions during reaction.

## METHANOL FORMATION

Interpretation of results for methanol formation is complicated by the finding that cobalt ions induced the degradation of methanol under the conditions employed for MBG degradations (see Methanol Stability). A further complicating factor is that cobalt ions also promoted the degradation of certain

TABLE VI

METHOXYL CONTENT OF REACTION SOLUTIONS AS DETERMINED BY  
HCl AND HI HYDROLYSIS<sup>a</sup>

Reaction No.	Hours of Reaction	Initial Cobalt Concentration	Percent Reaction <sup>b</sup>	Methoxyl Content, mM	
				with HCl	with HI
<u>Extracted NaOH</u>					
IV	8	0.00 mM	42.6	--	95.6
	60	0.00	82.7	91.3	94.8
V	2	0.01	28.9	--	94.9
	4	0.01	42.5	--	96.2
	8	0.01	57.5	--	91.7
	16	0.01	72.4	84.0	85.4
VI <sup>c</sup>	2	0.05	41.4	--	92.7
	4	0.05	65.7	--	90.9
	8	0.05	83.0	--	82.6
	16	0.05	90.7	73.0	74.1
VII	2	0.25	43.1	--	95.3
	4	0.25	56.0	--	89.7
	8	0.25	65.7	--	89.1
	16	0.25	72.1	--	85.2
<u>Ultrapure NaOH</u>					
X	0	0.00 mM	0.0	95.0	--
	16	0.00	53.7	93.8	--
XIII	2	0.05	59.8	88.1	--
	2 <sup>d</sup>	0.05	59.8	88.1	--
IX	16	0.25	51.6	91.2	--
XI	16	0.25	53.2	90.1	--

<sup>a</sup>Initial methoxyl content = 95.5 mM.

<sup>b</sup>Determined by GLC of acetylated reaction samples.

<sup>c</sup>Reaction VI was conducted under conditions of limited agitation.

primary methoxyl-containing products relative to uncatalyzed systems. This is discussed in the section on Acidic Products. Nonetheless, results of methanol analyses for reactions conducted in both extracted and ultrapure NaOH (Fig. 14 and 15) indicate that cobalt ions did not induce a significant shift in the extent of MBG degradation which occurred through glycosidic bond cleavage (ca. 70%). The rate of methanol degradation was roughly an order of magnitude slower than the rate of methanol formation, and a cobalt ion-induced increase in the extent of glycosidic bond cleavage would have resulted in plots of differing slopes in Fig. 14 and 15, depending on cobalt ion concentration. The essentially constant extent of methanol formation (ca. 70% on a mole percent reacted MBG basis) regardless of cobalt ion concentration indicates that cobalt ions did not significantly alter the extent of MBG glycosidic bond cleavage. It is likely that cobalt ion-induced methanol decomposition was largely balanced by enhanced methanol formation due to cobalt ion-catalyzed degradation of primary methoxyl-containing products.

#### ACIDIC PRODUCTS

##### GENERAL COMMENTS

The major acids produced during MBG degradation were examined to determine whether the presence of cobalt caused a shift in the types of acids formed, or a change in the acidic product distribution. The major acidic products produced during oxygen-alkali degradation of MBG have been identified (15, 19). Acidic products were analyzed as their per-O-trimethylsilyl (TMS) derivatives, and tentative identification of products was made by comparison of GLC product patterns to the product pattern reported by Ericsson et al. (15) for oxidative alkaline MBG degradation. Positive identification of the major reaction products was made by GLC interfaced with a mass spectrometer.

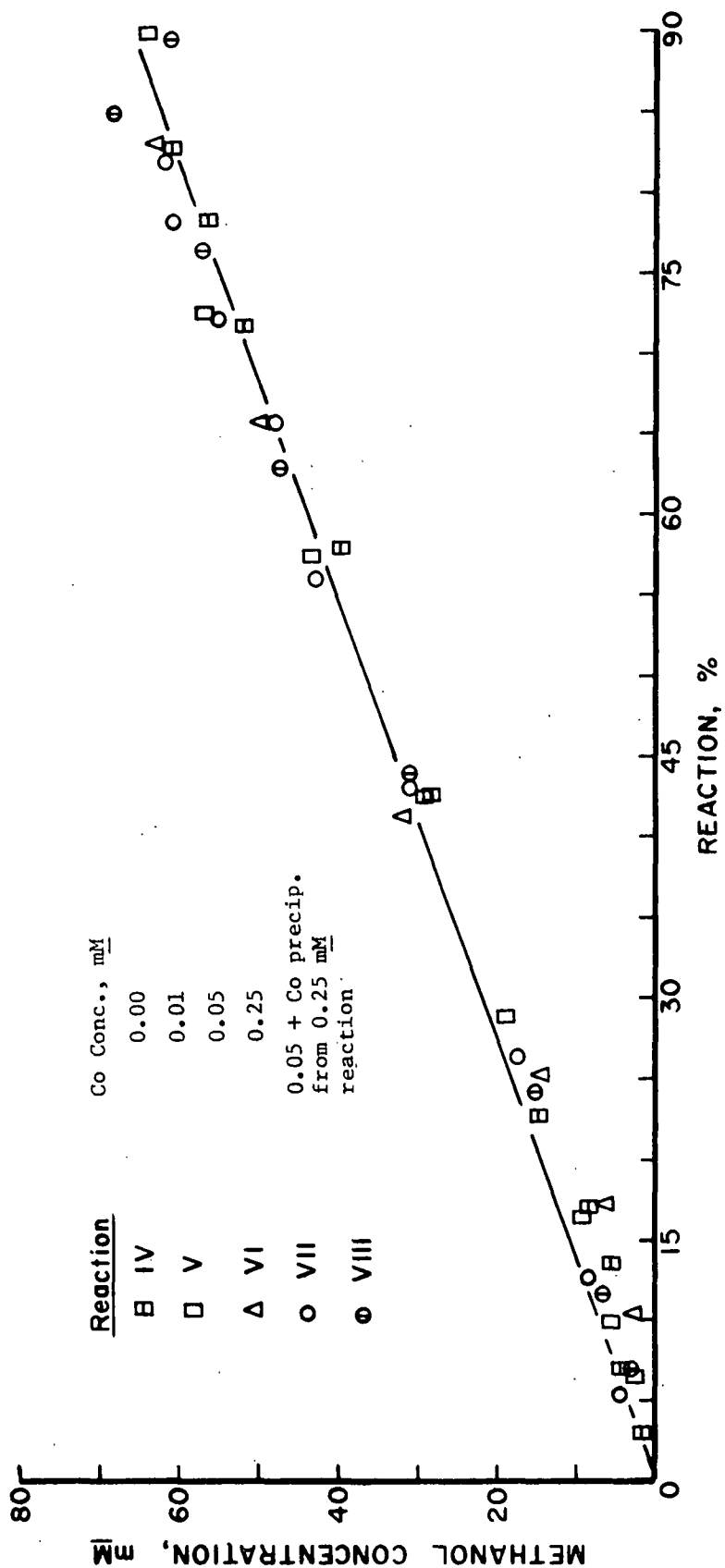


Figure 14. Yield of Methanol as a Function of Percent Reaction for MBG Degradations Conducted in Extracted NaOH



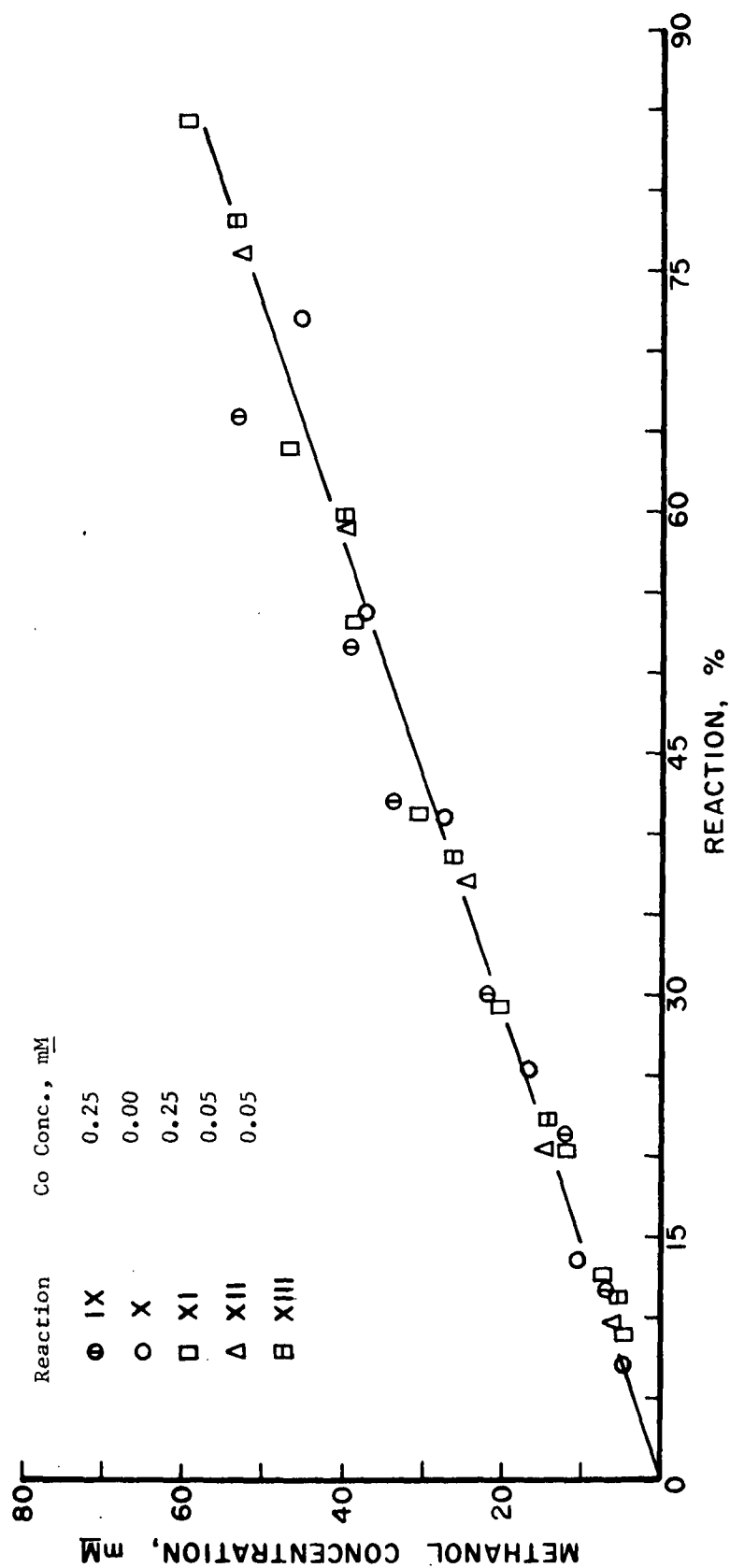


Figure 15. Yield of Methanol as a Function of Percent Reaction for MBG Degradations in Ultrapure NaOH

Semiquantitative estimates of acidic product concentrations were made by estimating response factors for acids on a molecular weight basis, and *n*-butyl- $\beta$ -D-glucopyranoside was used as an internal standard. The sample workup procedure is detailed in the Experimental section. Appendices II, IV, and V present, respectively, tabulated acidic product results, GLC conditions and response factors, and GLC-MS conditions and results.

#### INFLUENCE OF COBALT

A sample GLC chromatogram of the acidic reaction products from MBG degradation in ultrapure NaOH with 0.05 mM added cobalt(II) [a very degradative level of cobalt(II)] is shown in Fig. 16. The major acidic products which were identified are shown in Table VII. Fig. 17 is a GLC chromatogram of acidic MBG degradation products obtained in the absence of cobalt, as reported by Ericsson et al. (15). Chromatographic product patterns obtained in this work in the absence of cobalt were comparable to the GLC product pattern reported by Ericsson et al. (15) (Fig. 17).

The qualitative product patterns of Fig. 16 and 17 are very similar and show that cobalt did not induce major changes in the types or quantities of acidic products produced during MBG degradation. Table VIII compares acidic product concentrations in the presence and absence of cobalt at ca. 20, 40 and 60% reaction in ultrapure NaOH. Comparisons are made on a mole percent reacted MBG basis. The results indicate that soluble cobalt did not alter the product distribution measurably until after ca. 20% reaction. At greater than 20% reaction, the presence of soluble cobalt in reaction solutions led to an increase in the relative concentrations of dicarboxylic acids and a decrease in the concentrations of methyl-C-carboxy- $\beta$ -D-pentafuranosides.

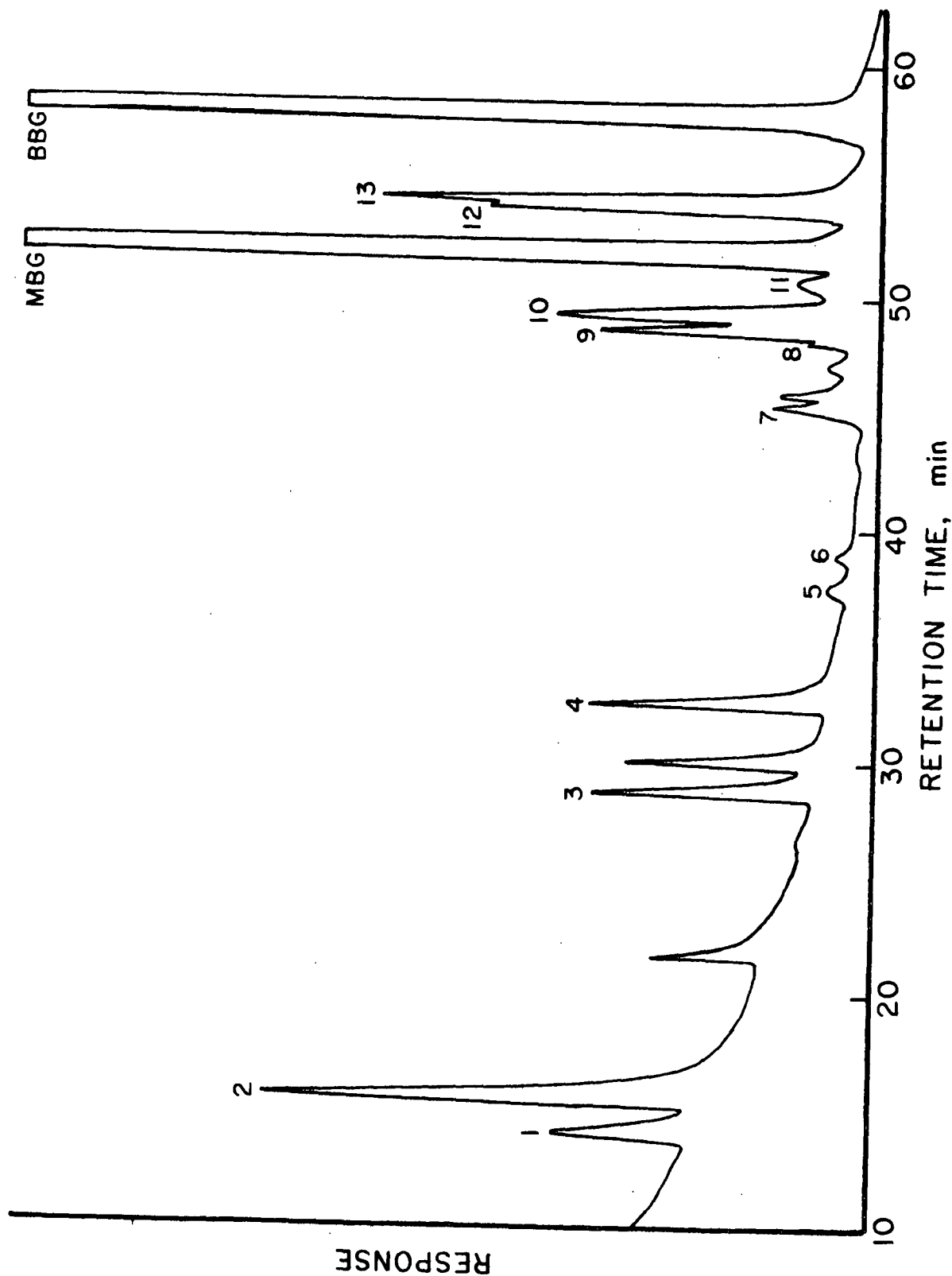


Figure 16. Sample GLC Chromatogram of the Acidic Degradation Products of MBG in Oxygen and Alkali with 0.05 mM Added  $\text{CoSO}_4 \cdot 7\text{H}_2\text{O}$ . Reaction was Conducted in 1.25M NaOH at 120°C and 0.68 MPa Partial  $\text{O}_2$  Pressure (Reaction XIII, Sample Obtained After 2 Hours Reaction). 1-Lactic Acid, 2-Glycolic Acid, 3-Glyceric Acid, 4-2,4-Dihydroxybutyric Acid, 5-Erythronic Acid, 6-Threonic Acid, 7-Arabinonic Acid, 8-11-Methyl-C-Carboxy  $\beta$ -D-Pentafuranosides, 12-13-Dicarboxylic Acids

TABLE VII  
ACIDIC DEGRADATION PRODUCTS

Product	Product Identification	Identification Method <sup>a,b</sup>
1	Lactic acid	GLC, MS
2	Glycolic acid	GLC, MS
3	Glyceric acid	GLC, MS
4	2,4-Dihydroxybutyric acid	GLC, MS
5	Erythronic acid	GLC
6	Threonic acid	GLC
7	Arabinonic acid	GLC
8-11	Methyl-C-carboxy β-D-pentafuranosides	GLC, MS <sup>c</sup>
12-13	Dicarboxylic acids	GLC, MS <sup>d</sup>

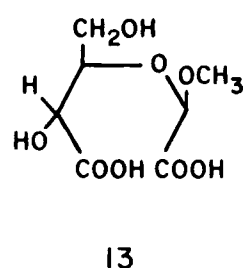
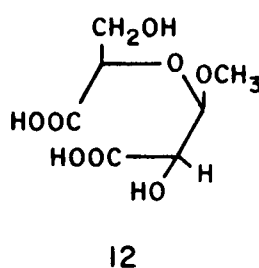
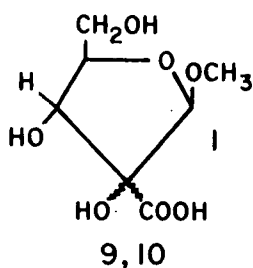
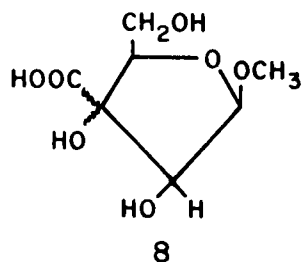
<sup>a</sup> GLC — identified by qualitative comparison to the GLC product pattern reported by Ericsson *et al.* (15). GLC conditions and retention times are given in Appendix IV.

MS — identified by gas chromatography-mass spectrometry.

<sup>b</sup> Mass spectra of acids 1-7 have been published (88). Mass spectral data for acids analyzed in this work are tabulated in Appendix V.

<sup>c</sup> Mass spectra were not obtained for peaks 8 and 11 due to the low concentrations of these products. Mass spectra obtained on peaks 9 and 10 were essentially identical, and the major fragments corresponded to those reported by Ericsson *et al.* (15). Using the assignments of Ericsson *et al.* (15) and Hearne (25), product 8 is methyl 3-C-carboxy β-D-pentafuranoside, and products 9 and 10 are isomers of methyl 2-C-carboxy β-D-pentafuranoside (see diagrams below). Product 11 has been reported as an unidentified furanoid acid in previous work (15).

<sup>d</sup> Mass spectra from peaks 12 and 13 were very similar and agreed with the fragmentation patterns reported by Ericsson *et al.* (15) for structures 12 and 13 shown below.



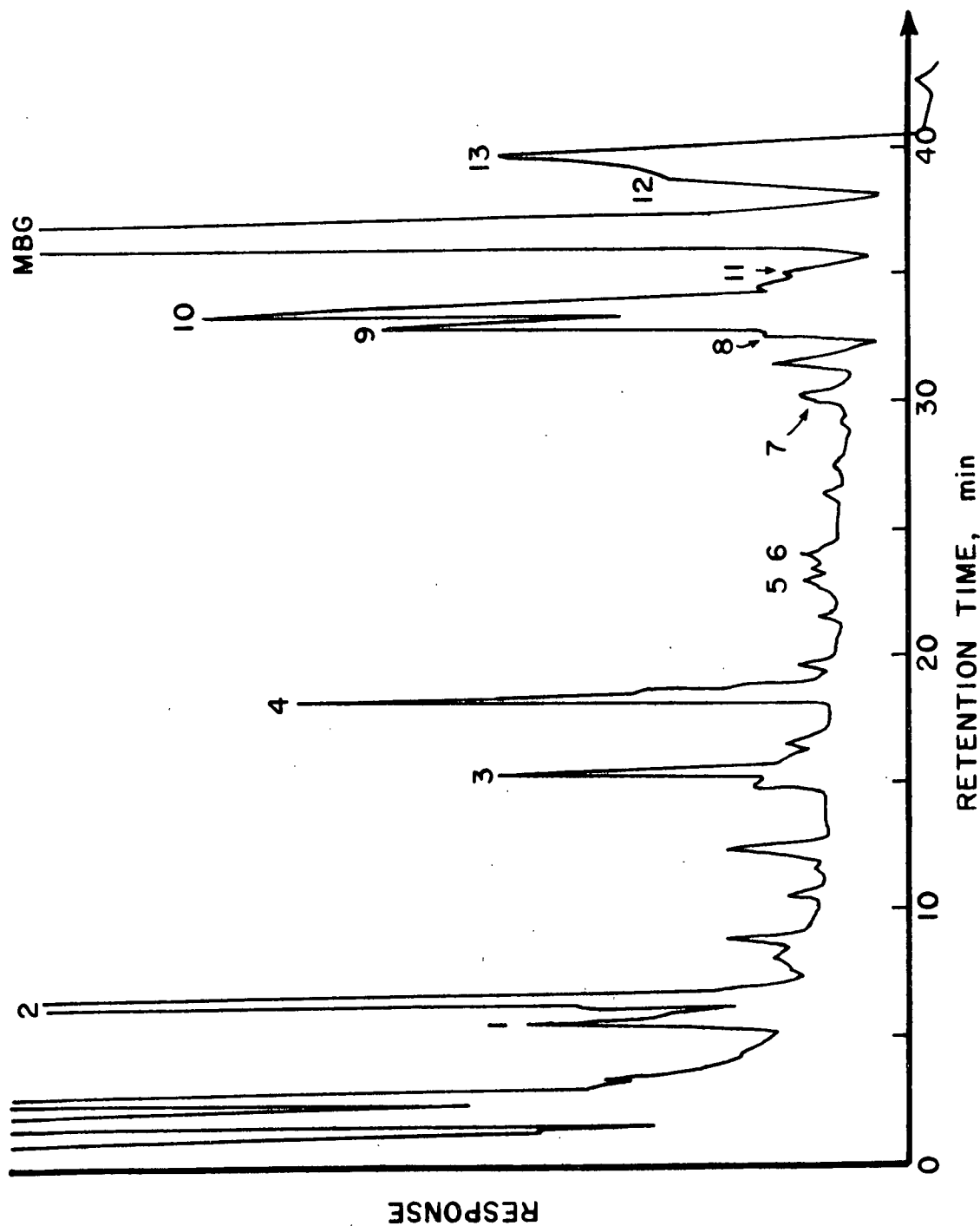


Figure 17. Sample Chromatogram of MBG Degradation in Oxygen-Alkali from Ericsson et al. (15) (1-Lactic Acid, 2-Glycolic Acid, 3-Glyceric Acid, 4-2,4-Dihydroxybutyric Acid, 5-Erythronic Acid, 6-Threonic Acid, 7-Arabinonic Acid, 8, 9, 10, 11-Methyl-C-Carboxy  $\beta$ -D-Pentafuranosides, 12, 13-Dicarboxylic Acids)

TABLE VIII

ACIDIC PRODUCT DISTRIBUTION FROM MBG DEGRADATION IN ULTRAPURE NaOH IN THE PRESENCE AND ABSENCE OF ADDED  $\text{CoSO}_4 \cdot 7\text{H}_2\text{O}$ . YIELDS ARE GIVEN IN MOLE PERCENT REACTED MBG<sup>a</sup>

	ca. 20% Reaction						ca. 40% Reaction						ca. 60% Reaction					
	0	0.25	0.25	0.05	0.05	0.05	0	0.25	0.25	0.05	0.05	0.05	0	0.25	0.25	0.05	0.05	0.05
Added cobalt, mM <sup>b</sup>	0	0.25	0.25	0.05	0.05	0.05	0	0.25	0.25	0.05	0.05	0.05	0	0.25	0.25	0.05	0.05	0.05
Reaction	X	IX	XI	XII	XII	XII	X	IX	XI	XII	XIII	XIII	X	IX	XI	XII	XIII	XIII
Reaction time, hr	4	2	2	0.5	8.5	8	8.5	8	8	1	1	1	16	32	32	2	2	2
Percent reaction <sup>c</sup>	25.6	20.1	20.3	20.4	41.0	42.0	41.0	42.0	41.2	37.1	38.6	53.7	65.9	64.0	58.2	59.8		
<u>Acidic Products</u>																		
1 Lactic	12	5	4	6	9	4	9	4	4	5	5	10	5	9	6	6		
2 Glycolic	25	22	18	12	19	19	19	19	19	13	20	19	20	28	18	22		
3 Glyceric	9	6	5	5	8	6	8	6	8	4	5	11	5	7	10	6		
4 2,4-Dihydroxy- butyric	4	5	6	6	3	5	3	5	4	5	7	5	4	5	5	7		
5 Erythronic	1	1	1	1	1	1	1	1	1	1	1	1	1	1	1	1		
6 Threonic	1	1	1	1	1	1	1	1	1	1	1	1	1	1	1	1		
7 Arabinonic	2	1	1	2	1	1	1	1	1	1	1	1	1	1	1	2		
8-11 Methyl-C- carboxy $\beta$ -D- pentafuranosides	32	33	38	35	30	25	30	25	26	23	21	29	12	11	15	13		
12-13 Dicarboxylic acids	4	5	8	5	4	5	4	5	4	9	12	5	5	4	11	13		

<sup>a</sup>GLC peak area was assumed to be proportional to molecular weight. Response factors used in semi-quantitative acidic product yield calculations are given in Appendix IV. For a given acidic product, the standard deviation for duplicate silylations was generally in the range of +25-30%. The significant inaccuracies involved in acidic product analyses mean that yields must be considered as estimates.

<sup>b</sup>Due to the nature of solution preparation, initial concentrations of cobalt(II) in reaction solutions follow the order  $\text{X} < \text{IX} = \text{XI} < \text{XII} = \text{XIII}$ .

<sup>c</sup>Percent reaction determined from acetylated samples.

Acidic product results at ca. 40% reaction for degradations in extracted NaOH (Table IX) show the same trends as reactions conducted in ultrapure NaOH. At ca. 40% reaction in extracted NaOH the presence of cobalt ions in reaction solutions resulted in increased dicarboxylic acid concentrations and decreased carboxyfuranoside concentrations relative to uncatalyzed MBG degradation.

TABLE IX

ACIDIC PRODUCT DISTRIBUTION AFTER ca. 40% REACTION OF MBG IN EXTRACTED NaOH IN THE PRESENCE AND ABSENCE OF ADDED  $\text{CoSO}_4 \cdot 7\text{H}_2\text{O}$ . YIELDS ARE GIVEN IN MOLE PERCENT OF REACTED MBG<sup>a</sup>

Added cobalt, mM <sup>b</sup>	0.0	0.01	0.25
Reaction	IV	V	VII
Reaction time, hr	8	4	2
Percent reaction <sup>c</sup>	42.6	42.5	43.1
<u>Acidic Products</u>			
1 Lactic	8	7	5
2 Glycolic	28	29	21
3 Glyceric	15	7	5
4 2,4-Dihydroxybutyric	6	6	5
5 Erythronic	2	1	1
6 Threonic	1	1	1
7 Arabinonic	1	1	2
8-11 Methyl-C-carboxy β-D-pentafuranosides	24	18	15
12-13 Dicarboxylic acids	4	13	11

<sup>a</sup>GLC peak area was assumed to be proportional to molecular weight. Response factors used in semiquantitative acidic product yield calculations are given in Appendix IV. For a given acidic product, the standard deviation for duplicate silylations was generally in the range of  $\pm 25-30\%$ . The significant inaccuracies involved in acidic product analyses mean that yields must be considered as estimates.

<sup>b</sup>Due to the nature of solution preparation, initial concentrations of cobalt(II) in reaction solutions follow the order IV<V<VII.

<sup>c</sup>Percent reaction determined from acetylated samples.

The considerable error encountered in the acidic product analyses (standard deviations of  $\pm 25$ -30% for individual acids from duplicate silylations) may have masked small cobalt ion-induced shifts in the quantities of acidic products which formed during MBG degradation. Nonetheless, the presence of silicate anions in reaction solutions did not significantly influence the acidic product distribution. Further, the presence of cobalt ions in reaction solutions did not alter the types of acids produced during MBG degradation. Within experimental error, cobalt ions did not significantly influence the initial distribution of MBG degradation products, as shifts in acidic product distribution were not clearly evident until after considerable MBG degradation had occurred.

#### MECHANISM OF COBALT-CATALYZED MBG DEGRADATION

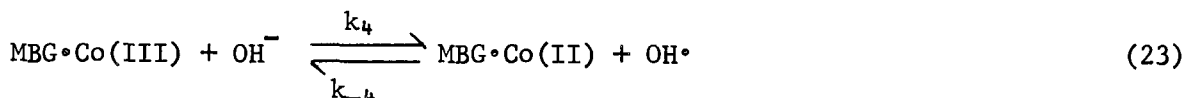
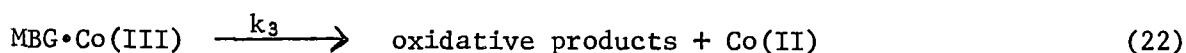
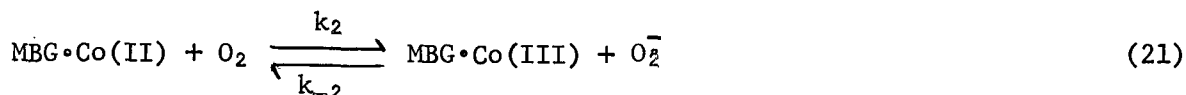
##### GENERAL COMMENTS

The presence of cobalt in reaction solutions did not result in a major shift in the extent of glycosidic bond cleavage, or in the initial distribution of acidic MBG degradation products. This indicated that the primary action of cobalt in oxygen-alkali MBG degradation was to accelerate the rate of MBG degradation. Only soluble cobalt was found to exert a major influence on the catalysis of MBG degradation, and precipitated cobalt reduced the effect of the soluble cobalt through removal of soluble cobalt from solution.

A mechanism of metal ion enhanced oxygen-alkali carbohydrate degradation attributable solely to free radical decomposition of peroxidic intermediates does not adequately account for the extent of degradation encountered in metal ion-catalyzed systems. Hydrogen peroxide levels are known to rapidly reach constant low levels in iron-catalyzed oxygen-alkali MBG degradation (3,29), and it is unlikely that the range of variation in metal ion activity



with metal ion concentration is entirely due to promotion of peroxide decomposition. Indeed, iron is known to promote the formation of stable organic peroxides during oxygen-alkali MBG degradation (29). The series of reactions in Fig. 18 are proposed to more adequately account for the observed catalytic ability of cobalt ions during MBG degradation. Equations (20)-(23) illustrate how an MBG-cobalt complex may participate in catalytic oxidation-reduction reactions comparable to those depicted in Fig. 18.



According to the mechanism in Fig. 18, the addition of alkali to an aqueous cobalt(II) solution results in the precipitation of cobalt(II) hydroxide, and in the solubilization of cobalt(II) as  $\text{Co(OH)}_3(\text{H}_2\text{O})^-$  and  $\text{Co(OH)}_4^{2-}$ , depending on hydroxide ion concentration. An increase in alkalinity, or the presence of silicate anions or coordinating polyols, shifts the equilibrium in favor of soluble ionic cobalt(II). The precipitation (in the absence of oxygen) of cobalt(II) from an alkaline solution supersaturated with respect to cobalt can result in the formation of a highly adsorptive precipitate.  $\text{Co(OH)}_2$  is readily oxidized by oxygen to produce a hydrous cobalt(III) oxide precipitate (54,63). In the presence of certain coordinating species the stability of cobalt(III) in oxidative alkaline solution can be greatly improved [and precipitation of cobalt(III) inhibited] (57) and an oxidation-reduction cycle

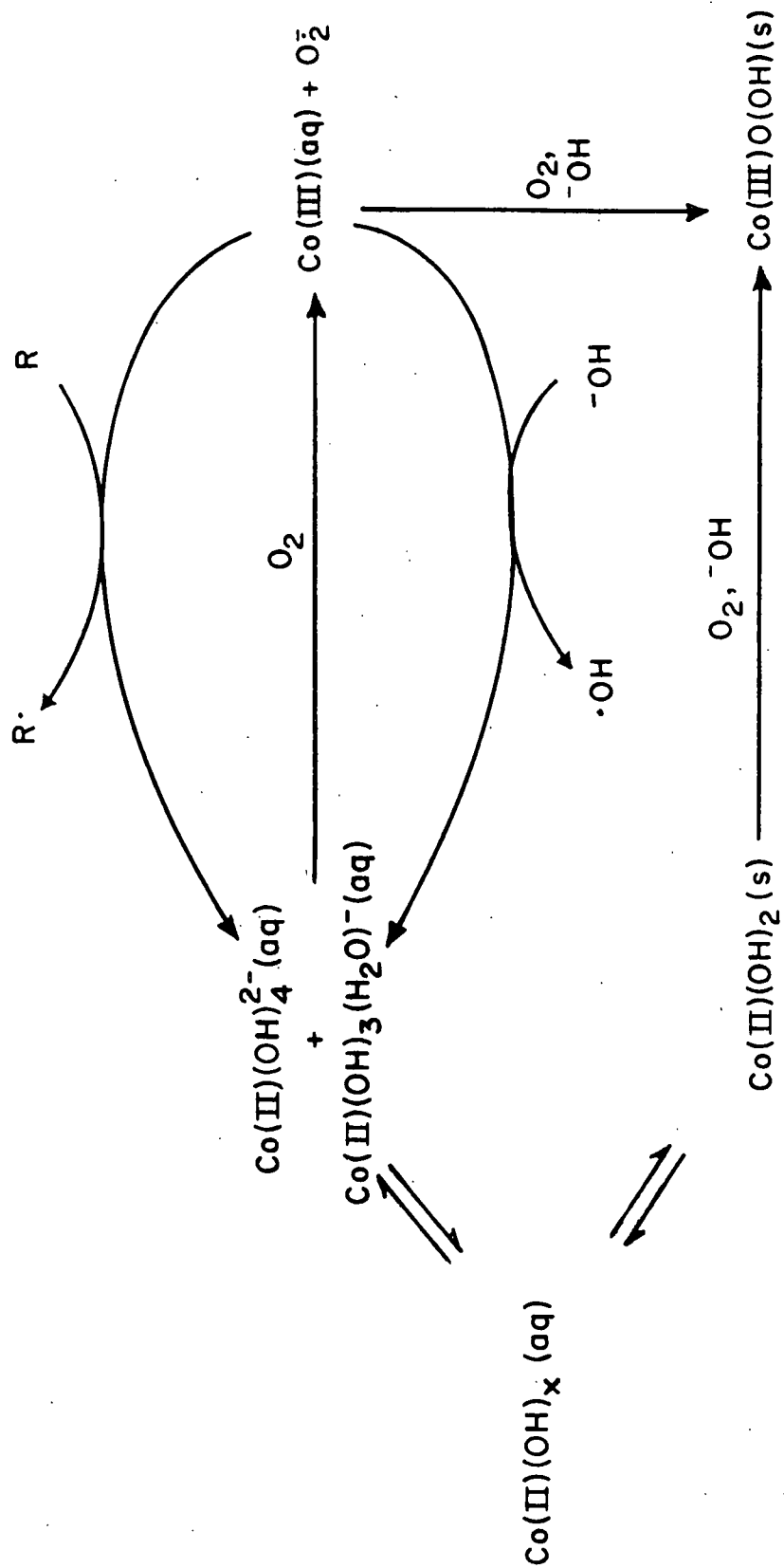


Figure 18. Proposed Pathways of Cobalt-Catalyzed Carbohydrate Degradation and Free Radical Generation

between cobalt(II) and cobalt(III) may be established as shown in Fig. 18.

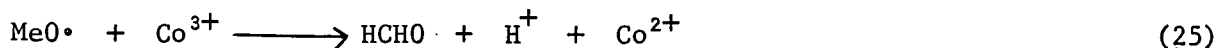
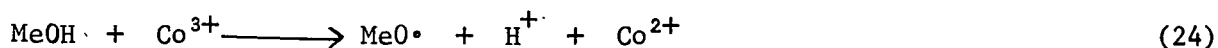
The oxidation of a substrate by a metal ion that exists in two (or more) oxidation states followed by rapid reoxidation of the metal ion by molecular oxygen commonly serves as the basis for a free radical catalytic system (89). Precipitation of cobalt(III) from alkaline solution can result in the formation of a highly adsorptive cobalt(III) precipitate. It seems likely that silicate anions, while solubilizing cobalt(II), also promote the oxidative precipitation of cobalt(III) from solution during MBG degradation. Evidence for the direct oxidation of cobalt(II) by oxygen in solution, and for the consequent degradation reactions which are promoted by such a reaction, is presented in the next section.

#### OXIDATION-REDUCTION OF COBALT

Under acidic conditions, the oxidation of organic compounds by soluble cobalt(III) is well established (53), and in acidic solution under suitable conditions oxygen is capable of oxidizing cobalt(II) to cobalt(III) with the production of hydroperoxy radical ( $\text{HOO}\cdot$ ) (90,91). Also under acidic conditions, the cobalt(III) species is capable of either oxidizing hydroxyl ion to produce hydroxyl radical, or it may oxidize an organic substrate with the production of reactive intermediate free radicals, the latter being the favored reaction (92-94).

Under alkaline conditions the ability of a cobalt(III)-glycerol complex to oxidize aldehydes and methyl ketones under strongly alkaline conditions at room temperature has already been noted (57) (see Cobalt-Carbohydrate Complexation and MBG Degradation). Evidence for oxidation of cobalt(II) to cobalt(III) by oxygen, followed by highly degradative reactions under oxygen-alkali conditions, is provided by the degradation of methanol encountered in the

presence of cobalt ions (see Table V in the section on Methanol Stability). In the absence of cobalt, methanol is stable under the conditions employed during MBG degradations (25,28). In the presence of cobalt, however, methanol was found to be degraded (Table V), indicating that a simple alcohol could be degraded under oxidative alkaline conditions in the presence of cobalt ions. Under acidic conditions, if  $\text{Co}^{3+}$  is produced electrolytically, methanol is degraded according to the mechanism (92-94):



The rate of reaction of cobalt(III) ion with an ionized form of organic compound is also known to be faster than reaction with the unionized compound (93). Under alkaline conditions, the mechanism of cobalt-catalyzed degradation of methanol probably involves the steps shown above, but cobalt(III) would be produced by electron transfer with oxygen in solution (reaction 26).



Superoxide radical, produced in reaction 26, is a potent oxidant and would participate in degradative reactions in the presence of carbohydrates (19,24,95). Cobalt ion-promoted production of superoxide radicals would result in higher steady state concentrations of various radical species. Thus, degradation of MBG may be accelerated by free radical production due to initial oxidation of cobalt(II) by oxygen (Fig. 18). The increase in the pool of degradative radical species in cobalt-containing reaction solutions would result in an enhanced rate of MBG degradation. This is discussed further in the next section.

## INFLUENCE OF COBALT-MBG COORDINATION ON MBG DEGRADATION

Further investigations must be conducted to more completely determine the influence of soluble cobalt ions on the mechanism of MBG degradation in oxygen-alkali. The results presented in this work have shown that soluble cobalt ions are the catalytic species in oxygen-alkali, and that cobalt(II) ions coordinate with MBG in alkaline solution. Cobalt ions did not promote a major shift in glycosidic bond cleavage, as reflected in methanol formation, and cobalt ions did not initially induce significant shifts in the types and amounts of acidic MBG degradation products.

Since cobalt was found to coordinate with MBG, this in itself suggests that cobalt ions alter (possibly in several ways) the mechanism of MBG degradation. One pathway of MBG-cobalt interaction is suggested by the finding at extended reaction times (40-60% reaction) that cobalt ions enhanced the concentrations of dicarboxylic acids detected in cobalt-containing reaction solutions (Tables VIII and IX). In reactions which initially contained soluble cobalt(II) (e.g., reactions XII, XIII, V, and VII) the concentrations of dicarboxylic acids at ca. 40-60% reaction were between 2 and 3 times higher than in the absence of cobalt(II) (Tables VIII and IX). The mechanism shown in Fig. 19 is proposed to account for the enhanced formation of dicarboxylic acids in cobalt ion-containing reactions.

According to this mechanism, cobalt(II) complexes with MBG either at the 2- and 3- positions (I in Fig. 19), or at the 3- and 4- positions. Coordinated cobalt(II) is then oxidized to cobalt(III) by oxygen with the production of superoxide radical, and cobalt(III) in turn oxidizes MBG. In Fig. 19 the oxidation of MBG by cobalt(III) results in the disproportionation of the cobalt ion-MBG complex, and in the formation of the free radical

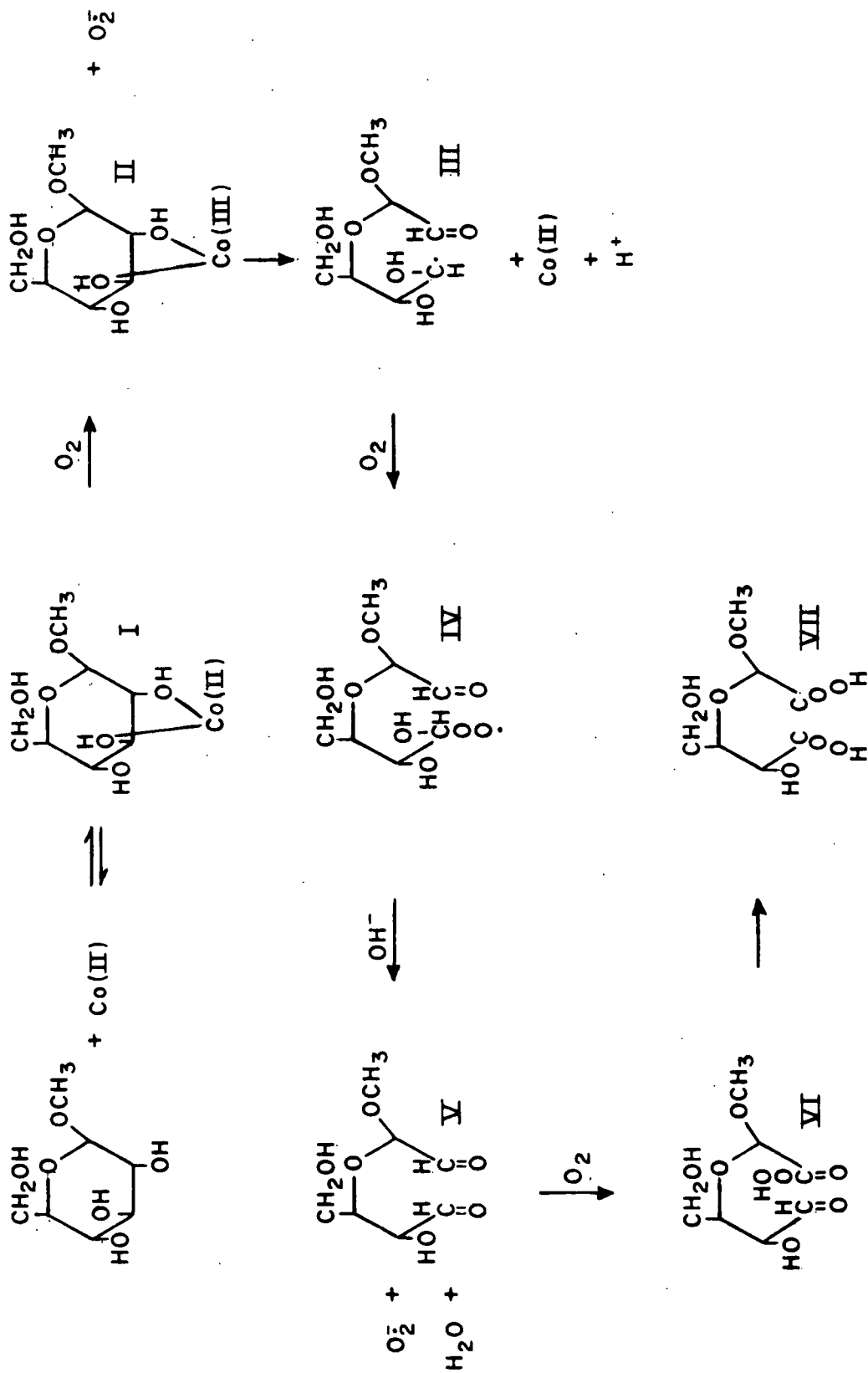


Figure 19. Proposed Mechanism of Cobalt Ion-Catalyzed Dicarboxylic Acid Formation

III and cobalt(II). A comparable reaction has been reported for the ceric(IV) ion oxidation of glucose (96). The free radical III then adds oxygen to produce peroxy radical IV. Radical IV is subject to a rapid base catalyzed elimination reaction producing the dialdehyde V and superoxide radical (97). Either aldehyde moiety in V can be readily oxidized by oxygen to yield a peroxy acid, as shown in VI (98). Peroxy acids are known to react with aldehydes to produce dicarboxylic acids (Eq. 27) (92,93,98), and it is proposed that an intramolecular rearrangement of the peracid species VI produces the dicarboxylic acid VII.



Due to the proximity of the aldehyde and peracid groups in intermediate VI, the reaction resulting in dicarboxylic acid formation would presumably be facilitated.

Since cobalt ion-enhanced dicarboxylic acid formation appears to be favored at extended reaction times, this suggests that cobalt ions initially increase the rate of MBG degradation predominantly through an intermediate species which is also present (but in smaller quantities) in the absence of cobalt ions. Such a species would most likely be superoxide radical. Superoxide radical is formed in the first step of the proposed mechanism of dicarboxylic acid formation (Fig. 19). If cobalt(III) in the cobalt(III)-MBG complex (Fig. 19) oxidized MBG relatively slowly, then cobalt ion-enhanced dicarboxylic acid formation would be delayed (as results in Table VIII suggest). The consequence of a relatively delayed cobalt(III) oxidation of MBG would be cobalt ion promoted production of radical species with MBG serving to maintain cobalt(III) in solution [i.e.,  $k_2 \gg k_3$  in Eq. (21) and (22)].

Superoxide radicals produced by oxygen oxidation of cobalt(II) to cobalt(III) would promote radical chain reactions which would accelerate the rate of MBG degradation. An alternate reaction competing with cobalt(III) oxidation of coordinated MBG may be the cobalt(III) oxidation of other species also coordinated with cobalt(III) (i.e.,  $\text{OH}^-$  and  $\text{H}_2\text{O}$ ). At later reaction times a complicating factor may be stable complex formation between cobalt(III) and acidic MBG degradation products as discussed in the section on Cobalt-Carbohydrate Complexation and MBG Degradation.

The difficulty in establishing the action of cobalt(III) in oxygen-alkali arises from a lack of information on the chemistry of alkaline cobalt(III). To further clarify how cobalt ions influence the mechanism of MBG degradation some fundamental work on the chemistry and stability of cobalt(III) in alkaline solution should first be conducted. For instance, cobalt(III) could be produced electrolytically in alkaline solutions, and measurements of the oxidizing action of cobalt(III) could be made both in the presence and absence of coordinating species. Degradation products produced due to cobalt(III) oxidation of selected carbohydrates in the absence of oxygen could pinpoint preferred sites of cobalt(III) (as opposed to oxygen) oxidation. Such experiments could be coupled with spectral (C-13, Raman, and UV-Visible) investigations of alkaline cobalt-carbohydrate complexation to establish the sites of cobalt-carbohydrate complexation. For example, comparison of the ability of MBG, methyl  $\beta$ -D-ribopyranoside (MBR), and methyl  $\beta$ -D-xylopyranoside (MBX) to stabilize cobalt(II) in alkaline solution would provide needed information on coordination sites, and on the importance of ring hydroxyl orientation on cobalt ion-carbohydrate complexation. Studies with simple alcohols (e.g., glycerol and 1,3-propanediol) would help clarify the strength of 1,2-versus 1,3- chelation of cobalt ion with polyols. Clearly, much fundamental



work needs to be done before the action of cobalt ions (and by extension other similarly catalytic transition metals) on oxygen-alkali carbohydrate degradation is fully understood.

#### COBALT-CATALYZED MBG DEGRADATION IN $\text{H}_2\text{O}_2$ -ALKALI AND $\text{O}_2$ -ALKALI

The results discussed in this work indicate that the precipitation and adsorption characteristics of alkaline cobalt ion solutions are such that the rate of MBG degradation is dependent upon the concentration of soluble cobalt ion in a given reaction solution. Results also show that cobalt ions do not induce a major shift in favor of glycosidic bond cleavage during MBG degradation in oxygen-alkali. This is in accord with Ericsson et al. (15) who analyzed a single sample from an MBG degradation in oxygen-alkali at  $10^{-5}\text{M}$  cobalt(II) level and found no significant cobalt-induced shift in MBG degradation products.

However, in the degradations of MBG in  $\text{H}_2\text{O}_2$ -alkali in the presence of cobalt(II) conducted by Weaver et al. (27,50) glycosidic bond cleavage was found to vary with cobalt ion concentration. At the  $10^{-4}\text{ mM}$  cobalt level glycosidic bond cleavage was enhanced (90-95% of MBG degradation occurred through glycosidic bond cleavage), while an increase in cobalt(II) concentration to  $10^{-3}\text{ mM}$  resulted in a decrease in glycosidic bond cleavage to roughly the level found in the absence of cobalt (ca. 60%). Why the extent of glycosidic bond cleavage in  $\text{H}_2\text{O}_2$ -alkali should vary with cobalt ion concentration while remaining constant in the oxygen-alkali system investigated in this work is not entirely clear. Numerous rationalizations are possible. First, the initial conditions employed by Weaver et al. (27,50) in  $\text{H}_2\text{O}_2$ -alkali degradation of MBG [ $10\text{-}30\text{ mM}$  MBG,  $1.25\text{M}$  NaOH,  $1\text{ mM}$   $\text{MgSO}_4$ ,  $50\text{-}60^\circ\text{C}$ ,  $200\text{ mM}$   $\text{H}_2\text{O}_2$ ,  $10^{-3}\text{-}10^{-4}\text{ mM}$  Co(II)] were very different from those used in this work

[95.5 mM MBG, 1.25M NaOH, 0.68 MPa  $O_2$  pressure, 120°C, 0.01-0.25 mM Co(II)].

It is also possible that the reaction of cobalt(II) with hydrogen peroxide, rather than with oxygen, may have resulted in a significantly different initial distribution of degradative radical intermediates, and this may have altered the mechanism of MBG degradation at the  $10^{-4}$  mM level. A third possibility is that the use of magnesium ion by Weaver et al. (27,50) (to improve the reproducibility of reactions) may have altered the mechanism of MBG degradation when cobalt ions were present. At this time there is insufficient information to choose which, if any, of the above explanations can account for the cobalt ion-induced shift in mechanism found by Weaver et al. (27,50) in an  $H_2O_2$ -alkali system at the  $10^{-4}$  mM cobalt(II) level.

## CONCLUSIONS

The catalysis of oxygen-alkali MBG degradation by cobalt(II) is a function of cobalt ion solubility. Increasing the concentration of cobalt ions in solution increases the rate of MBG (methyl  $\beta$ -D-glucopyranoside) degradation, as reflected in an initial 0.5 order pseudo rate dependence on dissolved cobalt ions.

During the precipitation of cobalt ions from alkaline solution, the concentration of ionic cobalt in solution can be drastically reduced due to the incipient formation of adsorptive cobalt(II) and cobalt(III) precipitates. In the absence of oxygen, formation of an adsorbent cobalt(II) hydroxide precipitate in a solution initially supersaturated with cobalt(II) results in the removal of otherwise soluble cobalt ions from solution. The consequent decrease in soluble cobalt ion concentration results in a reduced rate of oxidative MBG degradation. Cobalt ions precipitated from supersaturated solution under anaerobic conditions lose essentially all catalytic ability. Cobalt which precipitates from oxidative alkaline solution during MBG degradation is also very highly adsorbent, and the onset of precipitation coincides with a rapid decline in the rate of MBG degradation. Other than being adsorptive, the precipitate of cobalt formed under oxidative conditions is comparatively inert.

Silicates and certain polyols (MBG, glycerol, sorbitol, and ethylene glycol) coordinate with, and stabilize, cobalt(II) in alkaline solution. The sequence of preparation of alkaline cobalt solutions containing polyols or silicates is very important in the stabilization of cobalt in alkaline solution. For stabilization of cobalt(II) in alkaline solution to occur, the stabilizing agent must form a complex prior to adsorptive precipitate formation. Addition

of aqueous cobalt(II) to an alkaline polyol or alkaline silicate solution results in the stabilization of cobalt(II) in alkaline solution. The enhanced solubility of cobalt(II) attributable to complexation results in an increased rate of MBG degradation under oxidative alkaline conditions.

The ability of cobalt to increase the rate of MBG degradation is explained in terms of a catalytic system consisting of MBG and carbohydrate substrates, cobalt(II) and cobalt(III) ions, and oxygen. It is proposed that cobalt(II) is oxidized to cobalt(III) by oxygen with the production of degradative superoxide radical ( $O_2^{\cdot-}$ ). This reaction is then followed by the oxidation of organic substrates by cobalt(III) to produce radical organic species which are subject to further oxidative decomposition reactions.

The products of MBG degradation are influenced only to a limited extent by cobalt ions. Glycosidic bond cleavage is not significantly influenced by the presence of cobalt ions, and the same acidic products are produced both in the presence and absence of cobalt. Soluble cobalt increases the concentrations of dicarboxylic acids present in reaction solutions relative to uncatalyzed degradations. A mechanism involving oxidation of MBG by coordinated cobalt(III) is proposed to account for enhanced dicarboxylic acid concentrations in cobalt-containing reaction solutions.

## EXPERIMENTAL

### GENERAL ANALYTICAL PROCEDURES

Melting points were determined on a Thomas Hoover capillary melting point apparatus which had been calibrated with known compounds.

Optical rotations were measured on a Perkin-Elmer Model 141 MC recording polarimeter at room temperature and at 589 nm.

Thin-layer chromatography (TLC) was conducted on microscope slides coated with Silica gel G (Brinkman Instruments, Inc.). Slides were developed with ethyl acetate and detection was completed by spraying with methanolic sulfuric acid (20%, v/v) followed by charring on a hot plate.

Quantitative gas-liquid chromatography (GLC) was conducted on a Varian Aerograph 1200 gas Chromatograph equipped with a hydrogen flame detector. The Aerograph output was fed into either a Honeywell Electronic 16 recorder with a Disc integrator, or a Perkin-Elmer Sigma 10 Chromatography Data Station. Prepurified nitrogen (Matheson Gas Products) was used as the carrier gas. Columns and operating conditions are given in Appendix IV.

Mass spectral analyses were conducted on a Hewlett-Packard 5985 GC/MS System interfaced with a jet separator to a Hewlett-Packard 5840A gas chromatograph. Helium (prepurified, Matheson Gas Products) was used as the carrier gas. Chromatographic conditions and mass spectrometer control settings are reported in Appendix V.

## SOLUTIONS AND REAGENTS

### WATER

Triply-distilled (3-D) water was used in preparing reaction solutions, and in cleaning reactors and labware. The second distillation was from alkaline permanganate to remove any organic contaminants.

### OXYGEN AND NITROGEN

Oxygen was obtained from Airco, Inc. New York, NY and had a minimum guaranteed purity of 99.5%. Nitrogen was obtained prepurified from Matheson Gas Products, Joliet IL.

### SODIUM HYDROXIDE

#### Extracted Sodium Hydroxide

The purified sodium hydroxide solution used in this work was the same as that prepared and used by Hearne (25). The purification procedure involved filtration and extraction of complexed transition metals from a solution of reagent grade sodium hydroxide according to the method of Reiner and Poe (51). Only a general description of the preparative procedure is included here.

To an aqueous solution of reagent grade sodium hydroxide in a round bottomed flask was added phenyl-2-pyridyl ketoxime (Eastman Chemical Co., Hauppauge, NY) in a minimum of hot ethanol, and 10% palladium on charcoal catalyst. Hydrogen gas was bubbled through the mixture, which was heated to 100°C for 8 hours. The mixture was cooled, filtered through a sintered glass filter, and unprecipitated complexes of iron, copper, cadmium, cobalt, and nickel were extracted into 1/3 (v/v) ethanol/isopentyl alcohol. The

procedure was then repeated in the absence of catalyst and with nitrogen rather than hydrogen bubbling. This was followed by extraction with chloroform, in the place of ethanol/isopentyl alcohol, and the extracted sodium hydroxide was boiled for 6 hours (with nitrogen bubbling) to remove the last traces of solvent. The purified sodium hydroxide solution was stored in a paraffin-lined teflon-stoppered glass jar under a nitrogen atmosphere. Analysis of the caustic by GLC showed no traces of ethanol, and a UV spectrum was identical to a spectrum obtained with unextracted caustic, showing that the phenyl-2-pyridyl ketoxime had been removed (UV detection limit of  $6 \times 10^{-7} \text{M}$  with a 1 cm cell (51).

#### Ultrapure Sodium Hydroxide

Ultrapure sodium hydroxide was purchased as a 30% solution from Alfa Division, Ventron Corporation, Danvers, MA. Maximum assays of impurities in the concentrated NaOH were, in ppm: copper, 0.01; nickel, 0.01; cobalt, 0.01; iron, 0.05; zinc, 0.05; cadmium, 0.01; aluminum, 0.05; manganese, 0.01; magnesium, 0.2; calcium, 1; silicate ( $\text{SiO}_2$ ), 5.

#### METHYL $\beta$ -D-GLUCOPYRANOSIDE (MBG)

Methyl  $\beta$ -D-glucopyranoside was obtained from Pfanstiehl Laboratories, Inc. (Waukegan, IL). Traces of reducing sugars were removed by refluxing in 1M NaOH for 1 hour, followed by deionization over a mixture of Amberlite MB-3 and IR-120 ion exchange resins, and recrystallization from ethanol (2X). The product had a melting point of 109-111°C, and softened at 105°C:  $[\alpha]_D^{19} = -34.5^\circ$  ( $\text{H}_2\text{O}$ ,  $c = 2.0$ ), calculated as hemihydrate. The MBG was chromatographically pure. Literature values for the melting point range from 104-111°C and specific rotations vary from -31.4 to -34.2 (99).

## INTERNAL STANDARDS

### n-BUTYL $\beta$ -D-GLUCOPYRANOSIDE (BBG)

n-Butyl  $\beta$ -D-glucopyranoside was prepared by deacetylation of n-butyl-2,3,4,6-tetra-O-acetyl- $\beta$ -D-glucopyranoside, which was prepared via a modified Koenigs Knorr synthesis involving mercuric salts (100). The tetraacetate (25 g) was deacetylated with sodium methoxide (1N, 3.5 mL) in methanol (175 mL) by stirring the solution at room temperature. The reaction was complete after 45 minutes as followed by thin layer chromatography (see General Analytical Procedures for a description of the thin layer chromatography technique). The solution was neutralized with Amberlite MB-3 ( $H^+$ ,  $OH^-$ ) ion exchange resin, filtered, and concentrated to a syrup. Two crystallizations from ethyl acetate afforded n-butyl  $\beta$ -D-glucopyranoside: 12 g (63%), m.p. 66-67°C,  $[\alpha]_D^{21} = -36.4$  ( $H_2O$ ,  $c = 1.99$ ). Literature: m.p. 64-65°C,  $[\alpha]_D = -34.1$  ( $H_2O$ ) (101).

### ETHANOL

Reagent grade ethanol (95%) was used as an internal standard in methanol analyses.

## REACTION CONDITIONS AND SOLUTION ANALYSIS

### REACTOR SYSTEM

The reactor vessel and air-driven magnetic stirrer were the same as those described by Millard (24). The oil bath, temperature control apparatus and sampling system were the same as those described by Hearne (25). The reader is referred to these authors for detailed descriptions of the reactor apparatus.



Briefly, the reactor (Fig. 20) was a completely teflon-lined brass container which could be sampled while hot and under pressure. An air-driven turbine containing magnets was clamped to the bottom of the reactor and provided agitation. The reactor-stirrer assembly was raised and lowered into an insulated oil bath via a rack and pinion mechanism. An immersion circulator equipped with a preset thermostat controlled reactor temperature ( $120^{\circ}\text{C}$ ) to  $\pm 0.2^{\circ}\text{C}$  as sensed by the output of a thermocouple lead built into the reactor lid. The reactor was sampled under pressure through teflon lines which were controlled by pressure-tight inert valves. The sampling lines were arranged such that a small sample (ca. 0.8 mL) could be taken through a sample loop, or a larger sample of random size could be taken through a bypass loop.

#### CONDITIONING OF REACTOR AND LABWARE

All labware (glass and polypropylene) and teflon reactor surfaces were cleaned by successive washings with Alconox, distilled water, acetone, 35% nitric acid (v/v) and triply distilled water. The reactor and labware were allowed to air-dry before use.

#### PREPARATION OF REACTION SOLUTIONS

Triply distilled water (ca. 500 mL) was boiled, with the aid of teflon boiling chips, for 10 minutes and allowed to cool in a nitrogen atmosphere inside a glove bag. Sufficient stock sodium hydroxide solution (33.5 g extracted NaOH or 33.0 g ultrapure NaOH) was weighed into a volumetric flask (250 mL) such that dilution to the mark with cooled 3D water provided a  $1.25\text{M}$  solution of NaOH. If necessary, adjustments of concentration were made to attain an alkali concentration of  $1.25\text{M} \pm 0.05\text{M}$  as determined by titration against potassium acid phthalate to a phenolphthalein end point.

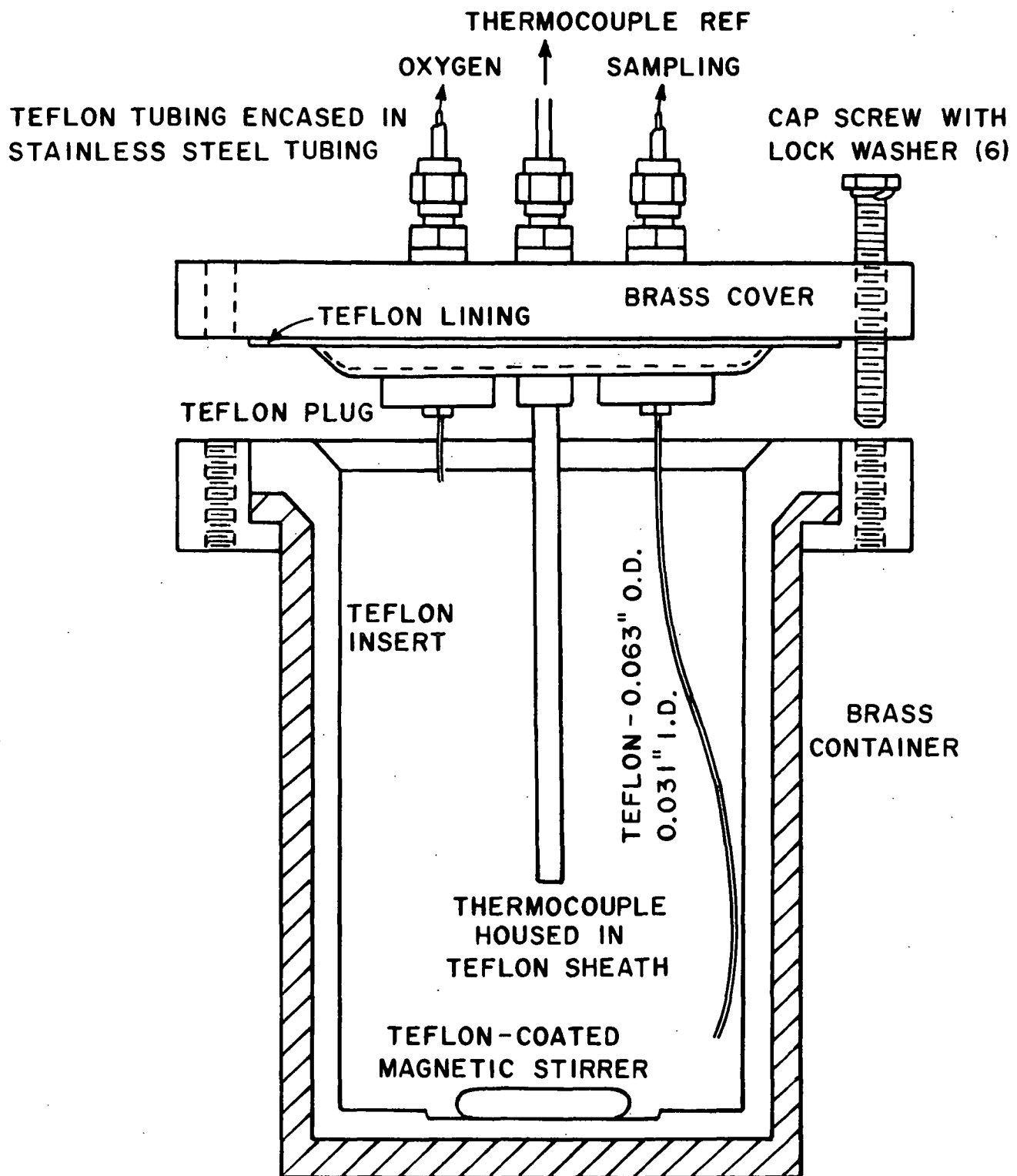


Figure 20. Teflon-lined Reactor Vessel

The alkaline solution (ca. 200 mL) was then poured (under nitrogen) into the reactor and from the weight of the volumetric flask before and after addition of the solution to the reactor, the volume added was calculated from the density of 1.25M NaOH solution (1.0529 g/mL). Sufficient MBG was then added to the reactor to achieve a concentration of 95.5 mM, the reactor cover was bolted into place, and the solution was back-flushed through the sample line with nitrogen (5 min). The reactor was then mounted on the stirrer, sample and oxygen lines were connected (with valves closed), the thermocouple was zeroed, and the reactor was lowered into the oil bath and the bath turned on.

Cobalt-containing reaction solutions were prepared in the same manner (under nitrogen) as solutions not containing added cobalt(II). A stock aqueous  $\text{CoSO}_4 \cdot 7\text{H}_2\text{O}$  solution was prepared [with boiled and cooled (under nitrogen) 3-D water] to be 25 times as concentrated in cobalt(II) as the desired reaction solution. To the stock NaOH solution in the 250 mL volumetric flask was added ca. 200 mL of 3-D water. The mixture was thoroughly shaken and 10 mL of the stock aqueous cobalt(II) solution was pipetted, with shaking, into the flask. The volumetric flask was filled to the mark with 3-D water, shaken, and the reactor was charged with the reaction solution. Sufficient powdered MBG was added to make the solution 95.5 mM in MBG, and the reactor was sealed and nitrogen purged in the usual fashion. In a reaction at the 0.25 mM cobalt(II) level with reversed reaction solution preparation procedure (reaction XVIII) the powdered MBG was dissolved in ultrapure NaOH prior to addition of stock aqueous cobalt sulfate.

The reaction with added cobalt(III) precipitate (reaction VIII) was conducted by isolating the precipitate from a reaction (reaction VIIla, 0.25 mM  $\text{CoSO}_4 \cdot 7\text{H}_2\text{O}$ , extracted NaOH, reaction run for 14 hours) and adding

the precipitate formed to a reaction solution prepared to be 0.05 mM in  $\text{CoSO}_4 \cdot 7\text{H}_2\text{O}$  (reaction VIII). The precipitate formed in reaction VIIIA was centrifuged from reaction solution (190 mL), and the precipitate was washed and centrifuged twice more with two 5 mL volumes of 1.25M NaOH. The precipitate was added to reaction solution VIII (200 mL, 0.05 mM in added soluble  $\text{CoSO}_4 \cdot 7\text{H}_2\text{O}$ , 1.25M extracted NaOH) as a suspension in 0.5 mL 1.25M NaOH. The elapsed time between precipitate isolation and initiation of reaction VIII was 20 hours.

Degradation of methanol (51.4 mM) in the presence of cobalt(II) (0.25 mM) was conducted as if it was an MBG degradation, except that aqueous methanol was added to stock ultrapure NaOH prior to mixing with aqueous cobalt(II), and no MBG was present during reaction.

#### REACTION SAMPLING

After the thermocouple output indicated that the reactor temperature had stabilized at 120°C (ca. 5 hr for a cold oil bath), the sample lines were purged with reaction solution, a time zero sample was taken, and the reactor was pressurized with oxygen (0.68 MPa partial  $\text{O}_2$  pressure at 120°C). Generally, three samples were obtained each time the reactor was sampled. Two samples (ca. 0.8 mL) were taken into tared 4 mL vials, one sample being used for glycoside analysis and the other for methanol analysis. A larger sample (ca. 8 mL) was retained for acidic product, methoxyl, and acid hydrolysis analyses. After samples were obtained, the sample tubing was back-flushed with water and acetone and vacuum dried. Before samples were taken, sample lines were vented twice with ca. 2 mL reaction solution each time to purge any solution caught between the reactor and the sampling valves from earlier samplings.

## ANALYSIS OF REACTION SOLUTIONS

### Glycoside Analysis

To an accurately weighed sample of reaction solution (ca. 0.8 g), internal standard (an aqueous solution of BBG) was added gravimetrically. The mixture was deionized over an Amberlite MB-3 ( $H^+$ ,  $OH^-$ ) resin column (5 mL) and eluted with distilled water (3 x 4 mL). The deionized sample was evaporated in vacuo to dryness. Each dried sample was dissolved in dry pyridine (1.0 mL) and acetylated by addition of acetic anhydride (0.4 mL). After 18 hr of mechanical shaking, ice water (8 mL) was added to each sample and the shaking was continued for an additional 0.5 hr. The aqueous mixture was extracted with  $CHCl_3$  (2 x 5 mL), and the combined chloroform extracts were washed with 1N HCl (15 mL) and distilled water (10 mL). The chloroform extract was then dried over sodium sulfate, decanted, and evaporated in vacuo to ca. 1 mL in volume. The acetylated glycosides were analyzed in triplicate by GLC (Appendix IV, conditions A).

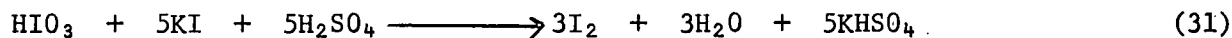
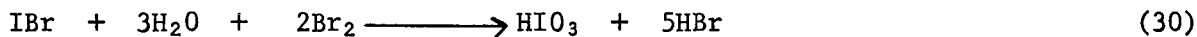
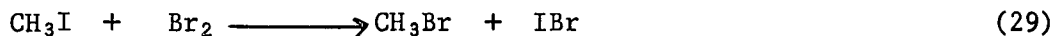
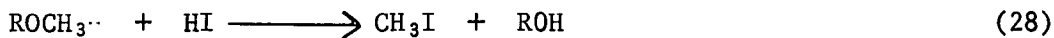
### Methanol Analysis

To an accurately weighed sample of reaction solution (ca. 0.8 g) internal standard (aqueous ethanol) was added gravimetrically and the mixture was analyzed directly, in triplicate, by GLC (Appendix IV, conditions B). The method of analysis was based on the technique reported by Sims (102).

### Methoxyl Analysis

Methoxyl concentrations of reaction solutions were determined by a method based on Institute Method 18 (103). The procedure involves the reaction of methoxyl groups with hydriodic acid to produce methyl iodide (reaction 28). The methyl iodide reacts with bromine to form iodobromine (reaction 29) and the iodobromine reacts with water and bromine to form

iodic acid (reaction 30). Iodic acid is determined by thiosulfate titration of the iodine liberated according to reaction (31). One mole of methoxyl produces three moles



of iodine. A diagram of the methoxyl apparatus employed is shown in Fig. 21. The procedure for methoxyl analysis was as follows.

A sufficient amount of a water suspension of red phosphorous (0.06 g/100 mL  $\text{H}_2\text{O}$ ) was placed in the scrubber (D) such that the scrubber inlet was covered to a depth of 4 mm. Into the reaction flask (A) was placed 10 mL of hydriodic acid and 3 drops of hypophosphorous acid. The reaction flask was attached to the air-cooled condenser (C), and  $\text{CO}_2$  gas was bubbled (B) through the mixture at the rate of 2 bubbles/second as determined at the scrubber. The solution was then heated to boiling for 45 minutes (to purge the system of any impurities) with a microburner such that the height of the refluxing liquid reached approximately half way (ca. 10 cm) up the condenser. The absorbing solution was prepared by placing 30 drops of bromine (approximately 0.6 mL) in 20 mL of a 10% solution of potassium acetate in glacial acetic acid. This solution was placed in receivers E (15 mL) and F (5 mL). The reaction flask was allowed to cool to room temperature, and following the rapid addition of a weighed sample of reaction solution (ca. 1 g) to the reaction flask the system was closed. The flask was then heated, as before, to reflux for 75 minutes. This was determined to be sufficient time to complete the reaction and sweep out the apparatus. The contents of both receivers were then

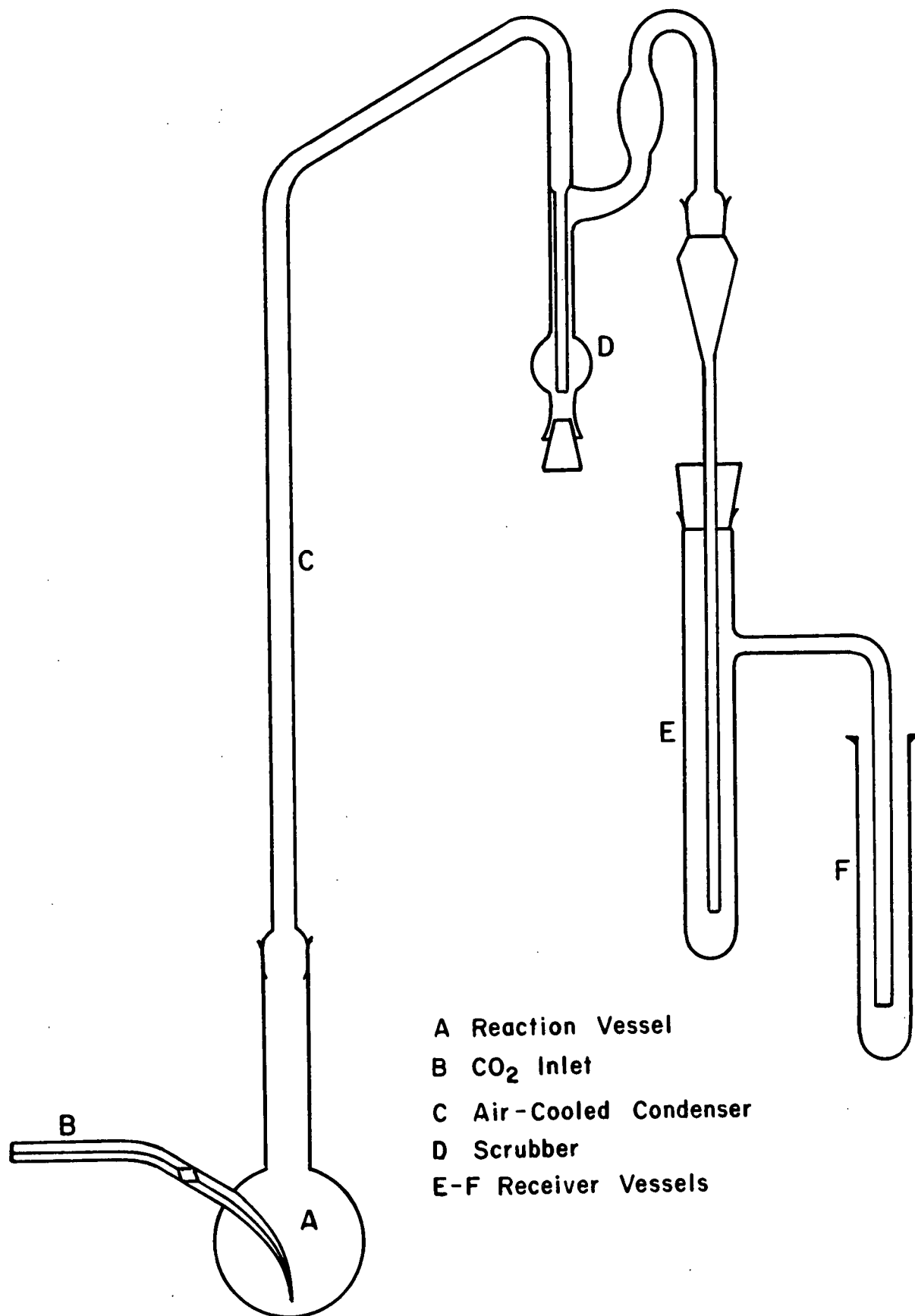


Figure 21. Apparatus Used for Methoxyl Determinations

washed into a 250 mL Erlenmeyer flask which contained 25 mL of 25% sodium acetate solution, and the mixture was diluted to ca. 125 mL with distilled water. Formic acid (88%, ca. 10 drops) was added until the color of the remaining bromine disappeared and 12 additional drops were added. After two minutes, 10 mL of 10% KI solution and 10 mL of 10% sulfuric acid were added to the solution. Free iodine was titrated with sodium thiosulfate (0.1 or 0.01N) to a starch endpoint. Methoxyl concentration was calculated using Eq. (32).

$$\text{CH}_3\text{O} = \frac{(N)(V)(\rho)}{(6)(W)} \quad (32)$$

where:  $\text{CH}_3\text{O}$  = concentration of methoxyl groups in the sample,  
moles/liter

N = normality of thiosulfate solution, N

V = volume of thiosulfate solution, mL

$\rho$  = density of reaction solution, g/mL

W = weight of reaction sample, g.

### Acid Hydrolysis

To complement the technique of methoxyl analysis mentioned above, selected reaction samples were hydrolyzed with hydrochloric acid to measure the methanol produced. This hydrolysis released methanol from MBG methyl esters. Authentic methoxyacetic acid, a reported product in oxidative alkaline reactions of glycosides (25), was found to be unaffected by the hydrolysis procedure.

Hydrolyses were conducted in 5 mL sealable glass ampules. To each ampule was added 0.5 g of reaction sample, 0.5 g of aqueous ethanol internal standard and 1 mL of 5N HCl. The ampules were immediately sealed with the aid of an oxy-acetylene flame and were heated in a water bath maintained at 80°C for a minimum of 24 hrs. to complete hydrolysis. The samples were



then cooled, made slightly alkaline with a 20% solution of NaOH, and analyzed for methanol by GLC (Appendix IV, conditions B).

#### Acidic Product Analysis

To ca. 2 mL of reaction sample (determined gravimetrically), internal standard (BBG, as an aqueous solution) was added gravimetrically. The mixture was deionized over an Amberlite IR-120 ( $H^+$ ) resin column (5 mL) and eluted with distilled water (3 x 8 mL). The deionized solution was immediately made alkaline by addition of  $NH_4OH$  (ca. 1 mL) and the sample was concentrated in vacuo ( $<60^\circ$ ) to ca. 1 mL in a pear shaped flask and transferred to a 4 mL screw-top vial. Following evaporation in vacuo ( $<60^\circ$ ) to dryness, the sample was stored in a vacuum desiccator over  $P_2O_5$  for a period of at least two hours to remove the last traces of water.

Each sample vial was fitted with a septum and the sample residue was dissolved in pyridine (0.5 mL, silylation grade, Pierce Chemical Co.) and, to assist dissolution, the vial was heated in a block heater ( $60^\circ C$ , 15 min). The mixture was then treated with BSTFA + 1% TMCS (0.5 mL, Pierce Chemical Co.) and mechanically shaken for 12 hours. The silylated sample was analyzed in duplicate by GLC (Appendix IV, conditions C), or GLC-MS (Appendix V).

#### TRACE METAL ANALYSIS

##### PLASMA EMISSION SPECTROMETRY

Samples of reaction solutions obtained at the end of reaction runs were analyzed for trace element content by inductively coupled argon plasma emission spectrometry. Analyses were conducted by Trace Elements, Inc., Park Ridge, IL, for aluminum, boron, cadmium, chromium, cobalt, copper, iron,

magnesium, manganese, nickel, silicon, and zinc. Results of these analyses are tabulated in Appendix I.

#### ATOMIC ABSORPTION SPECTROSCOPY

Atomic absorption analyses were conducted for cobalt and silicon on selected reaction solution samples and alkaline solutions. Analyses were performed on a Perkin-Elmer Model 305 spectrophotometer at 240.7 nm using an air-acetylene flame for cobalt, and at 251.6 nm using a nitrous oxide-acetylene flame for silicon.

For cobalt analyses of alkaline solutions, standard cobalt reference solutions were prepared to be 1.25M in NaCl, and 0.0, 0.8, 2.5, 5.0, and 8.5 ( $\times 10^2$ ) mM in cobalt sulfate (0.0, 0.5, 1.5, 3.0, and 5.0 mg/L). Reaction solution samples were centrifuged (2000 rpm, 5 min) to remove any suspended material from solution immediately prior to analysis. Other alkaline solutions analyzed for soluble cobalt concentration were filtered (ashless filter paper) immediately prior to analysis.

For silicon analyses, a standard silicon solution was prepared by fusing 0.2139 g silicon dioxide powder with 2 g sodium carbonate in a platinum crucible. The melt was dissolved in deionized water and was transferred to a 100 mL volumetric flask and diluted to the mark, to yield a 1000 mg/L silicon solution. Standard reference solutions were prepared to be 0.31M in NaOH, and 20, 40, 80, 120, and 140 mg/L in silicon. Reaction solutions were diluted to four times their original volume with distilled water (to make them 0.31M in sodium) immediately prior to analysis.

## VISIBLE SPECTRA OF ALKALINE COBALT SOLUTIONS

Visible spectra were obtained on a Perkin-Elmer 576 ST spectrophotometer. Alkaline cobalt solutions containing silicates, borates, or polyols were all prepared in the same manner. To 1 mL of 10M NaOH in a 5 mL volumetric flask continuously purged with nitrogen through a capillary tube was added 1 mL of an aqueous stock solution containing the additive of interest (silicate, borate, or polyol). To this mixture was added 1 mL of 6.25 mM  $\text{CoSO}_4 \cdot 7\text{H}_2\text{O}$ . Stock silicate solutions (0.021, 0.036, 0.108, 0.213M) were prepared with sodium meta-silicate ( $\text{Na}_2\text{SiO}_3 \cdot 7\text{H}_2\text{O}$ ). A stock borate solution was prepared to be 0.210M in sodium borate ( $\text{Na}_2\text{B}_4\text{O}_7 \cdot 10\text{H}_2\text{O}$ ). Stock polyol solutions were: 0.300M in MBG; 0.300M in sorbitol; 0.303M in glycerol; 0.303M in ethylene glycol. Samples were centrifuged (2000 rpm, 5 min) to remove unsettled precipitate, and visible spectra of the supernatant solutions were immediately obtained. Time lag between sample preparation and completion of analysis was 15-20 minutes.

#### ACKNOWLEDGMENTS

The author gratefully acknowledges the guidance and assistance provided by the members of his thesis advisory committee: Drs. R.H. Atalla, L.R. Schroeder, and N.S. Thompson, (chairman). Special thanks go to Drs. Schroeder and Thompson for the continued interest and encouragement they offered in countless discussions.

Thanks also go to the many members, past and present, of the faculty, staff and students of The Institute of Paper Chemistry for their professional help and personal friendship.

Above all I thank my parents and especially my wife for their support and understanding.

LITERATURE CITED

1. Robert, A., Traynard, P., and Martin-Borret, O., Fr. pat. 1,387,853 (Dec. 28, 1968); U.S. pat. 3,384,553 (May 21, 1968).
2. Smith, L., Calvert, D. W., Robert, A., and Viallet, A., U.S. pat. 3,657,065 (1972).
3. Sinkey, J. D., and Thompson, N. S., Paperi Puu 56(5):473 (1974).
4. Gustavsson, R. and Swan, B., Tappi 58(3):120 (1975).
5. Gilbert, A. F., Pavlovova, E., and Rapson, W. H., Tappi 56(6):95 (1973).
6. Manouchehri, M. and Samuelson, O., Svensk Papperstid. 76(13):486 (1973).
7. Robert, A., and Viallet, A., Revue ATIP 25:237 (1971).
8. Samuelson, O., and Stolpe, L., Tappi 52(9):1709 (1969).
9. Ericsson, B., Lindgren, B. O., and Theander, O., Svensk Papperstid. 74(22):757 (1971).
10. Kolmodin, H., and Samuelson, O., Svensk Papperstid. 76:71 (1973).
11. Ericsson, B., Lindgren, B. O., and Theander, O., Cellulose Chem. Technol. 7:581 (1973).
12. Akim, G. L., Paperi Puu 55(5):389 (1973).
13. Brooks, R. D., and Thompson, N. S., Tappi 49:362 (1966).
14. Minor, J. L., and Sanyer, N., J. Polymer Sci., Part C 36:73 (1971).
15. Ericsson, B., Lindgren, B. O., and Theander, O., Cellulose Chem. Technol. 8:363 (1974).
16. Ericsson, B., Lindgren, B. O., Theander, O., and Petersson, G., Carbohyd. Res. 23:323 (1972).
17. Ericsson, B., and Malinen, R., Cellulose Chem. Technol. 8:327 (1974).
18. McCloskey, J. T., Schroeder, L. R., Sinkey, J. D., and Thompson, N. S., Paperi Puu 57:131 (1975).
19. Malinen, R., and Sjostrom, E., Cellulose Chem. Technol. 9:231 (1975).
20. Millard, E. C., Schroeder, L. R., and Thompson, N. S., Carbohyd. Res. 56:259 (1977).
21. Haskins, J. F., and Hogsed, M. J., J. Org. Chem. 15:1264 (1950).

22. Theander, O., Tappi 48:105(1965).
23. Malinen, R., Paperi Puu 57:193(1975).
24. Millard, E. C. The degradation of selected 1,5-anhydroalditols by molecular oxygen in alkaline media. Doctor's Dissertation. Appleton, Wis., The Institute of Paper Chemistry, 1976.
25. Hearne, D. O. The effect of the aglycon and hydroxyl orientation on alkali-oxygen degradations of methyl glucosides. Doctor's Dissertation. Appleton, Wis., The Institute of Paper Chemistry, 1978.
26. Weaver, J. W., Schroeder, L. R., and Thompson, N. S., Paperi Puu 61(1): 31(1979).
27. Weaver, J. W. The alkaline hydrogen peroxide reaction of methyl  $\beta$ -D-glucopyranoside and methyl 4-O-methyl- $\beta$ -D-glucopyranoside. Doctor's Dissertation. Appleton, Wis., The Institute of Paper Chemistry, 1976.
28. McCloskey, J. T. The degradation of methyl  $\beta$ -D-glucopyranoside by oxygen in alkaline solution. Doctor's Dissertation. Appleton, Wis., The Institute of Paper Chemistry, 1971.
29. McCloskey, J. T., Sinkey, J. D., and Thompson, N. S., Tappi 58(2): 56(1975).
30. Kochi, J. K., ed., Free Radicals, vol. 1, p. 628-642. New York, John Wiley & Sons, 1973.
31. Schaumb, W. C., Satterfield, C. N., and Wentworth, R. L. Hydrogen Peroxide, American Chemical Society Monograph Series, no. 128. p. 447-514, 542. New York, Reinhold Publishing Corporation, 1955.
32. Niebauer, R. J. The degradation of ethyl 3,4,6,tri-O-methyl- $\beta$ -D-arabino-hexopyranosidulose in aqueous alkaline hydrogen peroxide solutions. Doctor's Dissertation. Appleton, Wis. The Institute of Paper Chemistry, 1979.
33. Landucci, L. L., and Sanyer, N., Tappi 57(10):97(1974).
34. Landucci, L. L., and Sanyer, N., Tappi 58(2):60(1975).
35. Samuelson, O., and Stolpe, L., Svensk Papperstid. 77(14):513(1974).
36. Lowendahl, L., and Samuelson, O., Svensk Papperstid. 77(16):593(1974).
37. Abrahamsson, K. and Samuelson, O., Svensk Papperstid. 78(4):135(1975).
38. Manouchehri, M., and Samuelson, O., Cellulose Chem. Technol. 12:105(1978).

39. Sjöström, E., and Välttilä, O., Paperi Puu 60(1):37(1978).
40. Malinen, R., and Sjöström, E., Paperi Puu 54(8):451(1972).
41. Samuelson, O., and Stolpe, L., Svensk Papperstid. 74(18):545(1971).
42. Ericsson, B. Oxygen oxidation of cellulose in aqueous alkaline medium. Doctors Dissertation, Stockholm, 1974.
43. Entwistle, D., Cole, E. H., and Wooding, N. S., Textile Research J. 19:527(1949); 19:609(1949).
44. MacDonald, D. M., Tappi 48(12):708(1965).
45. Khan, M. M. T., and Martell, A. E. Homogeneous Catalysis by Metal Complexes, vol. 1, p. 114-160. New York, Academic Press, 1974.
46. Michie, R. I. C., and Neale, S. M., J. Polymer Sci. 2A:2063(1964).
47. Samuelson, O., and Stolpe, L., Svensk Papperstid. 72(20):662(1969).
48. Samuelson, O., and Thede, L., Tappi 52:99(1969).
49. Abrahamsson, K., and Samuelson, O., Svensk Papperstid. 76(13):480(1973).
50. Weaver, J. W., and Thompson, N. S., Unpublished work.
51. Reiner, D., and Poe, D. P., Anal. Chem. 49(6):889(1977).
52. Schenk, J. E., and Weber, W. J., Jr., J. Amer. Water Works Assoc. 60:199(1968).
53. Cotton, F. A., and Wilkinson, G., Advanced Inorganic Chemistry, 3rd ed. p. 875-885, 918. New York, Interscience Publishers, 1972.
54. Trotman-Dickenson, A. F., exec. ed., Comprehensive Inorganic Chemistry, vol. 3, p. 1071-1094. New York, Pergamon Press, 1973.
55. Gordon, S., and Schreyer, J. M., Anal. Chem. 23(2):381(1951).
56. Rendleman, J. A., Jr. Ionization of Carbohydrates in the Presence of Metal Hydroxides and Oxides, in Carbohydrates in Solution, Advances in Chemistry Series, no. 117, p. 51-69. Washington, American Chemical Society, 1973.
57. Gordon, S. Properties of cobalt(II) and cobalt(III) in strongly alkaline solutions. Doctor's Dissertation. Lexington, Kentucky, University of Kentucky, 1951.
58. Baes, C. F., Jr., and Mesmer, R. E., The Hydrolysis of Cations, p. 238-242, 336-342. New York, John Wiley & Sons, 1976.
59. Cotton, F. A., Goodgame, D. M. L., and Goodgame, M., J. Amer. Chem. Soc. 83:4690(1961).

60. Gayer, K. H., and Garrett, A. B., J. Am. Chem. Soc. 72:3921(1950).
61. Bourne, E. J., Nery, R., and Weigel, H., Chemistry and Industry 998(1959).
62. Charley, P. J., Sarkar, B., Stitt, C. F., and Saltman, P., Biochim. Biophys. Acta 69:313(1963).
63. Behl, W. K., and Toni, J. E., J. Electroanal. Chem. 31:63(1971).
64. Stumm, W., and Morgan, J. J., Aquatic Chemistry, p. 243-258, 472-494. New York, John Wiley & Sons, 1970.
65. Leckie, J. O., and James, R. O. Control Mechanisms for Trace Metals in Natural Waters, in Aqueous-Environmental Chemistry of Metals, Alan J. Rubin, ed., p. 1-76. Ann Arbor, Michigan, Ann Arbor Science Publishers, Inc. 1976.
66. Rollinson, C. L. Olation and Related Chemical Processes, in The Chemistry of Coordination Compounds, American Chemical Society Monograph Series, no. 131, J.C. Bailar, Jr., ed., p. 448-471. New York, Reinhold Publishing Corp., 1956.
67. Healy, T. W., James, R. O., and Cooper, R. The Adsorption of Aqueous Co(II) at the Silica-Water Interface, in Adsorption from Aqueous Solution, Am. Chem. Soc. Advances in Chemistry Series, no. 79, p. 62-73, Washington, 1968.
68. Morgan, J. J. and Stumm, W., J. Colloid Sci. 19:347(1964).
69. Murray, K. J., Healy, T. W., and Fuerstenau, D. W. The Adsorption of Aqueous Metal on Colloidal Hydrous Manganese Oxide, in Adsorption from Aqueous Solution, Am. Chem. Soc. Advances in Chemistry Series, no. 79, p. 74-81, Washington, 1968.
70. Kurbatov, M. H., Wood, G. B., and Kurbatov, J. D., J. Phys. Chem., 55:1170(1951).
71. Weiser, H. B., Inorganic Colloid Chemistry, vol II, The Hydrous Oxides and Hydroxides, p. 21, 160-167. New York, John Wiley & Sons, 1935.
72. Weiser, H. B., Colloid Chemistry, 2nd ed., p. 140-141, New York, John Wiley & Sons, 1949.
73. James, R. O., and Healy, T. W., J. Colloid Interface Sci. (40):42-52, 53-64, 65-81(1972).
74. Weast, R. C., ed., CRC Handbook of Chemistry and Physics, 54th ed., Cleveland, Ohio, CRC Press, 1973.
75. Gayer, K. H., and Garrett, A. B., J. Am. Chem. Soc. 71:2973(1949).
76. Gayer, K. H., and Woontner, L., J. Phys. Chem. 60:1569(1956).



77. Fox, R. K., Swinehart, D. F., and Garrett, A. B., J. Am. Chem. Soc. 63: 1779(1941).
78. McDowell, L. A., and Johnston, H. L., J. Am. Chem. Soc. 58:2009(1936).
79. Gordon, S., and Schreyer, J. M., J. Am. Chem. Soc. 74:3169(1952).
80. Grube, G., and Feucht, O., Z. Elektrochem. 28:568(1922).
81. Dugger, D. L., Stanton, J. H., Irby, B. N., McConnell, B. L., Cummings, W. W., and Maatman, R. W., J. Phys. Chem. 68:757(1964).
82. Iler, R. K. The Chemistry of Silica, p. 4, 84, 138, 667-673. New York, John Wiley & Sons, 1979.
83. Trotman-Dickenson, A. F., exec. ed., Comprehensive Inorganic Chemistry, vol. 1, p. 1413. New York, Pergamon Press, 1973.
84. Weber, W. J., Jr., and Stumm, W., J. Inorg. Nucl. Chem. 27:237(1965).
85. Schenk, J. E. Interactions of monomeric silica with iron, manganese, and aluminum in aqueous solution. Doctor's Dissertation. Ann Arbor, Michigan. The University of Michigan, 1969.
86. Beeman, L. A., and Reichert, J. S. Peroxides in Pulp Bleaching Processes, in The Bleaching of Pulp, Tappi Monograph no. 10, p. 221. New York. Technical Association of the Pulp and Paper Industry, 1953.
87. Boehm, H. P., Adv. Catal. 16:226(1966).
88. Petersson, G., Tetrahedron 26(13):3413(1970).
89. Khan, M. M. T., and Martell, A. E. Homogeneous Catalysis by Metal Complexes, vol. 1, Activation of Small Inorganic Molecules, p. 114-123. New York, Academic Press, 1974.
90. Jones, M. M. Ligand Reactivity and Catalysis, p. 88-108. New York, Academic Press, 1968.
91. Fallab, S., Angew. Chem. Internat. Edit. 6:496(1967).
92. Bawn, C. E. H., and White, A. G., J. Chem. Soc. 331, 339, 343(1951).
93. Bawn, C. E. H., Disc. Faraday Soc. 14:181(1953).
94. Bawn, C. E. H., and Jolley, J. E., Proc. Roy. Soc. (London) A237: 19(1956).
95. Isbell, H. S., and Frush, H. L., Carbohydr. Res. 59:C25-C31(1977).
96. Pottenger, C. R., and Johnson, D. C., J. Polymer Sci. 8:301(1970).
97. Bothe, E., Schulte-Frohlinde, D., and Von Sonntag, C., J.C.S. Perkin II, 416(1978).

98. Swern, D. Organic Peroxy Acids — Preparation, Properties, and Structure, in Organic Peroxides, vol. 1, Daniel Swern, ed., p. 62, 313-324. New York, Wiley-Interscience, 1970.
99. Bollenback, G. N. Methyl Glucoside, p. 19. New York, Academic Press, 1958.
100. Schroeder, L. R., and Green, J. W., J. Chem. Soc. (C) 530(1966).
101. Timell, T. E., Can. J. Chem. 42:1456(1964).
102. Sims, E. W., J. Chromat. Sci. 14:65(1976).
103. Standard Method 18, The Institute of Paper Chemistry, Appleton, Wisconsin, 1951.

## APPENDIX I

TABLE X

## TRACE METALS IN ALKALINE REACTION SOLUTIONS

Reaction	Initial Co Charge to Reactor	Final Co Concentration	Metal, mg/L = ppm <sup>a</sup>										
			Al	B	Cd	Cr	Cu	Fe	Mg	Mn	Ni	Si	Zn
IV	0.00	<0.05	--	--	<0.05	0.13	<0.05	0.21	0.22	<0.05	<0.05	516	0.52
V	0.59	0.41 (0.6)	13.2	232	<0.05	<0.05	<0.05	0.13	<0.05	<0.05	<0.05	492 (491)	<0.05
VI	2.95	0.22 (0.4)	12.0	241	<0.05	<0.05	<0.05	0.11	<0.05	<0.05	<0.05	500 (414)	<0.05
VII	14.73	<0.05	13.6	263	<0.05	<0.05	<0.05	0.08	<0.05	<0.05	<0.05	501 (485)	<0.05
X	0.00	<0.05	<0.5	<0.5	<0.05	<0.05	<0.05	0.26	0.10	<0.05	<0.05	<0.05	0.14
XI	14.73	<0.05 (0.1)	0.12	0.10	<0.05	<0.05	<0.05	0.20	<0.05	<0.05	<0.05	<0.05	0.35
XIII	2.95	0.11 (0.2)	0.06	<0.05	<0.05	<0.05	<0.05	0.11	<0.05	<0.05	<0.05	<0.05	0.27
XVII	2.95	2.3 (2.3)	13.1	40	<0.05	<0.05	<0.05	0.40	<0.05	<0.05	<0.05	394	0.05
XVIII	14.73	0.22	0.08	<0.05	<0.05	<0.05	<0.05	<0.05	<0.05	<0.05	<0.05	0.43	<0.05

<sup>a</sup>Metal ion analyses were conducted by Trace Elements, Inc. (Park Ridge, IL) using inductively coupled argon plasma emission spectrometry. Values in parentheses were obtained by atomic absorption spectroscopy using Institute equipment. Samples for metals analysis were obtained after reactions were terminated.

<sup>b</sup>Starting cobalt concentrations in mmoles/liter are: IV, X, 0.00; V, 0.01; VI, XIII, XVII, 0.05; VII, XI, XVIII, 0.25.

# APPENDIX II

## EXPERIMENTAL DATA

All degradations of methyl  $\beta$ -D-glucopyranoside (MBG) were conducted with 95.5 mM MBG in 1.25M NaOH (either extracted or ultrapure) at 120°C and 0.68 MPa partial O<sub>2</sub> pressure at 120°C. Mole percent methanol is methanol formed expressed as a percentage of reacted MBG on a molar basis. Except for zero-time values, all MBG analyses given in Tables XI-XXII were by GLC of acetates.

TABLE XI

REACTION IV. EXTRACTED NaOH, NO ADDED CoSO<sub>4</sub>·7H<sub>2</sub>O

Time, hr	MBG, mM	MeOH, mM	Mole % MeOH
0.0	95.5 <sup>a</sup>	--	--
0.25	92.7	1.6	57
0.50	88.8	4.0	60
1.00	82.6	5.7	44
2.00	79.3	8.1	50
4.00	73.8	14.6	67
8.00	54.8	27.9	69
16.00	39.6	39.3	70
32.00	26.9	51.7	75
48.00	20.7	56.1	75
60.00	16.5	60.8	77

---

<sup>a</sup>By GLC of acetates, 96.4 mM.

TABLE XII

REACTION V. EXTRACTED NaOH, 0.01 mM ADDED CoSO <sub>4</sub> ·7H <sub>2</sub> O			
Time, hr	MBG, mM	MeOH, mM	Mole % MeOH
0.00	95.5 <sup>a</sup>	--	--
0.25	89.1	2.5	39
0.50	86.1	5.2	55
1.00	79.8	9.5	61
2.00	67.9	18.5	67
4.00	54.9	28.4	70
8.00	40.6	43.0	78
16.00	26.4	55.2	80
32.00	15.3	60.2	75
48.00	9.8	63.7	74

<sup>a</sup>By GLC of acetates, 95.1 mM.

TABLE XIII

REACTION VI. EXTRACTED NaOH, 0.05 mM ADDED CoSO <sub>4</sub> ·7H <sub>2</sub> O <sup>a</sup>			
Time, hr	MBG, mM	MeOH, mM	Mole % MeOH
0.00	95.5 <sup>b</sup>	--	--
0.25	85.6	2.9	29
0.50	79.1	6.2	38
1.00	71.4	14.3	59
2.00	56.0	31.8	81
4.00	32.8	49.4	79
8.00	16.2	62.9	79
16.00	8.9	67.0	77

<sup>a</sup>Conducted under conditions of limited agitation.

<sup>b</sup>By GLC of acetates, 93.7 mM.

TABLE XIV

REACTION VII. EXTRACTED NaOH, 0.25 mM ADDED  $\text{CoSO}_4 \cdot 7\text{H}_2\text{O}$

Time, hr	MBG, mM	MeOH, mM	Mole % MeOH
0.00	95.5 <sup>a</sup>	--	--
0.25	90.3	4.3	83
0.50	83.4	8.3	69
1.00	70.3	17.2	68
2.00	54.4	30.1	73
4.00	42.0	42.5	79
8.00	32.8	47.4	76
16.00	26.7	54.6	79
32.00	20.8	60.0	80
48.00	17.3	61.4	79

<sup>a</sup>By GLC of acetates, 95.4 mM.

TABLE XV

REACTION VIII. EXTRACTED NaOH, 0.05 mM ADDED  $\text{CoSO}_4 \cdot 7\text{H}_2\text{O}$ <sup>a</sup> AND THE PRECIPITATE ISOLATED FROM A 0.25 mM COBALT-CONTAINING REACTION

Time, hr	MBG, mM	MeOH, mM	Mole % MeOH
0.00	95.5 <sup>a</sup>	--	--
0.25	88.9	3.1	47
0.50	84.4	6.4	58
1.00	72.4	15.0	65
2.00	53.5	30.9	74
4.00	35.3	47.0	78
8.00	22.1	56.8	77
16.00	14.5	67.9	84
32.00	10.1	60.4	71
48.00	8.2	60.0	69

<sup>a</sup>By GLC of acetates, 93.5 mM.

TABLE XVI

REACTION IX. ULTRAPURE NaOH, 0.25 mM ADDED  $\text{CoSO}_4 \cdot 7\text{H}_2\text{O}$

Time, hr	MBG, mM	MeOH, mM	Mole % MeOH
0.00	95.5 <sup>a</sup>	--	--
0.17	91.8	--	--
0.42	89.1	2.8	44
0.67	86.5	--	--
1.00	84.4	7.0	63
2.00	76.3	12.2	63
4.00	67.1	21.9	77
8.00	55.4	33.5	83
16.00	46.2	39.5	80
32.00	32.6	54.8	87

<sup>a</sup>By GLC of acetates, 93.7 mM.

TABLE XVII

REACTION X. ULTRAPURE NaOH, NO ADDED  $\text{CoSO}_4 \cdot 7\text{H}_2\text{O}$

Time, hr	MBG, mM	MeOH, mM	Mole % MeOH
0.00	95.5 <sup>a</sup>	--	--
0.25	94.9	--	--
0.50	91.4	--	--
1.00	88.7	4.1	60
2.00	82.4	8.8	67
4.00	71.1	16.2	66
8.50	56.4	26.7	68
16.00	44.2	37.7	72
32.00	26.7	44.4	65

<sup>a</sup>By GLC of acetates, 96.4 mM.

TABLE XVIII

REACTION XI. ULTRAPURE NaOH, 0.25 mM ADDED  $\text{CoSO}_4 \cdot 7\text{H}_2\text{O}$

Time, hr	MBG, <u>mM</u>	MeOH, <u>mM</u>	Mole % MeOH
0.00	95.5 <sup>a</sup>	--	--
0.25	90.8	2.8	58
0.50	87.1	4.4	52
1.00	83.5	7.3	61
2.00	76.1	12.0	62
4.00	67.6	20.8	74
8.00	56.2	30.3	77
16.00	44.7	38.8	76
32.00	34.4	46.9	77

---

<sup>a</sup>By GLC of acetates, 95.5 mM.

TABLE XIX

REACTION XII. ULTRAPURE NaOH, 0.05 mM ADDED  $\text{CoSO}_4 \cdot 7\text{H}_2\text{O}$

Time, hr	MBG, <u>mM</u>	MeOH, <u>mM</u>	Mole % MeOH
0.00	95.5 <sup>a</sup>	--	--
0.25	86.2	6.1	65
0.50	76.0	14.2	73
1.00	60.1	24.7	70
2.00	39.9	39.4	71
4.00	22.5	52.8	72
8.00	14.9	60.0	74

---

<sup>a</sup>By GLC of acetates, 94.0 mM.



TABLE XX

REACTION XIII. ULTRAPURE NaOH, 0.05 mM ADDED  $\text{CoSO}_4 \cdot 7\text{H}_2\text{O}$

Time, hr	MBG, mM	MeOH, mM	Mole % MeOH
0.00	95.5 <sup>a</sup>	--	--
0.13	90.2	2.4	45
0.25	84.8	5.6	52
0.50	74.1	14.7	69
1.00	58.7	26.2	71
2.00	38.4	40.0	70
4.00	22.0	54.3	74

---

<sup>a</sup>By GLC of acetates, 96.5 mM.

TABLE XXI

REACTION XVII. ULTRAPURE NaOH, 0.05 mM ADDED  $\text{CoSO}_4 \cdot 7\text{H}_2\text{O}$

Time, hr	MBG, mM
0.00	95.5 <sup>a</sup>
0.25	84.9
0.50	74.5
1.00	62.4
2.00	42.0
4.00	24.8
8.00	14.9

---

<sup>a</sup>By GLC of acetates, 93.7 mM.

TABLE XXII

REACTION XVIII. ULTRAPURE NaOH, 0.25 mM ADDED COBALT

Time, hr	MBG, <u>mM</u>
0.00	95.5 <sup>a</sup>
0.25	80.5
0.50	61.7
1.00	47.6
2.00	35.9
4.00	30.4
8.00	25.9

---

<sup>a</sup>By GLC of acetates, 98.7 mM.

TABLE XXIII

ACIDIC PRODUCT DISTRIBUTION WITH TIME<sup>a</sup>

Reaction	IVb				VC				VIId			
	1	2	4	8	48	2	4	16	2	8	16	
Reaction time, hr												
Percent reaction <sup>e</sup>	13.5	17.0	22.7	42.6	78.3	28.9	42.5	72.4	43.1	65.7	72.1	
Acidic Products	Estimated Concentration of Products, mM <sup>f</sup>											
1 Lactic	1.1	1.7	3.3	3.2	5.2	1.3	2.7	5.0	2.2	4.5	7.1	
2 Glycolic	4.0	4.9	7.4	15.1	22.7	7.4	11.9	20.0	8.5	13.6	20.4	
3 Glyceric	1.5	2.0	2.4	6.9	9.3	1.8	2.7	4.7	1.9	3.7	5.1	
4 2,4-Dihydroxybutyric	0.7	1.0	1.6	2.6	10.1	2.2	2.6	4.0	2.2	4.0	4.4	
5 Erythronic	0.2	0.2	0.3	0.8	1.0	0.3	0.4	0.3	0.2	0.3	0.5	
6 Threonic	0.1	0.2	0.2	0.5	1.7	0.2	0.2	0.1	0.1	0.1	0.1	
7 Arabinonic	0.1	0.1	0.1	0.4	0.4	0.9	0.3	1.0	0.6	1.0	1.6	
8-11 Methyl-C-carboxy $\beta$ -D-penta-furanosides	2.6	5.9	5.9	9.6	8.5	8.7	7.2	4.9	6.1	4.2	5.1	
12-13 Dicarboxylic acids	0.1	0.5	1.6	1.4	0.8	3.1	5.1	6.0	4.3	6.1	4.3	

<sup>a</sup>Reactions conducted in 1.25M extracted NaOH at 120°C and 0.68 MPa partial O<sub>2</sub> pressure. Starting

MBG concentrations = 95.5 mM.

<sup>b</sup>Reaction IV contained no added cobalt.

<sup>c</sup>Reaction V prepared to be 0.01 mM in cobalt.

<sup>d</sup>Reaction VII prepared to be 0.25 mM in cobalt.

<sup>e</sup>Determined from acetylated samples.

<sup>f</sup>Response factor calculation is described in Appendix IV.

TABLE XXIV

ACIDIC PRODUCT DISTRIBUTION WITH TIME<sup>a</sup>

Reaction	x <sup>b</sup>				XII <sup>c</sup>			XIII <sup>c</sup>		
	2	4	8.5	16	32	0.5	1	2	1	2
Reaction time, hr										
Percent reaction <sup>d</sup>	13.7	25.6	41.0	53.7	72.1	20.4	37.1	58.2	38.6	59.8
Estimated Concentration of Products, mM <sup>e</sup>										
<u>Acidic Products</u>										
1 Lactic	1.9	3.4	4.2	5.1	6.6	0.5	1.5	2.2	2.0	3.4
2 Glycolic	3.0	6.1	7.3	9.7	10.9	2.3	3.7	10.1	7.4	12.6
3 Glyceric	1.0	2.1	3.3	5.7	5.9	0.6	1.1	5.3	1.9	3.2
4 2,4-Dihydroxybutyric	0.6	1.0	1.2	2.6	2.2	0.9	1.6	2.5	2.5	3.7
5 Erythronic	0.5	0.2	0.2	0.7	0.5	0.1	0.1	0.2	0.3	0.3
6 Threonic	0.1	0.2	0.2	0.4	0.5	0.1	0.1	0.1	0.2	0.2
7 Arabinonic	0.3	0.4	0.1	0.4	0.4	0.3	0.5	0.1	0.5	0.9
8-11 Methyl-C-carboxy $\beta$ -D-pentafuranosides	5.6	7.8	11.6	15.1	13.1	6.8	8.2	8.1	7.9	7.5
12-13 Dicarboxylic acids	0.9	1.0	1.5	2.6	1.2	0.9	1.9	5.9	4.5	7.2

<sup>a</sup>Reactions conducted in 1.25M ultrapure NaOH at 120°C and 0.68 MPa partial O<sub>2</sub> pressure. Starting MBG concentrations = 95.5 mM.

<sup>b</sup>Reaction X contained no added cobalt.

<sup>c</sup>Reactions XII and XIII each contained 0.05 mM added cobalt.

<sup>d</sup>Determined from acetylated samples.

<sup>e</sup>Response factor calculation is described in Appendix IV.

TABLE XXV

ACIDIC PRODUCT DISTRIBUTION WITH TIME<sup>a</sup>

Reaction	IX <sup>b</sup>			XI <sup>b</sup>		
Reaction time, hr	2	8	32	2	8	32
Percent reaction <sup>c</sup>	20.1	42.0	65.9	20.3	41.2	53.2 64.0
<u>Acidic Products</u>	Estimated Concentration of Products, mM <sup>d</sup>					
1 Lactic	0.9	1.5	2.5	0.5	0.8	2.7 5.6
2 Glycolic	4.2	7.6	12.7	3.4	7.3	14.1 17.1
3 Glyceric	1.1	2.2	3.4	0.9	3.0	3.6 4.0
4 2,4-Dihydroxybutyric	0.9	1.8	2.2	1.1	1.4	3.0 3.2
5 Erythronic	0.2	0.2	0.2	0.1	0.1	0.3 0.3
6 Threonic	0.1	0.2	0.2	0.2	0.2	0.3 0.3
7 Arabinonic	0.1	0.2	0.3	0.2	0.2	0.5 0.5
8-11 Methyl-C-carboxy $\beta$ -D-pentafuranosides	6.4	10.0	7.3	8.4	10.1	10.4 6.7
12-13 Dicarboxylic acids	0.8	1.8	3.2	2.1	1.5	3.5 2.6

<sup>a</sup>Reactions conducted in 1.25M ultrapure NaOH at 120°C and 0.68 MPa partial O<sub>2</sub> pressure. Starting MBG concentrations = 95.5 mM.

<sup>b</sup>Reaction IX and XI were prepared to be 0.25 mM in cobalt.

<sup>c</sup>Determined from acetylated samples.

<sup>d</sup>Response factor calculation is described in Appendix IV.

APPENDIX III

DETERMINATION OF SIGNIFICANT DIFFERENCES BETWEEN  
SETS OF MBG RESULTS

To determine significant differences between sets of results for MBG concentration versus reaction time, a multiple regression was performed by computer using the following model.

$$1/y = b_1X_1 + b_2X_2 + b_3X_3 + b_{12}X_1X_2 + b_{13}X_1X_3 + b_{11}X_1^2 \quad (33)$$

where  $y$  = MBG concentration, mM

$X_1$  = reaction time, hours

$X_2X_3$  = dependent variables assigned either a 0 or a 1 in value  
(e.g.,  $X_2 = 0$  for extracted NaOH and 1 for ultrapure NaOH,  
and  $X_3 = 0$  for no added cobalt and 1 for added cobalt)

$X_1X_2$  and  $X_1X_3$  = interaction terms between  $X_1$  and  $X_2$  or  $X_3$

$b_1, b_2, b_3, b_{12}, b_{13}, b_{11}$  = coefficients for variable X terms.

The number of terms in the model depended on the number of variables involved and on the goodness of fit. A difference between sets of MBG degradation results was considered significant if a student's t value for the dependent variable being investigated exceeded the 0.05 probability level of a student's t distribution. The results are tabulated in Table XXVI.

TABLE XXVI  
SIGNIFICANT DIFFERENCES BETWEEN SETS OF MBG RESULTS

Reaction in Data Set	Variable	Curve Fit ( $r^2$ )	Student's t from Regression	Tubular Student's t at 0.05 Level	Conclusion
IV, X, IX, XI	Ultrapure <u>vs.</u> extracted NaOH	0.99	0.249	1.706	Difference not signi- ficant
IV, X, IX, XI	Added Co <u>vs.</u> no added Co	0.99	3.298	1.706	Difference significant
XII, XIII, XVII	Ultrapure <u>vs.</u> extracted NaOH	1.00	1.559	1.771	Difference not signi- ficant
XII, XIII, VIII	Presence <u>vs.</u> absence of precipitated Co	1.00	2.153	1.771	Difference significant

# APPENDIX IV

## GAS-LIQUID CHROMATOGRAPHY

Quantitative and semiquantitative GLC was accomplished through the use of an appropriate internal standard. Molar response factors were calculated relative to internal standards according to Eq. (34).

$$F_X = A_r \times M_r \quad (34)$$

where  $F_X$  = response factor for compound X relative to the internal standard

$A_r$  = ratio of GLC peak area of compound X to the peak area of the internal standard

$M_r$  = mole ratio of the internal standard to compound X

Response factors were experimentally determined by subjecting a series of solutions, prepared with varied mole ratios, to the appropriate workup and analysis procedures. The solutions were then analyzed by GLC in triplicate, and response factors were calculated as an average of the values obtained. Semiquantitative GLC analysis involved either estimation of response factors on a molecular weight basis, or calculation of response factors from workup and analysis of a single reference solution containing the compound of interest. Table XXVII lists GLC conditions used for the various analyses conducted in this work, and Table XXVIII gives retention times and response factors for compounds encountered in this work.

The concentration of a compound X was determined by using Equation (35).

$$X = (A_r)(M)(I)/(S)(F_X) \quad (35)$$

where X = concentration of compound X, moles/liter

M = molarity of internal standard, moles/liter

I = internal standard volume, mL

S = sample volume, mL.



TABLE XXVII  
GAS-LIQUID CHROMATOGRAPHIC CONDITIONS

Conditions	A	B	C
Column type	SE-30 <sup>a</sup>	Carbowax 20M <sup>b</sup>	SP-2250 <sup>c</sup>
Derivative	Acetylated	Underivatized	Trimethylsilylated
Column temperature programming, °C	205	70	60 for 10 min, 3/min to 220
Injector temperature, °C	260	120	265
Detector temperature, °C	260	260	260
N <sub>2</sub> flow rate, mL/min	15	35	20

<sup>a</sup>Stainless steel column (5 ft x 0.125-inch) rigged for on-column injection and packed with 10% SE-30 on 60/80 mesh DMCS-AW Chromosorb W.

<sup>b</sup>Stainless steel column (4 ft x 0.125-inch) rigged for off-column injection and flash vaporization and packed with 5% Carbowax 20M on 80/100 mesh Chromosorb 101.

<sup>c</sup>Stainless steel column (9 ft x 0.125-inch) rigged for off-column injection and flash vaporization and packed with 3% SP-2250 on 100/120 mesh Supelcoport.

TABLE XXVIII

RETENTION TIMES ( $T_r$ ) AND RESPONSE FACTORS ( $F_x$ )

Conditions	Compound	$T_r$ , min	$F_x$
A	Methyl $\beta$ - <u>D</u> -glucopyranoside	6.2	$0.713 \pm 0.012^a$
	<u>n</u> -Butyl $\beta$ - <u>D</u> -glucopyranoside	12.2	1.000 <sup>a</sup>
B	Methanol	2.8	$0.517 \pm 0.015^b$
	Ethanol	7.0	1.00 <sup>b</sup>
C	Lactic acid	13.4	0.45 <sup>c</sup>
	Glycolic acid	15.2	0.43 <sup>c</sup>
	Glyceric acid	28.7	0.63 <sup>d</sup>
	2,4-Dihydroxybutyric acid	32.6	0.64 <sup>c</sup>
	Erythronic	37.7	0.81 <sup>c</sup>
	Threonic	39.1	0.81 <sup>c</sup>
	Arabinonic	45.5	1.00 <sup>c</sup>
	Methyl <u>C</u> -carboxy $\beta$ - <u>D</u> -penta- furanosides	47.9 48.7 49.4 50.9	0.95 <sup>c</sup>
	Methyl $\beta$ - <u>D</u> -glucopyranoside	52.4	0.90 <sup>d</sup>
	Dicarboxylic acids	53.9 54.3	0.98 <sup>c</sup>

<sup>a</sup>Calculated relative to n-butyl  $\beta$ -D-glucopyranoside at the specified conditions.

<sup>b</sup>Calculated relative to ethanol at the specified conditions.

<sup>c</sup>Estimated on a molecular weight basis relative to n-butyl  $\beta$ -D-glucopyranoside.

<sup>d</sup>Calculated from triplicate injections of a single sample relative to n-butyl  $\beta$ -D-glucopyranoside.

APPENDIX V

GAS CHROMATOGRAPHIC-MASS SPECTRAL ANALYSIS

Equipment used for gas chromatography-mass spectrometry is described in the Experimental section. Chromatographic separations were performed on a newly packed glass column (6 ft x 0.250 inch) packed with 3% OV-17 on 80/100 mesh Gas Chrom Q and rigged for on-column injection. Chromatographic conditions were as follows: helium flow rate, 34 mL/min; column temperature isothermal at 60° for 10 min, then 3°/min to 220°; injector temperature, 275°. The operating conditions for the mass spectrometer are given in Table XXIX.

TABLE XXIX

MASS SPECTROMETER OPERATING CONDITIONS

Jet separator temperature: 250°

GC transfer line probe: 250°

Analyzer manifold: 200°

Ion source temperature: 200°

Electron multiplier: 200 V

Ionizing voltage: 70 eV

Mass Scan Range: 50-550

The mass spectral data for trimethylsilylated acidic MBG degradation products are presented in Tables XXX-XXXVI. Spectra are uncorrected for background.

TABLE XXX

MASS SPECTRAL DATA FOR LACTIC ACID (TMS DERIVATIVE)

Reference: Petersson (88)

m/e	%	m/e	%	m/e	%
50	3	76	4	129	1
51	5	77	5	131	4
52	13	78	3	133	6
53	2	79	21	134	1
55	3	80	1	147	73
57	1	87	2	148	11
58	2	88	6	149	6
59	6	93	1	170	1
60	1	101	2	175	1
61	2	102	3	190	18
66	13	103	1	191	16
69	2	115	1	192	4
70	1	116	2	193	2
72	3	117	84	204	1
73	100	118	9	219	9
74	9	119	4	220	2
75	41	120	2	221	1

TABLE XXXI

MASS SPECTRAL DATA FOR GLYCOLIC ACID (TMS DERIVATIVE)

Reference: Petersson (88)

m/e	%	m/e	%	m/e	%
51	2	79	4	149	9
52	4	81	4	150	1
57	1	88	2	161	6
58	3	89	1	162	1
59	5	95	1	177	14
61	1	103	4	178	3
66	20	115	1	179	1
72	3	117	5	190	1
73	100	131	3	205	17
74	9	133	8	206	3
75	14	134	1	207	2
76	1	147	92		
77	1	148	14		

TABLE XXXII

MASS SPECTRAL DATA FOR GLYCERIC ACID (TMS DERIVATIVE)  
Reference: Petersson (88)

m/e	%	m/e	%	m/e	%
50	2	89	1	175	3
51	4	93	1	189	35
52	8	101	4	190	10
53	1	102	10	191	6
55	2	103	23	204	1
57	2	104	3	205	16
58	1	105	2	206	3
59	5	115	1	207	2
61	1	116	2	217	4
66	1	117	10	219	2
69	2	118	1	221	2
71	1	119	1	292	37
72	2	130	3	293	10
73	100	131	4	294	5
74	10	133	13	295	1
75	20	134	3	307	9
76	2	135	2	308	2
77	2	147	69	309	1
78	2	148	11	322	1
79	16	149	7		

TABLE XXXIII

MASS SPECTRAL DATA FOR 2,4-DIHYDROXYBUTYRIC ACID (TMS DERIVATIVE)  
Reference: Petersson (88)

m/e	%	m/e	%	m/e	%
50	1	85	1	175	1
51	2	101	3	177	3
52	4	102	2	189	3
55	5	103	100	190	3
57	1	104	10	203	4
58	1	105	4	204	1
59	4	115	2	219	60
66	1	117	2	220	16
69	1	129	10	221	7
71	1	130	2	222	1
72	2	131	5	291	1
73	68	133	7	293	1
74	6	134	1	321	6
75	14	147	37	322	2
77	2	148	6		
79	8	149	3		

TABLE XXXIV

MASS SPECTRAL DATA FOR METHYL 2-C-CARBOXY  $\beta$ -D-PENTAFURANOSIDE<sup>a</sup>  
(TMS DERIVATIVE)

Reference: Ericsson et al. (15)

m/e	%	m/e	%	m/e	%
52	2	144	2	233	1
55	2	145	1	243	2
57	2	147	42	245	3
59	4	148	7	247	11
69	2	149	8	248	3
71	2	150	1	249	1
72	2	157	2	257	4
73	100	159	2	259	1
74	9	163	5	261	1
75	12	165	1	275	3
76	1	169	2	303	1
77	2	171	1	305	8
79	4	173	1	306	2
83	2	177	2	307	1
85	2	187	2	319	1
87	1	189	4	331	8
89	6	190	1	332	3
93	2	191	3	333	97
95	1	203	1	334	31
97	1	204	2	335	17
101	1	205	1	336	4
103	12	207	3	337	1
104	1	215	2	345	2
105	2	217	20	346	8
117	3	218	4	347	4
119	1	219	5	348	2
129	4	220	1	378	2
131	4	221	5	421	2
133	31	222	1	436	7
134	4	229	1	437	3
135	2	230	1	438	2
143	9	231	1	481	1

<sup>a</sup>The spectrum for dicarboxylic acid 9 (Table VII) was essentially identical to that for dicarboxylic acid 10.

TABLE XXXV

MASS SPECTRAL DATA FOR DICARBOXYLIC ACID 12 (TABLE VII) (TMS DERIVATIVE)

Reference: Ericsson et al. (15)

m/e	%	m/e	%	m/e	%
52	2	131	6	218	5
55	3	132	1	219	25
57	1	133	18	220	6
59	4	134	2	221	4
61	1	135	1	233	3
71	1	143	6	234	26
72	3	145	1	235	9
73	100	146	1	236	3
74	9	147	29	245	39
75	14	148	5	246	9
76	1	149	4	247	6
77	2	157	1	248	1
79	4	159	1	261	3
83	4	161	25	263	2
85	1	162	3	291	2
89	6	163	3	292	12
93	2	173	1	293	8
95	1	175	1	294	3
101	3	177	1	305	13
102	1	189	5	306	4
103	12	190	1	319	1
104	1	191	4	335	5
105	1	203	2	336	2
116	1	204	10	393	1
117	3	205	4	395	2
119	1	206	1	409	3
129	8	207	1	410	1
130	2	217	23		

TABLE XXXVI

MASS SPECTRAL DATA FOR DICARBOXYLIC ACID 13 (TABLE VII) (TMS DERIVATIVE)  
Reference: Ericcson et al. (15)

m/e	%	m/e	%	m/e	%
52	2	133	15	221	3
55	3	134	2	233	20
59	3	135	1	234	7
71	1	143	2	235	4
72	2	146	2	245	5
73	100	147	22	246	1
74	9	148	3	247	5
75	10	149	3	248	1
76	1	159	1	249	1
77	2	161	4	263	5
79	3	163	2	264	1
85	2	175	1	292	4
89	4	189	20	293	24
93	2	190	4	294	7
101	7	191	8	295	3
102	2	192	1	305	3
103	6	204	7	307	11
116	5	205	2	308	3
117	6	217	7	309	2
129	2	218	2	335	1
131	10	219	18	391	1
132	1	220	6	407	1